POLYACRYLAMIDE POLYMER FLOW THROUGH CARBONATE ROCKS FOR ENHANCED OIL RECOVERY: AN EXPERIMENTAL STUDY OF POLYMER - BRINE STABILITY, RESISTANCE FACTOR, AND RELATED GEOLOGIC CHARACTERISTICS

James A. Hunt

Graduate School
Chemical and Petroleum Engineering Department
Tertiary Oil Recovery Project
The University of Kansas

July 1981

This work is presented to my parents, in appreciation of their love and understanding so generously offered during my early learning years.

POLYACRYLAMIDE POLYMER FLOW THROUGH CARBONATE ROCKS FOR ENHANCED OIL RECOVERY: AN EXPERIMENTAL STUDY OF POLYMER-BRINE STABILITY, RESISTANCE FACTOR, AND RELATED GEOLOGIC CHARACTERISTICS

by

James A. Hunt
B.S., University of Akron, 1975

Submitted tc the Department of Chemical and Petroleum Engineering and the Faculty of the Graduate School of the University of Kansas in partial fulfillment of the requirements for the degree of Master of Engineering.

Dr. D. W. Green, Professor in Charge

Committee Members:

Dr. G. P. Willhite

Dr. R. E. Terry

For the Department

ABSTRACT

A large portion of the world's crude oil reserves is contained in carbonate reservoirs. The addition of low concentrations of high molecular weight, water-soluble polymers to injection waters has been employed primarily in sandstones to increase oil recovery by improving reservoir areal sweep and displacement efficiency. Based on a comprehensive study of the technical literature, very little experimental work has been performed using polymers in carbonate rocks. A research program was developed to investigate the application of polyacrylamide as a mobility control agent in limestone and dolomite rocks.

The research program was divided into three phases. In the first phase, limestone material obtained from three wells cored in the Lansing and Kansas City Group was examined for adequate porosity and permeability to conduct laboratory core flood experiments. Twenty polyacrylamides were tested for stability in sodium, calcium, and magnesium chloride brine mixtures at 25°C (77°F) and 43.3°C (110°F) for periods up to seven months. Most of the polyacrylamides investigated were found stable in brines containing 27,300 ppm calcium ion and in brines containing 78,700 ppm sodium ion.

In the second phase, ten core flood experiments were performed in reservoir core samples from the Lansing and Kansas City Group, three in Baker dolomite, and one in Berea sandstone. For sections of the core, resistance factors and residual resistance factors to polymer and brine were determined from pressure drop measurements. Both resistance factors and residual resistance factors were found to be significantly higher in carbonates than in Berea sandstone.

In the third phase, an attempt was made to relate rock microscopic properties with macroscopic measurements determined from the core flood experiments. Thin sections of the rock material flooded in the laboratory were studied for mineral content, grains, textures, cements, and porosities. The scanning electron microscope (SEM) was used to examine rock and pore cast samples for pore structure. Finally, mercury porosimetery was used to measure the pore size distribution of rock samples flooded in the laboratory. An attempt was made to correlate the resistance factors and residual resistance factors to the geological characteristics studied by thin sectioning, SEM, and mercury porosimetery techniques.

Presented in this paper is a study of the technical literature and each of the above described research phases. Conclusions drawn from the experimental results and recommendations for future research are also presented.

keywords: Baker dolomite; Lansing and Kansas City Group; carbonate; compatability; dolomite; limestone; mercury porosimetery; polyacrylamides; polymers; reservoir core; residual resistance factor; resistance factor; sandstone; scanning electron microscope (SEM); stability; thin section; enhanced oil recovery.

AUTHOR'S NOTE

Over the time in which the research was performed and the documentation completed, considerable input and support was provided by many individuals. The author particularly wishes to acknowledge Dr. D.W. Green, Dr. R.E. Terry, and Dr. G.P. Willhite of the University of Kansas.

Dr. Green, the author's major advisor, offered untiring assistance during the sometimes troublesome phases of the experimental research program. The author is appreciative to Dr. Green for reviewing and editing this long manuscript. His examination of sections submitted piece by piece insured that the final document was accurate and complete.

Dr. Terry and Dr. Willhite, both members of the Master's committee, were valuable in directing the research effort and in reviewing and editing the final documentation. Each person's instructive method of problem solution was utilized frequently during all stages of the experimental program. The guidance and support of Dr. Green, Dr. Terry, and Dr. Willhite is greatly appreciated. Many times throughout when an end to the work appeared nonexistent, the encouragement offered by these men proved invaluable to the successful completion of the research and documentation.

The author wishes to acknowledge the assistance offered by Mr. Al Smith, machinist at the University of Kansas. His skills in construction of most of the experimental equipment enabled the laboratory research to advance rapidly and on schedule.

Special appreciation is given to Dr. Bernard J. Hunt, both brother and friend, who offered unending encouragement and assistance during much of the research and writing of the final documentation. Bernard was extremely helpful in producing a completed document which is both readable and understandable.

Final documentation of this work was performed by Pat Owens of the Chemical and Petroleum Engineering Department at the University of Kansas. Her diligent assistance in expediting the final document is recognized and greatly appreciated.

To fellow students at the University of Kansas, the author wishes to thank them for their assistance and understanding throughout many of the difficult stages of the research endeavor.

As a final note, whenever beginning such an undertaking as the one at hand, many times we envision the task as huge and insurmountable with no method of completion in sight. Sir William Osler, an advocate of Carlyl's dictum that: "Our main business is not to see what lies dimly at a distance, but to do what lies clearly at hand," wrote the following poem which typifies this idea; a concept which helped immensely in the successful completion of this learning enterprise.

Listen to the Exhortation of the Dawn!

Look to this Day!

For it is Life, the very Life of Life.

In its brief Course lie all the

Varieties and Realities of your Existence:

The Bliss of Growth,

The Glory of Action,

The Splendour of Beauty;

For Yesterday is but a Dream

And Tomorrow is only a Vision;

But Today well lived makes

Every Yesterday a Dream of Happiness,

And every Tomorrow a Vision of Hope.

Look well therefore to this Day!

Such is the Salutation of the Dawn!

Table of Contents

List of Figures

List of Tables

I was, being human, born alone;
I am, being woman, hard beset;
I live by squeezing from a stone;
The little nourishment I get.

-Elinor Hoyt Wylie

CHAPTER 1

Introduction

1.1 Background

With the rapid depletion of existing oil reserves, new methods have been developed beyond waterflooding to improve oil production by recovering additional amounts of oil-in-place from reservoirs. Polymer flooding is one technique used to increase oil recovery.

A large portion of the crude oil reserves in Kansas reside in carbonate rocks. In response to an interest by Kansas oil producers to recover additional oil from carbonate rocks, an experimental research program was undertaken at the University of Kansas to investigate the behavior of polymer flooding in carbonate rocks.

In polymer flooding, high molecular weight, water-soluble polymers are added in low concentrations to injection waters to increase viscosity and thereby reduce fluid mobility or ease-to-flow. An objective of polymer flooding is to control the injection or displacing fluid mobility; thus the term mobility control. Mobility of the displacing fluid is also reduced when polymer molecules become entrapped and adsorbed on the rock surfaces. Reduction in the mobility of the displacing fluid results in effective control of the paths which the fluid travels, thereby enhancing both reservoir sweep and displacement efficiency.

Two major types of polymers currently employed in polymer flooding are the synthetically manufactured polyacrylamides and the biologically

produced polysaccharides or biopolymers. Little information exists concerning the use of these polymers, especially in flooding carbonate rock formations for enhanced oil recovery. The use of polymers in carbonate rocks has been avoided because rock heterogeneities are numerous and brine salinities are high. Rock heterogeneities reduce mobility control because of low polymer adsorption and loss of the displacing fluid. High brine salinities tend to cause polymer degradation and thus loss of the polymer mobility control characteristics. The Kansas oil bearing carbonate rock formations have characteristically high salinities and numerous heterogeneities.

Since little information is available on polymer flooding in carbonate rocks and a large portion of the Kansas crude oil reserves reside in carbonate rocks, this experimental research program was undertaken.

1.2 Objective and Scope

The objective of the experimental research program was to investigate various aspects of polymer flow which govern the use of water-soluble polymer as mobility control agents in enhanced oil recovery operations in carbonate rocks. This study was limited to the investigation of polyacrylamide polymer flooding in both limestone and dolomite, two forms of carbonate rocks, with the exception of one comparison flood performed in Berea sandstone. Information available on polymer flooding in sandstone rocks was only referenced for possible contribution to this study.

In this paper, the experimental program is described. Suitable polyacrylamides are investigated for use in laboratory core flood experiments in carbonate and dolomite rocks. Recommendations are made on

the use of polyacrylamide polymers for application in carbonate reservoirs of high salinity. Resistance factors and residual resistance factors measured for carbonate rocks in the laboratory are presented. Microscopic properties of carbonate rocks were determined from studies using thin section, mercury porosimetery, and scanning electron microscopy (SEM). These microscopic properties were then related to the resistance effects of carbonate rocks to polymer and are presented herein.

1.3 Organization of the Document

This document consists of five chapters and five appendices. In Chapter 2 are presented the findings of an in-depth study of the polymer and carbonate geological literature.

In Chapter 3, the experimental research program is presented which was designed to study the flow behavior of polyacrylamide in carbonate rocks.

In Chapter 4 are presented the results of the experimental research program and a discussion of the findings.

In Chapter 5, the findings of the experimental research are summarized and recommendations are presented for direction of future studies of polymers in carbonate rocks.

In Appendix A, the experimental procedures are described for the mixing of polymer solutions.

In Appendix B, the procedure is presented for measuring and calculating laboratory core air permeabilities.

In Appendix C, equations are given for the calculation of the resistance factor and residual resistance factor from core pressure

data.

In Appendix D, a graph of pressure drop data for a sample core flood is given in which resistance to brine increased after polymer.

In Appendix E, references are listed for literature which was reviewed but was not discussed.

CHAPTER 2

Literature Review

2.1 Introduction

Since the recognition of the general need to improve oil displacement and sweep efficiency in petroleum reservoirs, extensive research has been conducted on the application of water-soluble polymers as mobility control agents. A study of the polymer literature, however, has revealed a lack of information concerning the use of water-soluble polymers in carbonate rocks for enhanced oil recovery techniques. Specifically, the application of polyacrylamides in carbonate reservoirs has been avoided. These reservoirs characteristically have high salinity and low permeability, both conditions unfavorable to polyacrylamide use. Most of the research was found to involve the use of biologically produced polysaccharides or biopolymers and synthetically manufactured polyacrylamides, two major types of polymer used in enhanced oil recovery operations, in sands and sandstone Much of this work performed in sand materials can be directly applied to carbonate rocks.

A computerized* search of the published literature was performed using key words related to polymers, carbonates or limestones, and enhanced or tertiary oil recovery topics. The data bases searched were:

---

* Lockheed Dialog Information Retrieval Service, Palo Alto, California.

- CA CONDENS (Corporation American Chemical Society) 1970-1971
- CA SEARCH (Corporation American Chemical Society) 1976-1980
- CLAIMS/CHEM 1950-1970
- CLAIMS/U.S. PATENTS 1950-1977
- COMPENDEX (Corporation Engineering Index Inc.) 1970-1980
- COMPREHENSIVE DISSERTATION ABSTRACTS 1861-1980
- CONFERENCE PAPERS INDEX 1973-1980
- ENERGYLINE (Corporation EIC Inc.) 1971-1978
- GEOARCHIVE (Corporation GEOSYSTEMS) 1974-1980
- SCISEARCH (Corporation ISI Inc.) 1974-1980

The search identified over 500 publications concerning water-soluble polymer application to enhanced oil recovery methods both in the laboratory and in the field. Many unrelated topics were found and discarded. References in the publications identified by the computer search made to other published material were noted. These articles were collected and examined for their technical content. Discussed in this chapter are those articles found which directly relate to polymer flow behavior in sandstones and carbonates and to carbonate geology. Articles read but found not applicable to this work are listed in a separate bibliography in Appendix E.

2.2 Polymers

2.2.1 General Description

The word polymer is derived from the Greek "polys" meaning many

---

* Citations in brackets point to a numbered bibliographic reference list.

and "meros" meaning parts or units [10]*. Polymers are high molecular weight compounds formed from simple molecules called monomers or single units. The molecular weight of the polymer molecule is proportional to the degree of polymerization.

Two types of polymer frequently used in enhanced oil recovery processes [9] are the synthetically manufactured polyacrylamides and biologically produced polysaccharides also called biopolymers. Both polymers are long-chain macromolecules ranging in average molecular weight between 1 and 30 million. Polyacrylamides are known to both increase the viscosity of the injection fluid and reduce the permeability of the reservoir rock. Unhydrolyzed, partially hydrolyzed, and anionic or cationic polymers manufactured by copolymerization of acrylamides are used. Polyacrylamide is hydrolyzed by reaction with sodium or potassium hydroxide. Polyacrylamides have the advantage over polysaccharides of lower cost and reduced filterability problems associated with polysaccharides. The chemical structure of portions of these polymer molecules are shown in Figure 3.1.

Water-soluble polymers used in many of the enhanced oil recovery operations are polar molecules capable of intermolecular and intramolecular hydrogen bonding. A lack of crystallinity in the structure enables the polymer molecules to bond with other polar components. Water can hydrate the polymer molecules by penetrating the network and forming hydrogen bonds with available sites. During the hydration process, solid polymer is added to water or brine and mixed until the solution is formed. A rapid wetting of the surface of the solid polymer causes the particles to swell and form a barrier to

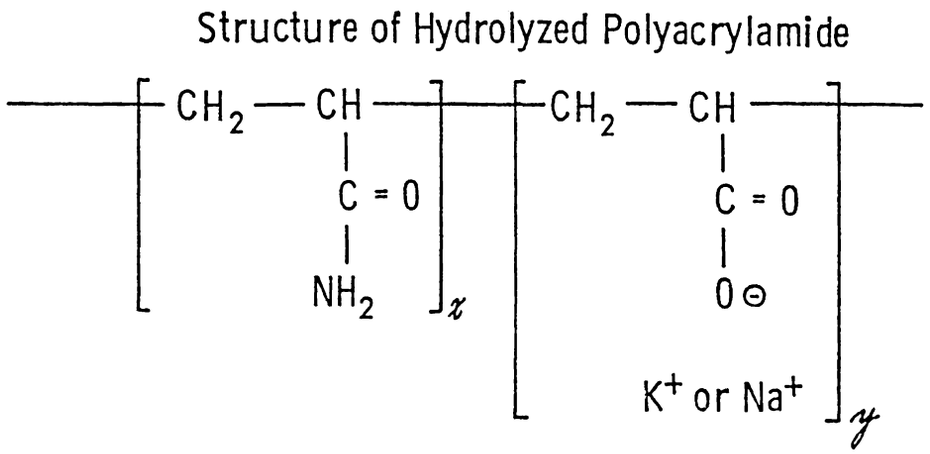

Polyacrylamide

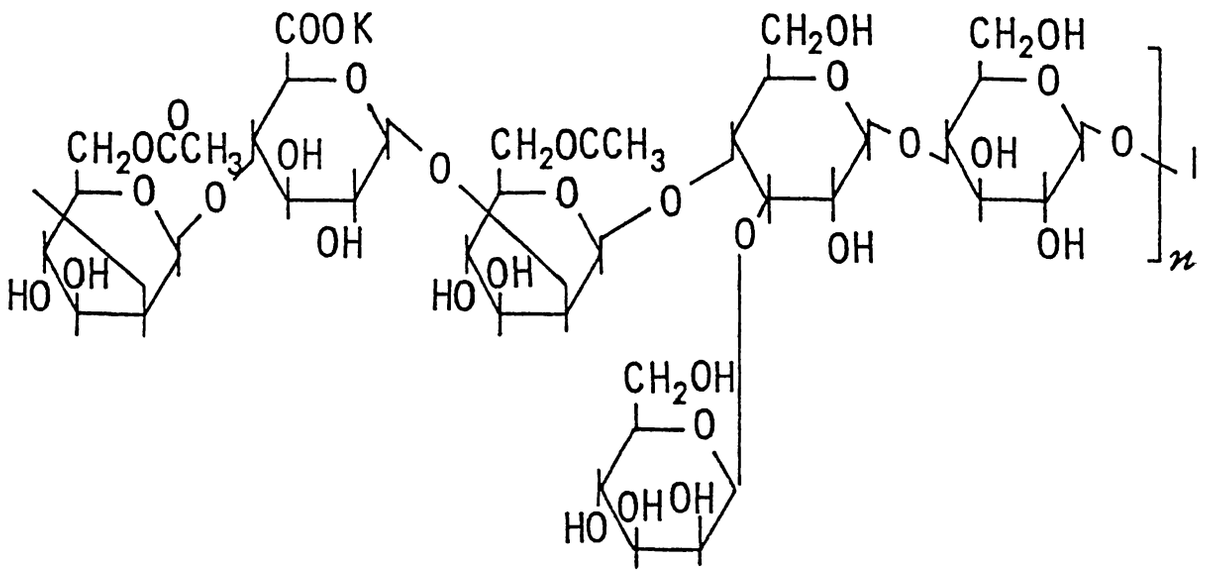

Polysaccharide

Figure 3.1 Structure of the polyacrylamide and polysaccharide molecule.

further hydration [10]. Insoluble aggregates called "fish eyes" or "gel balls" are formed which can plug injection faces. Fish eye formation can be eliminated by increasing the surface area of water to polymer by vigorous agitation of the water and slow addition of the polymer.

Burcik [4,7,8] and Lynch and MacWilliams [31] found the presence of gel-like particles or microgels in prepared polyacrylamide solutions. Both investigators found microgels to be detrimental to polyacrylamide performance. Burcik and Walrond [4] suggests that microgels were formed by cross-linking of the polymer molecules into larger gel-like aggregates during the drying process. He noticed that the amount of microgels present increased with increasing degree of hydrolysis of the polyacrylamide. Burcik [7,8] later studied the mechanism of microgel formation and found polymer cross-linking to be caused by anhydride linkages resulting from the elimination of carboxyl groups. Burcik [8] also discovered the formation of imide cross-linkages from amide and carboxyl groups. Both Burcik [7] and Lynch and MacWilliams [31] found microgel structures to be three dimensional stiff networks.

Both fish eyes and microgels can conceivably plug porous media during polymer flow if the pore throats are smaller than the size of these particles. Proper mixing and filtration procedures can eliminate fish eyes and microgels from polymer solutions.

2.2.2 Polyacrylamide Stability

Polyacrylamides are reported in the literature to be subject to thermal and divalent metal ion degradation. To be effective, the

polymer must remain in solution during the life of the flood at the reservoir temperature and salinity.

Davison and Mentzer [15] screened over 140 different polymers, among which included the general class of polyacrylamides, for compatibility with deoxygenated sea water from the North Sea. Most of the tests were conducted at 90°C (194°F) in sealed glass ampoules in which all the polyacrylamide solutions formed white precipitates within 60 days. The authors cite a study by Mentzer and Meldrum [36] investigating the dependence of precipitation on metal ion type, temperature, and degree of hydrolysis. In this study, calcium and magnesium ions were found to cause the precipitation of polyacrylamide. Precipitation was not observed in distilled water or in 30,000 ppm sodium chloride solutions after 500 days. The addition of high concentrations (more than 15,000 ppm) of EDTA, a divalent metal ion complexing agent, prevented precipitation of the polyacrylamide from sea water. Major elements present in sea water are as follows,

Element	ppm
Cl	18,980
Na	10,562
Mg	1,272
S	884
Ca	400
K	380
Br	65
C	28
Sr	13

Precipitation was not prevented by the addition of 200 ppm of sodium dithionite oxygen scavenger. Davison and Mentzer [15] investigated the effect of temperature on polyacrylamide with a 31% degree of hydrolysis and found the polymer solutions unstable above 70°C (158°F).

The authors found a linear relationship existed between degree of hydrolysis and precipitation time for 1000 ppm polyacrylamide solutions in sea water at 90°C. The addition of Ca^{+2} and Mg^{+2} ions to clear polyacrylamide solutions in distilled water which were 43% and 65% hydrolyzed caused immediate precipitation. Davison and Mentzer propose that amide groups on the polyacrylamide molecules are hydrolyzed at higher temperatures to carboxylate groups which then can interact with divalent metal ions forming the insoluble salt. A 1% hydrolyzed 10,000 ppm polyacrylamide solution in distilled water and sealed in a glass ampoule at 90°C for 130 days released ammonia and the degree of hydrolysis of the polymer increased to 42%. The addition of calcium chloride to the clear solution gave a precipitate in which the calcium concentration corresponded to a 42% hydrolysis level as determined by titration.

M. H. Akstinat [1] tested about 340 different polymers of various classes for application in reservoirs of extremely high salinity (more than 165,000 ppm total dissolved solids) and high temperature (up to 80°C; 176°F). The polyacrylamides and partially hydrolyzed polyacrylamides were among the most difficult to dissolve. Fe^{+2} was found to cause coagulation of the polyacrylamide. The addition of small quantities of EDTA prevented the coagulation process. Akstinat requires that oxygen be eliminated from polyacrylamide solutions to prevent degradation. Dissolved carbon dioxide in his synthetic brine eliminated the need for reducing agents and stabilizers like sodium-dithionite, hydrazine hydrate, or thiourea.

R. D. Shupe [52] investigated the chemical stability of Dow Pusher 500, a partially hydrolyzed polyacrylamide, in Sundance field brine at 46°C (115°F). He tested the effects of some 15 different components present during field injection of the polymer solution. The field brine contained about 10 ppm hardness (6 ppm Ca^{+2} and 4 ppm Mg^{+2}) and 3,841 ppm total dissolved solids. Among the components tested for compatibility with the polymer solution were metals, ferrous and ferric iron salts, and oxygen. The thermal stability of the polymer solution was also evaluated. Stability of the polyacrylamide solution was determined by viscosity and screen factor measurements. Precipitation of the polyacrylamide from solution was not apparent for the salinity and temperature conditions tested.

Most investigators of the chemical stability of polyacrylamide solutions in highly saline brines and at high temperatures found this class of polymers unsuitable for polymer flooding application. High temperature and divalent metal ions (Ca^{+2}, Mg^{+2}, and Fe^{+2}), caused precipitation of the polyacrylamide solutions.

2.2.3 Polymer Rheology

Viscosity

The viscosity of a fluid is defined as the proportionality constant relating the force per unit area or shear stress and the velocity decrease with distance or shear rate for a fluid sheared between two parallel plates [2]. For a Newtonian fluid, the shear stress is directly proportional to the shear rate. For a non-Newtonian fluid, the viscosity is dependent on shear rate and is termed the apparent viscosity. Mungan [39] defines an apparent rela-

tive viscosity for polymer solutions as the ratio of the measured polymer viscosity to the measured solvent viscosity.

Burcik [6,5] reports that ionizable carboxylate, COONa, groups have a marked effect on the degree of coiling of the polymer molecules when they are dissolved in water. The degree of coiling determines the viscosity of the solution and is a function of molecular weight, acid-amide ratio, ionic strength, and pH.

Pseudoplaticity

Polymer molecules have been represented [60] as random statistical coils in solution. The coils are free to change configuration under an imposed shear force. The polymer solutions exhibit a shear thinning or pseudoplastic behavior.

Mungan [40,39,38] investigated the pseudoplastic behavior of polymer solutions of various polymer molecular weight, concentration, and brine salinity. Mungan discovered that higher molecular weight polymers had a higher viscosity and greater dependency on shear rate. Mungan [40] found increasing polymer concentration to increase apparent viscosity and polymer shear rate dependency. He related this effect to the size, shape, and interactions of the polymer molecules. Also at low shear rates [38], the polymer viscosity is highly dependent on molecular weight.

Salinity Effects

In the presence of an electrolyte such as sodium chloride, the electrostatic repulsion between carboxylate groups on the polymer molecule is shielded. The polymer coils change from a distended configuration to a spherical shape. Mungan [40,39,38] discovered that

the viscosity and shear rate dependency decreased as sodium chloride was added to the polymer solutions. Research performed on a 25 percent hydrolyzed polyacrylamide [38] showed sodium chloride to reduce polymer solution viscosity and pseudoplasticity; however, divalent ions affect both parameters to a greater extent. Gogarty [23] also found divalent cations have a stronger effect on reducing polymer viscosity than monovalent cations. Szabo [56] found that the addition of sodium tripolyphosate (STP), a sequestering agent, did not reduce the effect of calcium ion on the shear rate dependency of polymer.

pH Effects

Mungan [39] found that a lower solution pH gave lower apparent viscosity for polymer solutions. Sparlin [54] also found that increasing pH caused increased solution viscosity. Szabo [56] however, discovered pH had little effect on polymer viscosity over flow rate ranges encountered in most reservoirs. The control of solution pH was not considered important for fluids used in the experimental study discussed in this paper.

Pseudo-dilatency

Burcik [6,5] found that partially hydrolyzed polyacrylamides were dilatent during flow through porous media if the polymer was adsorbed or entraped. Dilatent materials increase in viscosity with increasing rate of shear. This behavior was not observed in straight capillary tubes. Also, Burcik reports the flow of polymer solutions of about 500 ppm concentration in brine is Newtonian.

Burcik calls this type flow in porous media pseudo dilatent flow. It occurs because the bound polymer molecules are opened or uncoiled under the imposed velocity gradients within the pore channels and more of the molecules uncoil as the pressure drop increases. Burcik suggests this behavior should increase the efficiency of a displacement process in non-homogeneous porous media and porous media having a range of pore sizes.

The flow rates employed by Burcik [5] were from 3.1 to 16.8 m/da (10 to 55 ft/da). Smith [53] discovered polymers were dilatent at rates of 3.1 m/da or greater.

2.2.4 Mobility Control

Nonuniform permeabilities in the vertical direction of the reservoir causes injected fluids to travel more rapidly through the more permeable zones. A measure of the uniformity of water invasion is the verical sweep efficiency, E_I, defined by Craig [13] as the cross-sectional area contacted by the injected fluid divided by the cross-sectional area enclosed in all layers behind the injected fluid front. The vertical sweep efficiency is a two-dimensional measure of the reservoir nonuniformities. The volumetric sweep efficiency, Ev, a three-dimensional measure of reservoir nonuniformities, is defined by Craig as the pore volume contacted by the injected fluid divided by the total pore volume of the pattern.

Darcy's law is used to describe the flow of fluids in porous media. The proportionality factor relating the velocity of a fluid to the pressure gradient in Darcy's law is the fluid mobility. The fluid mobility [13] is the effective permeability of the rock to that

fluid divided by the fluid viscosity. A mobility ratio, M, can be defined for two fluids as the ratio of the displacing fluid mobility to the displaced fluid mobility. It is the objective during the flooding of a reservoir to control fluid mobility and thus control the direction of movement of the fluids. Water-soluble polymers are added in low concentration to injection water to improve oil recovery by increasing reservoir sweep and displacement efficiency. D. J. Pye [46] and B. B. Sandiford [48] first introduced the use of polymeric additives to reduce the mobility, the ability to flow, of the water or brine during waterflooding processes and thereby lower the water-oil mobility ratio. Dilute polymer solutions have been used effectively to control the movement of fl enhanced oil recovery operations.

2.2.5 Mobility Reduction

Dilute solutions of polyacrylamide can improve oil recovery by reducing the water mobility. Mobility reduction is achieved by [14,23,4,39,53,62,41] increasing the solution viscosity and, more importantly, by reducing the effective permeability of the reservoir. Reduced mobility of injected fluids causes more efficient oil displacement and improved sweep efficiency of non-linear displacements. Maerker [33] and Smith [53] define mobility reduction as the ratio of prepolymer brine mobility to the mobility of the polymer solution. Maerker [33] describes mobility reduction as a viscoelastic effect caused by the increased normal stresses developed in the elongational flow pattern. Mungan [40] found the mobility reduction to depend on sodium chloride content, pH, capillary proper-

ties of the rock, and shear rate.

Gogarty [23] describes a three-step mechanism for permeability reduction. (1) During flow stabilization, polymer is retained by adsorption on the rock surface and mechanical entrapment at the smaller pore openings. (2) After flow stabilization, polymer solution flow takes place between pores through the larger openings. (3) Polymer solution stops flowing through the smaller openings between pores and the rock permeability is reduced. White [62] also attributes physical plugging to the mechanism of mobility reduction.

The geometry of the porous media has been found to affect the permeability reduction by polymer solutions. Pye [46] and Jennings [27] found permeability to be reduced by polymer solutions only in tortuous passages and not in straight capillaries. Jennings [27] found polymer effectiveness to decrease as the pore sizes increased. White [62] suggests the pore size, pore size distribution, and tortuosity affect the magnitude of the permeability reduction. Mungan [40] found permeability reduction greater in sintered glass discs of smaller pore openings. Smith [53] discovered a greater mobility and permeability reduction in lower permeability cores. Smith suggests, however, that pore size distribution and pore geometry of interconnections should be used to correlate polymer effects on porous media.

A measure of the effect of polymer solutions or mobility and permeability reduction are the resistance factor and residual resistance factor. Jennings [27] defines the resistance factor as the decrease in mobility of a polymer solution in comparison with the

flow of the water or brine in which it was prepared. The residual resistance factor is defined as the decrease in mobility of water that follows a polymer solution to water flow before the flow of the polymer solution. White [62] found polymer type, degree of hydrolysis, and concentration to control both resistance factor and residual resistance factor. Both factors are experimentally obtained by pressure measurements during polymer and brine flow.

2.2.6 Adsorption and Retention

Polymer retention is known to occur in porous media by adsorption, mechanical entrapment, and hydrodynamic retention [64]. Adsorption of polymer occurs due to the attraction the molecules have for a charged surface. As polymer solutions flow through the porous media, the molecules are mechanically entraped because of their large size in relation to the size of the pores. Gogarty [23] reports most polymer units are between 0.5 and 1.5 micrometers. Hydrodynamic retention is used to describe polymer retained due to a flow rate dependency. Dominguez and Willhite [17] saw polymer produced from a teflon core when the flow rate was reduced.

Meister [35] studied the effect of rock matrix on retention of polyacrylamide in Berea sandstone, Baker dolomite, and Georgia kaolinite. He attributed observed retention to (1) hydrodynamic retention, (2) entrapment, and (3) surface adsorption. (1) Hydrodynamic retention was caused by what Meister called a recirculation vortex created during flow which trapped the polymer molecules. The hydrodynamic effect was absent in dulute polymer solutions. (2) For Meister's floods, entrapment was plugging of the pores by the polymer

molecules. (3) Surface adsorption occurred by electrostatic attraction or coordinate bonds between the polymer molecules and the surface. Entrapment and surface adsorption were controlled by (a) the nature of the surface, (b) the polymer type, and (c) the solvent.

Meister [35] investigated the adsorption of unhydrolyzed polyacrylamide and hydrolyzed polyacrylamide on Baker dolomite and found the unhydrolyzed polymer adsorption to be 17 % and the hydrolyzed polymer adsorption to be 94.6 %. Meister attributed the higher adsorption of the anionic polyacrylamide to an attraction of the molecules for the net positively charged surface of the dolomite. Sparlin [54] also found anionic polyacrylamides to adsorb highly on calcium carbonate. In Meister's study [35], the surface charge and accessible surface area control retention.

Smith [53], Szabo [57], and Meister [35] found increased sodium chloride concentration caused increased polyacrylamide adsorption. Meister [35] attributed this effect to the brine becoming a less effective solvent as the salinity was increased. Mungan [39] reports on the other hand less adsorption out of brine solutions of the polymer than from distilled water solutions. According to Mungan, the NaCl satisfies charges on the surface and thus reduces adsorption. Smith [53] found a low concentration of calcium ion promoted the adsorption of polymer onto silica yet the effect was diminished by high NaCl concentrations. Smith visualized a competition between calcium and sodium ions for adsorption. A small amount of calcium ion (400 ppm) inreased the adsorption of a polyacrylamide of molecular weight of 3 million on calcium carbonate in a 10 % NaCl

brine. Smith suggests the addition of calcium ions lowered the solution pH and increased adsorption of hydrogen ions which in turn promoted polymer adsorption.

In static adsorption tests of partially hydrolyzed polyacrylamide on calcium carbonate and silica, Szabo [56,57] found adsorption to be significantly higher on the carbonate than on silica for the same surface area. Retention values in his carbonate packs were three times the adsorption values indicating mechanical entrapment to be the dominant retention mechanism. Sparlin [54] reports most of the permeability reduction in calcium carbonate packs was due to adsorption because average pore sizes were 16 micrometers; a size much larger than the size of polymer molecules.

2.2.7 Inaccessible Pore Volume

High molecular weight polymer molecules do not flow through all the connected pore space in reservoir rocks. Polymer molecules are large in size relative to solvent molecules and pore in the rock and cannot enter this portion of the pore space. In addition, some of the polymer molecules are retained due to adsorption and mechanical entrapment. This volume occupied by the polymer contributes to what is called the inaccessible pore volume.

Dawson and Lantz [16] measured inaccessible pore volume in consolidated sandstone to be 30 %. The inaccessible pore volume allowed changes in polymer concentration to be propagated through the porous media more rapidly than similar changes in salt concentration. Dawson and Lantz also found the inaccessible pore volume effect was opposed by adsorption of polymer on the rock.

Szabo [58] measured the inaccessible pore volume to polyacrylamide in consolidated sandstone and unconsolidated sand packs to be between 25 and 28 %. Dominguez and Willhite [17] used the method of Dawson and Lantz [16] to measure inaccessible pore volume in teflon cores and found it to be 19 %.

Shah, et al. [51] investigated the mechanism causing inaccessible pore volume. Inaccessible pore volume was found to decrease with increasing polymer concentration in Berea sandstone cores. It was proposed that inaccessible pore volume depends on molecular size, shape, and interactions with flowing and retained polymer. The hydrodynamic size of polymer coils is largest in dilute solutions and thus increases the amount of inaccessible pore volume. Also as the polymer concentration increases, the interactions between polymer coils increase. The net effect is to reduce the velocity of polymer coils and thereby reduce the effect of inaccessible pore volume on polymer velocity.

Jennings [27] found that polymer reduced the permeability of the rock yet did not reduce the effective pore volume.

2.3 Mechanical Degradation

Dilute polyacrylamide solutions are viscoelastic fluids which behave partially like viscous liquids at low rates of deformation and partially like elastic solids at high rates of deformation [33]. Polyacrylamides are composed of segments of randomly coiled, long-chain polymer molecules that are entangled with each other. The molecules are stretched as they move through contrictions in the pore space. If the stretch rate is large enough such that the time scale of deformation is

short and on the order of the natural relaxation time of the molecules, the entangled molecules do not have time to unravel. Large stresses build up until the polymer molecules rupture. This process is called mechanical or shear degradation. Seright [50] describes mechanical degradation to occur when fluid stresses become large enough to fragment the polymer molecules resulting in an irreversible loss of viscosity and resistance factor.

Maerker [33] investigated the cause of mechanical degradation of dilute polymer solutions by studying the effects of polymer concentration, water salinity, permeability, flow rate, and flow distance in consolidated sandstone. Maerker found that mechanical degradation became more severe with larger fluxes, longer dimensionless flow distances, and lower brine permeabilities. Maerker described these effects using a correlation based, in part, on a theoretical viscoelastic fluid model and an analysis of the deformation of the polymer molecules in porous media.

Maerker [32] extended his previous work [33] to include mechanical degradation in unconsolidated sand packs. Maerker studied the effects of porosity, permeability, length, and flow rate on mechanical degradation of partially hydrolyzed polyacrylamides in sand packs. He found that mechanical degradation became more severe with larger fluxes, longer dimensionless flow distances, lower porosities, and lower brine permeabilities. Maerker's improved correlating group showed that degradation correlates with porosity by a power law.

Morris [37] studied mechanical degradation in sandstone plugs and sandpacks. He found that polymer shear degradation can be correlated by

plotting percent loss in screen factor versus the stretch rate times the dimensionless flow distance raised to the M^{th} power where M is the average polymer molecular weight divided by 107. The screen factor is defined by Jennings [27] as the ratio of flow time of polymer solution to flow time of solvent in a screen viscometer. A typical screen viscometer [28] has a pack of five 100-mesh stainless steel screens. Morris [37] found M to be independent of concentration from 500 to 2000 ppm. Mechanical degradation was dependent on concentration, with the higher concentrated polymer solution exhibiting the least degradation.

Smith [53] tested the effect of calcium ion on the flow of partially hydrolyzed polyacrylamide solutions. Calcium lowered the effectiveness of the polymer and caused further degradation at high rates. According to Smith, the calcium ion reduced the polymer solution viscosity and permitted higher flow rates and thus increased mechanical degradation.

Sparlin [54] found polyacrylamides to be shear sensitive. He discovered however, that shearing of the polymer solution did not affect the ability of the polymer to alter permeability.

2.4 Carbonate Rocks

2.4.1 General Description

Three main types of rocks, each formed in a different way, are igneous, sedimentary, and metamorphic rocks [59]. Sedimentary rocks, rocks most common in Kansas, are formed by the wearing down of other pre-existing rocks into small particles or sediment and by the later deposition, compaction, and cementation of these particles. Car-

bonate rocks and sandstone or quartz based rocks form the two major types of sedimentary rocks.

Carbonate rocks, so named because of the presence of carbonate ion, CO_3^-, usually originate from marine deposits consisting mainly of animal shells. These rocks have a very complex structure composed of many carbonate minerals. Three minerals found in most abundance are calcite, aragonite, and dolomite. Calcite and aragonite are both composed of calcium carbonate or $CaCO_3$. Calcite crystals are hexagonal while aragonite crystals are orthorhombic. Dolomite is composed of the mineral dolomite or $CaMg(CO_3)_2$. Calcite can also form the cement material in sandstones as well as carbonate rocks. Crystals of aragonite occur as radiating groups of fibrous or needle-like shapes. The white pearly layer found inside many sea shells is aragonite. Aragonite is usually the original form of calcium carbonate deposited but is easily dissolved and later converted to the more stable form of calcite. Dolomite crystals are rhomb-shaped having curved surfaces and usually result from the dissolution of calcite with the subsequent precipitation of dolomite. This process known as dolomitization [11] can occur according to the reaction

$$2CaCO_3 + Mg^{++} \rightarrow CaMg(CO_3)_2 + Ca^{++}$$

Dolomites are light colored and fine-to-coarse grained rocks. Pure dolomite [11] is composed of 45.7% $MgCO_3$ and 54.3% $CaCO_3$. Some dolomite rocks are formed by wave action on older dolomites. Other carbonate minerals present include magnesite, $MgCO_3$, ankerite, (Ca, Mg, Fe)CO_3, siderite, $FeCO_3$, rhodocrosite, $MnCO_3$, and smithsonite,

$ZnCO_3$ [63].

Until now, rocks of the nature described above have been referred to as carbonate rocks. In the litrature, authors have used the terms limestone and carbonate rock interchangeably to name this type of sedimentary rock. Much of the confusion in nomenclature may have resulted from the very complex composition and nature of these rocks. A limestone is defined in the Dictionary of Geology [63] as "any sedimentary rock consisting essentially of carbonates and composed mostly of calcite, dolomite, and small amounts of iron-bearing carbonates."

Both Feray and Whitten [20,63] describe limestones as rocks consisting of calcite, aragonite, and magnesium-calcium carbonate or dolomite. The distinction has also been made classifying limestone and dolomite as compositional divisions of carbonate rocks [11,24,25,30]. Limestone, then, is composed of 50% or more of carbonate minerals with most of these minerals being calcite and aragonite. An abundance of the mineral dolomite, 50% or more, would classify the rock as a dolomite as proposed by Chilingar and Horowitz [11,25]. Limestones have been classified [63] into three groups; 1) organic, 2) chemical, and 3) detrital or clastic. Organic limestones consist of the skeletal remains of organisms which secreted calcium carbonate. Limestones of the second group were formed by chemical precipitation of dissolved calcium carbonate. Whitten [63] defines clastic limestones as "mechanically deposited carbonate rocks made up essentially of fragments of organic carbonate or a pre-existing limestone rock".

The uncertainty of what constitutes a limestone, dolomite, or carbonate still remains. In many uses the differences are subtle. Therefore, for the purpose of this paper in classifying these rocks, a limestone is defined to contain mostly c a dolomite mostly the mineral dolomite. Both limestones and dolomites constitute the general class of rocks composed of carbonate minerals and called carbonate rocks.

2.4.2 Classification of Carbonates

Carbonate rocks are extremely complex because initial depositional patterns are complicated and varied and because post-depositional processes can extensively alter porosity and permeability. Many systems have been devised to classify this large group of sedimentary rocks. Most of these classification systems, as proposed by Horowitz [25], involve four fundamental building blocks for carbonate rocks, the 1) framework, 2) mud, 3) cement and 4) pores. The framework, also called the skeleton or grains of the rock, is made up of discrete particles of sediment. The mud or lime mud refers to the small, silt-sized particles filling any void space in the rock. The term matrix has been used for mud when it fills the interstices between larger grains [29]. Chemically precipitated cement, most often calcite, cements grains together and fills in void space by crystal growth. The pores of the rock are openings remaining between the rigid framework and can be partially or totally connected. These pores and pore connections constitute the pore system or porosity of the rock and account for the ability of the

rock to store and transmit fluids. Classification systems for carbonates are divided into two groups; systems based on rock classification and those based on porosity classification.

Rock Classification

The most widely used carbonate rock classification systems are those of R. L. Folk [21,22] and R. J. Dunham [19]. Folk's classification is based on the nature of the limestone matrix and on the types of particles present. Folk's system of classification groups carbonate constituents into three main groups; 1) allochems, 2) carbonate mud, and 3) sparry calcite cement. Allochems are the framework particles of the rock and include shells, oolites, and carbonate pellets. Oolites are spherical to elliptical coated grains less than 2 mm in diameter and formed by chemical precipitation of calcite around a nucleus. Pellets are silt-sized (0.04 to 0.08 mm [22]) grains of micrite or mud. The carbonate mud, also called microcrystalline ooze or micrite, is the clay-size (1 to 6 mm [22]) matrix consisting of fine detrital or clastic organic fragments and chemical precipitates. Mud is present in carbonates deposited in a low energy environment (low currents). The sparry calcite cement fills the pore space and cements the carbonate grains together. Folk also classifies clastic limestones according to particle size using the following nomenclature and scale.

calcirudites - 2 mm and above

calcarenites - 0.0625 to 2 mm

calcilulites - less than 0.0625 mm

Dunham's system of carbonate rock classification [19] defines class names based on depositional texture. Four major groups defined for detrital carbonates are defined according to the relative proportions of grains to lime mud or matrix and depending on whether the grains are in contact with one another (grain-supported) or not (mud-supported). They are mudstone, wackestone, packstone, and grainstone. Mudstone is carbonate rock composed of carbonate mud with less than 10% grains and is originally deposited in a calm environment. Wackestone is a mud-supported carbonate rock containing more than 10% grains. Packstone is a grain-supported carbonate rock with a carbonate mud matrix. Grainstone is a mud-free carbonate rock which is grain-supported. Dunham, through this system of rock classification, has attempted to describe the distribution and origin of porosity in carbonates.

Porosity Classification

The word pore, derived from the Greek word "poros" meaning passageway, refers to the local enlargements in the void space of the rock [12]. Pore throats are the constricted openings which serve as the pore interconnections. These pores and pore throats constitute what is called the pore system of the rock. The pores, according to Choquette [12], constitute most of the porosity and fluid storage volume of the rock while the pore throats control rock permeability. He defines three classes of regular pore shapes; 1) micropores, 2) mesopores, and 3) megapores. The size classification of these pores is as follows.

micropores - less than 0.0625 mm

- mesopores - 0.0625 to 4 mm
- megapores - 4 to 256 mm

The size, shape, and distribution of the pores can be described by macroscopic and microscopic visual observation. The pore throats are difficult to visualize but can be measured quantitatively by capillary pressure techniques. The porosity encompasses all openings in the mineral framework of the rock [12]. The porosity also has been referred to as the pore system and includes fractures as well. Primary and secondary porosity are two types found in carbonate rocks. Primary porosity includes all pore space present after final deposition while secondary porosity refers to porosity created after deposition as defined by Choquette [12]. Solution vugs ,defined below, and fractures are two common types of secondary porosity.

A widely used system of porosity classification for carbonates is that of P.W. Choquette and L.C. Pray [12]. Choquette and Pray classify porosity according to size, shape, and distribution of pores. Their genetically oriented system defines 15 porosity types; seven of which are most abundant in carbonate rocks. These seven types are 1) interparticle, 2) intraparticle, 3) intercrystal, 4) moldic, 5) fenestral, 6) fracture, and 7) vug porosity. Interparticle is porosity between the individual particles or grains. Intergranular porosity is often used synonymously with interparticle porosity. Choquette suggests that the grains in intergranular carbonate rocks be coarse (0.004 to 0.06 mm). Interparticle porosity, as preferred by Choquette, has no lower or upper size limitations.

Intraparticle porosity is porosity within the individual particles or grains and is abundant in carbonate rocks. Intercrystal porosity is porosity between crystals as found in many porous dolomites. Fenestral porosity consists of openings larger than the grain-supported interstices. Fracture porosity is formed by fracturing or cracking of the rock and is one common type of secondary porosity found in carbonates. Vugs are void spaces in the rock created by dissolution of the carbonated material. These types of porosity are shown in Figure 3.2. Most porosity in sedimentary carbonates is related to the diagenetic or sedimentary components which constitute the texture or fabric of the rock. Choquette terms this fabric selective porosity and is the type found in most carbonate producing reservoir rocks [12].

2.4.3 Carbonate Pore Geometry

The pore system of a rock comprises all void space within the mineral framework of the sediment [12]. As described above, the pore system of carbonates can be extremely heterogeneous [26] consisting of vugs and fractures in addition to the interstices between the carbonate grains. The porosity and permeability are two quantitative parameters used to characterize the rock. However, in carbonates, porosity and permeability alone may prove inadequate for a description of the fluid flow behavior in the pore system. Information about the size distribution and shape of the pores and pore throats is necessary. This information can be obtained by studying the pore geometry through the use of pore casts, pore-cast thin sections, and mercury porosimetry.

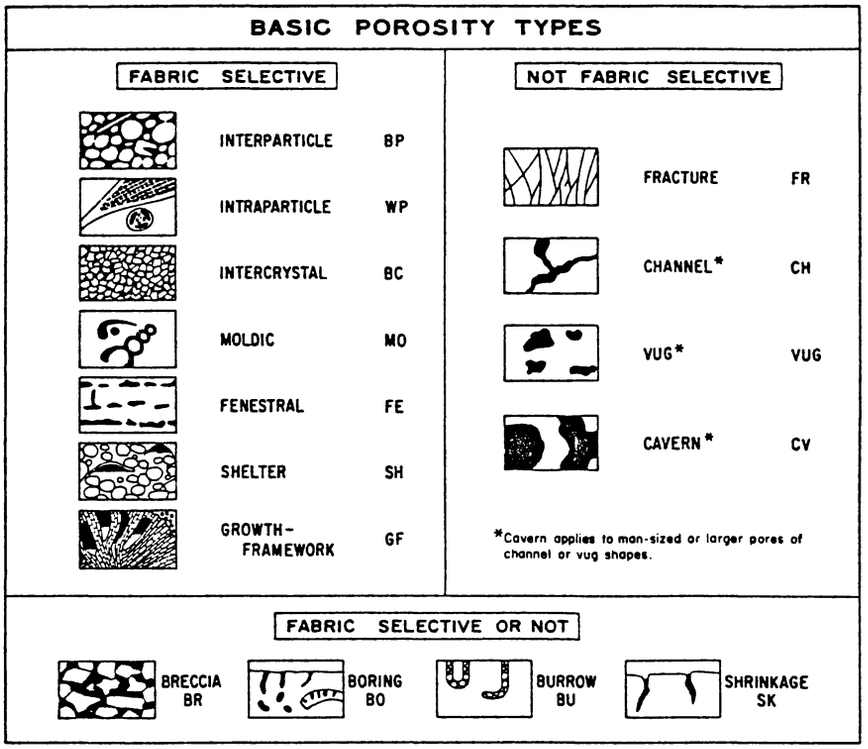

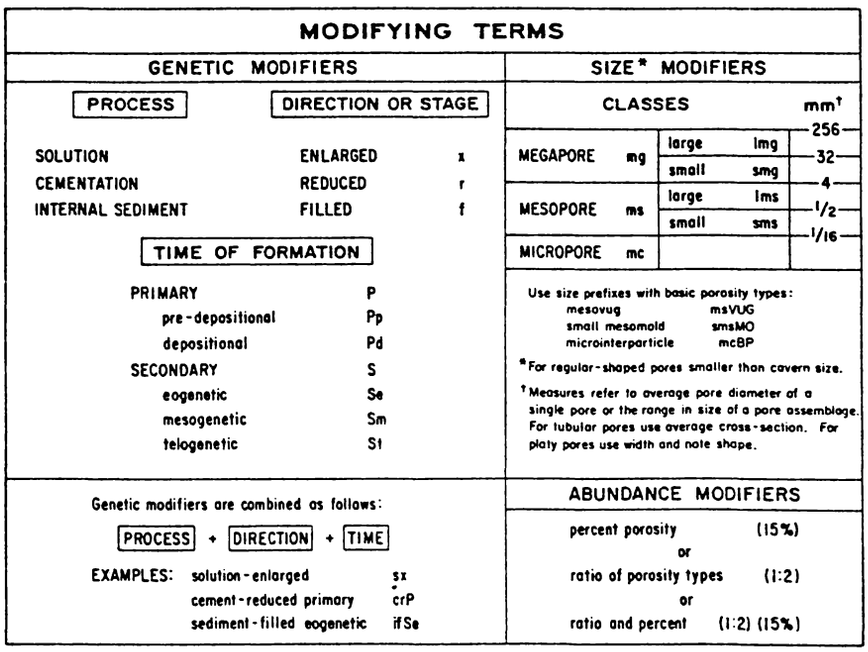

Figure 3.2 Porosity Classification of Choquette and Pray [12].

Pore casts of carbonate rock are replicas of the void space in the rock formed by impregnation of the rock with colored plastic [43,42,61] or Wood's metal [55] and by the subsequent dissolution of the rock matrix with dilute hydrochloric acid (15%). Pore-cast thin sections are mounted thin section slides prepared with colored epoxy impregnated rock. The rock is dissolved with dilute hydrochloric acid leaving a replica of the pore space. Both the pore casts and pore-cast thin sections can be examined with binocular, petrographic, or scanning electron microscopes.

Pittman et al. [43,44] realized the difficulty of visualizing the void space beyond the surface of the rock. These investigators found the scanning electron microscope (SEM) instrumental in viewing a three-dimensional image of the pore structure with larger magnification and greater depth of field than possible with conventional light microscopes. Samples of the rock are easily prepared and examined without destruction. A discussion of the operating principles of the SEM is presented by J. T. Black [3] and is not discussed herein.

Pittman [42] discovered the existence of a bimodal distribution of pore sizes in carbonate rocks. The larger pores, the macropores, and pore throats, formed intergranular and moldic porosity. The micropores, pores much smaller in size, formed intercrystalline or intraparticle porosity. These porosity types, defined earlier, follow Choquette and Pray's [12] system of porosity nomenclature. Micropores, as defined by Pittman, are pores and pore throats existing in the microcrystalline carbonate or micrite with a tabular

shape 1 micrometer or less in size [42] or as pore apertures with a radius of less than 0.5 micrometers [44]. These micropores were not visible until examined with the SEM at high magnification. Pittman [42] postulates that micropores in water wet rocks retain irreducible water not available for fluid flow.

Swanson [55] also discovered the dual size of pores in dolomite using Wood's metal* at low and high saturations. Pores filled at a low capillary pressure, thus low metal saturation (12%), were found to be tubular in shape. Pores filled at a high capillary pressure and metal saturation (87%), were found to be much smaller in size and very poorly connected.

Wardlaw [61] discovered many of the pore connections in dolomites to be sheet-like in shape rather than tubular. Wardlaw attributed this pore connection configuration to the transformation of polyhedral pores to tetrahedral pores to finally these inter-boundary sheet pores during dolomite crystal growth. Tetrahedral pores were found to be common in low porosity dolomites with the separation in the sheet pores measured to be 0.1 to 4 micrometers (2 micrometers average) both from pore casts and capillary pressure determination.

The pore structure of carbonate rocks is a complicated network of various sized openings. By porosity measurements the total void volume of the rock is obtained and by permeability measurement the extent of interconnection between pores can be determined. The limiting size of the connecting throats between pores can be measured by capillary pressure techniques.

Bismuth, lead, tin, and cadmium alloy with a melting point of 70 °C.

Two methods used to construct capillary pressure curves are the mercury injection method and the centrifuge method as described by Chilingar [11]. Mercury injection has been the preferred method for study of the pore geometry in carbonates. Early investigators of this method include Ritter, Drake, and Purcell [47,18,45]. Mercury porosimetry has been used both to obtain average pore throat radii and pore size distributions within the rock. Apparatus and procedures for obtaining the measurements are described by both Ritter and Purcell [47,45]. Ritter and Drake [47] define two ranges of pore size distribution in porous materials (not carbonates) based on radii of the pore throats. Micropores have radii less than 100 angstroms (0.01 micrometers); macropores have radii greater than 100 angstroms. Their radii calculations are based upon the capillary pressure relationship for intrusion of a non-wetting phase into circular constrictions as follows,

$$Pc(r) = -2\sigma \cos(\theta)$$

where

Pc = capillary pressure

σ = non-wetting phase surface tension

r = tube radius

θ = contact angle measured through the wetting phase

Wardlaw [61] modified this same equation for sheet pores by considering the separation of two plates to be half the pore diameter or equal to the radius defined above. This modification would yield pore "diameters" half the size of those computed for tubular pore

connections. Meister [34] reports a capillary pressure curve and pore size distribution for Baker dolomite without reference to techniques or procedures used. He reports the bulk of the dolomite being accessed by pores with neck diameters of 0.5 to 5 micrometers and 86% of the surface area being accessed through pore necks of 10^{-3} micrometers or less.

In addition to indicating the pore throat size, the shape of the capillary pressure curve will indicate the sorting and skewness of the pore throat size in carbonate rocks [11]. Sorting is a measure of the degree of spread from the finest to the largest pores. A well-sorted pore arrangement indicates that the primary sediments have undergone winnowing (weathering) or that the rock has been dolomitized. The skewness is the grouping of pores into a particle size fraction. A fine skewness indicates a fine compact crystalline matrix while a coarse skewness indicates vuggy porosity.

CHAPTER 3

Experimental Program

3.1 Introduction

The purpose of the experimental program was to investigate various aspects of polymer flow which govern the use of water-soluble polymers as mobility control agents in enhanced-oil recovery operations in carbonate rocks. Previous experimental work was discussed (Chapter 2) which involved studies of polymer behavior in sandstone rocks. Many aspects of polymer flooding observed in sandstones have direct application to carbonate rocks. Therefore, much of this previous experimental work in sandstones was used as a guide in developing the experimental studies in carbonate rocks.

The experimental program to study polymer behavior in carbonate rocks was divided into three phases. Phase I involved both the selection of carbonate reservoir core material and polymer for use in the fluid flow experiments. In Phase II, cores were assembled and flooded to determine both the resistance factor and residual resistance factor of the core to the polymer. Phase III concerned an in-depth study of the petrographic aspects of carbonate rocks using thin sectioning, scanning electron microscopy (SEM), and mercury porosimetry techniques. The experimental technique used in each phase of the research program is described in this chapter. The experimental results and conclusions are presented in Chapters 4 and 5.

3.2 Phase I. Preliminary Testing

3.2.1 Core Selection

Frequently in enhanced oil recovery research, fluid flow experiments are carried out on rock samples taken from the reservoir in an attempt to model the actual fluid flow behavior in the reservoir. A reservoir core, as the rock sample is called, is obtained during the drilling of an oil well. The reservoir core is drilled in the vertical direction and ranges in diameter from 10 to 15 cm (4 to 6 in). Laboratory cores are drilled in a perpendicular direction from the reservoir cores as shown in Figure 3.1. In the laboratory, reservoir conditions can then be modeled on a very small scale. The effects of rock heterogeneities become pronounced due to the small sample size and random selection technique. It is desirable to perform floods in a standard rock of uniform porosity and permeability, for comparison purposes. To date, Berea sandstone*, known for its uniform properties, is commonly used as a core flood standard for enhanced oil recovery experiments in sandstone rocks. No standard material exists for similar experiments in carbonate rocks.

Investigation of several sources of carbonate materials revealed a pure dolomite quarried by the J. E. Baker Co.** The dolomite comes from the Guelph formation, Niagaran Series, Silurian System and is finely crystalline and light colored in nature. The dolomite is thin-bedded and brittle yet porous and permeable (porosity 20%; per-

---

* Quarried by Cleveland Quarries in Amherst, Ohio.

Located in an isolated area of the West Quarry in Millersville, Ohio.

meability 100 to 300 md). The dolomite quarry material was obtained in blocks approximately 30 cm x 15 cm x 15 cm. Fluid flow experiments, similar to those performed in the actual reservoir rock samples, were performed in this material and the results compared.

A large amount of the oil in place in Kansas exists in rocks of the Lansing and Kansas City Group, part of the upper Missourian Stage in the Upper Pennsylvanian Series. Because this work could be coordinated with on-going geologic research projects at the University and because Kansas oil-producing companies are interested in using polymer flooding techniques in this zone of oil-bearing formation, the Lansing and Kansas City Group was chosen for study. Reservoir cores used in this project were obtained from three Kansas locations.

Stanolind Oil and Gas Company*, Number 3 Denker well, NE NW SW, section 10, T 22S, R 12W, Max oil field, Stafford County, Kansas.

Murfin Drilling Co., Souchek Number 1 well, 150' SE of C-SE-NE, section 2, T 15, R 34W, Rawlins County, Kansas.

Husky Oil Co., Brooks Number 6 well, Red Willow County, Nebraska.

Each reservoir core was examined for rock material which might have suitable porosity and permeability for core flooding. Oil staining of the rock and a grain-supported matrix (explained in

---

Now Pan American Petroleum Corporation.

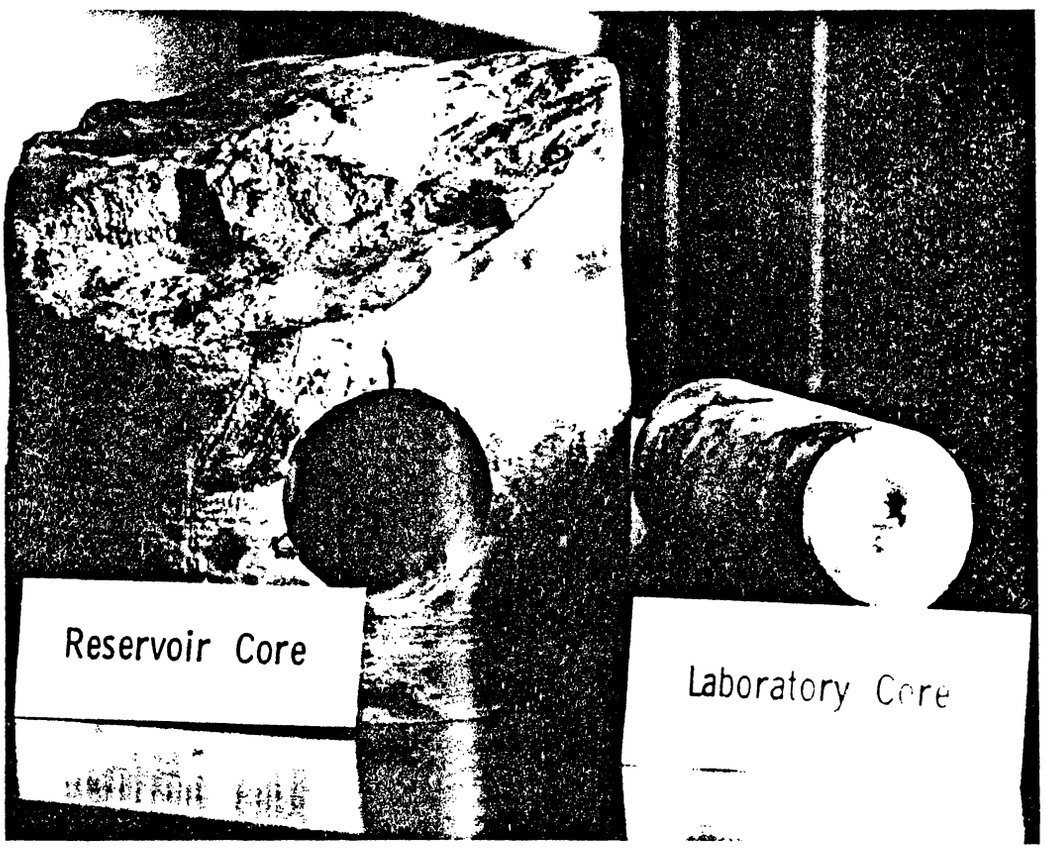

Figure 3.1 Reservoir and Laboratory Core Configuration.

Chapter 2) were two visual indications of good potential flood material. Plugs 1.91 cm (0.75 in) in diameter and approximately 2.54 cm (1 in) long were cut in the direction of the bedding plane from the reservoir core using a diamond core drill. Tap water was used both as a coolant and as a cutting lubricant. The plugs were placed in a Soxhlet extraction apparatus using tetralin* as the cleaning solvent. The plugs were extracted for periods ranging from 12 hours up to 3 days. Long periods of cleaning time were required for cores of low permeability. The cores were assumed to be clean when solvent surrounding the core plugs remained clear. The plugs were dried in a vacuum oven at approximately 85°C (185°F). The plugs were cooled to room temperature, dimensions were recorded, and air permeabilities were measured using a Ruska air permeameter by the procedure described in Appendix B.

The porosities of the plugs were measured by a gravimetric procedure. The dry core plugs were weighed on a Mettler triple beam balance. The plugs were placed in a vacuum flask connected to both a vacuum source and supply of distilled water. The plugs were evacuated to about 100 micrometers of mercury (0.1mm Hg) and the vacuum source was isolated from the system. Water was introduced into the vacuum flask to completely cover the plugs and fill the flask. The plugs were removed from the flask and a short thread was tied around each plug. The plugs were suspended from the center pan support of the Mettler balance and weighed both in air and in a beaker of distilled water to determine the bulk and buoyant weights. The

---

* 1,2,3,4-tetrahydro-naphthalene; BP = 207.2°C

ratio of these weights was used to calculate plug porosities.

3.2.2 Polymer Screening

Two types of polymers currently being used as mobility control agents in enhanced oil recovery processes in the field are the synthetically manufactured polyacrylamides and the biologically produced polysaccharides or biopolymers. The polyacrylamides offer distinct advantages over the biopolymers for field application as discussed in Chapter 2 and were investigated for use in the core flood experiments. Two criteria used for selection were that the polymer be commercially available and that it be compatible with salinities encountered in Kansas reservoirs; specifically salinities encountered in areas from which the reservoir core samples were taken. A listing* of ion concentrations in Kansas reservoir brines produced from the Lansing and Kansas City Groups was examined. The highest levels of sodium, calcium, and magnesium ions were selected for brine solution preparation used to test compatibility with the various polyacrylamides. A listing of these ion levels by County is given in Table 3.1.

Compatibility between polymer and brine was assumed if upon mixing, the solution remained clear for a period of one week; the duration of the longest flow test. Liquid polymers, all turbid when mixed, were centrifuged for eight hours to settle any precipitate formed. Samples of the polymer solutions were also tested for longer periods of time.

---

* Compiled by the Operations Research Section of the Kansas Geological Survey (KGS) at the University of Kansas.

Table 3.1 Cation Concentrations for Brines Produced from Lansing and Kansas City Group in Kansas by County.

COUNTY	Na CONCENTRATION (ppm)	Ca CONCENTRATION (ppm)	Mg CONCENTRATION (ppm)
Barber	--	13,000	4,500
Barton	56,000	13,000	3,500
Butler	60,000	10,000	3,700
Clark	50,000	12,000	2,800
Comanche	--	12,000	1,800
Decatur	42,000	32,000	14,000
Ellis	59,000	16,000	4,000
Graham	55,000	5,000	2,500
Harper	--	16,000	1,700
Kingman	43,000	16,000	5,000
Kiowa	69,000	12,000	2,400
Lyon	20,000	4,000	1,500
McPherson	60,000	15,000	5,000
Meade	65,000	10,000	2,500
Pawnee	45,000	7,000	2,000
Phillips	40,000	3,000	1,200
Pratt	80,000	17,000	4,000
Rawlins	--	1,700	500
Reno	78,000	17,000	4,500
Rice	54,000	12,000	4,000
Rooks	70,000	9,000	3,000
Rush	30,000	5,000	1,100
Russell	54,000	25,000	5,000
Scott	29,000	1,400	500
Sedgwick	75,000	12,000	5,000
Seward	88,000	10,000	2,600
Sheridan	33,000	2,500	700
Sherman	--	1,300	100
Stafford	60,000	14,000	5,000
Sumner	65,000	10,000	2,800
Trego	62,000	12,000	1,600

The mixing procedure for both the solid polyacrylamides and polyacrylamides in the emulsion or liquid form are given in Appendix A. In the usual polymer mixing procedures, polymer is added to the brine. Some of the solid polyacrylamides were determined incompatible with the brine because of observed precipitate formation. For these polymers, the solid polyacrylamide was first dissolved in distilled water and then the solid salts were added to this solution to form the final polymer mixture.

Mixtures found to be compatible for at least a one week period were prepared for long-term testing in a relatively oxygen-free environment and at an elevated temperature of 43.3°C (110°F). The polymer solution was purged of oxygen by bubbling nitrogen through the solution for about 3 minutes*. Disposable pipettes sealed on the bottom end with a glass blowing torch were purged for several minutes with nitrogen to exclude the air. Approximately 10 cc of the polymer solution was added to the sealed tube and the top end was sealed by fusing the glass with a torch. The tubes were placed in a vertical position in a constant temperature water bath maintained at 43.3°C (110°F). The polymer-brine screening tests indicated suitable polymers for flooding and fluid flow tests were pursued.

3.3 Fluid Flow Experiments

The main part of the research program involved fluid flow tests on the selected carbonate materials. The preliminary porosity and permeability measurements indicated potentially good core material for

---

Used only to reduce the oxygen level to an unknown, yet smaller value.

these flood tests. Presented in this section is a description of the fluid flow experiments which were conducted. suitable polymers for flooding.

3.3.1 Core Flooding Apparatus

The experimental apparatus used to conduct the fluid flow experiments in the core material is shown in Figures 3.2 and 3.3. A positive displacement pump was used to displace injection fluids from the transfer cylinders into the core flood cell. Pressure drops along the length of the core were monitored using diaphram pressure transducers. Voltages measured from the transducers were collected and stored on permanent disc files on a minicomputer.

3.3.2 Flood Cell Design

A core flood cell was designed to hold consolidated core samples for the fluid flow experiments. The holder consists of Schedule 80 PVC (polyvinylchloride) pipe nipples 3.81 cm (1.5 in) in diameter and 7.62 cm (3 in) and 10.16 cm (4 in) long depending on core length. End plates, 1.27 cm (0.5 in) thick, were bolted on to the core assembly after the core was encapsulated in the PVC pipe. The core assembly is shown in Figure 3.4.

3.3.3 Core Preparation

Laboratory cores* 2.54 cm (1 in) in diameter were drilled in the direction of the bedding plane out of the reservoir core from areas which indicated good porosity and permeability (15 to 30 % porosity;

---

* The laboratory cores will be referred to simply as cores henceforth.

20 to 100 md permeability). Similar laboratory cores were cut from the dolomite quarry material. The length of these lab cores was restricted by either the diameter of the reservoir core or by the length of the core drill. This length ranged from 5 to 10 cm (2 to 4 in). Again, tap water was used for the cutting process. The cores cut from the reservoir material were cleaned by the same procedure used for the core plugs as described in the preliminary phase of the experimental work. The dolomite quarry material was not cleaned but was only dried in a vacuum oven at 85°C (185°F).

Triangular spacers were cut from 0.16 cm (1/16 in) Plexiglas and were epoxied* to the ends of the cores as shown in Figure 3.5. The core was coated with epoxy** and allowed to set and dry. One end of the pipe nipple was closed by glueing a sheet of 0.16 cm (1/16 in) Plexiglas to it. Epoxy was poured into the nipple to about half full and the core was inserted. Additional epoxy was added if necessary to cover the core. After hardening overnight, the core assembly was machined in a lathe to expose both faces of the core. A flat was machined on one side of the core assembly to accept a pressure tap boss. The pressure tap boss was glued onto the side of the core assembly according to directions for using PVC pipe cement (cleaning, priming, and glueing). The core assembly was clamped in a bench vice and allowed to dry.

---

* EASYPOXY manufactured by Conap, Inc., Olean, New York.

** STYCAST 2850 GT epoxy casting resin plus 3.3% CATALYST 9 both manufactured by Emerson & Cuming, Inc., Canton, Massachusetts 02021.

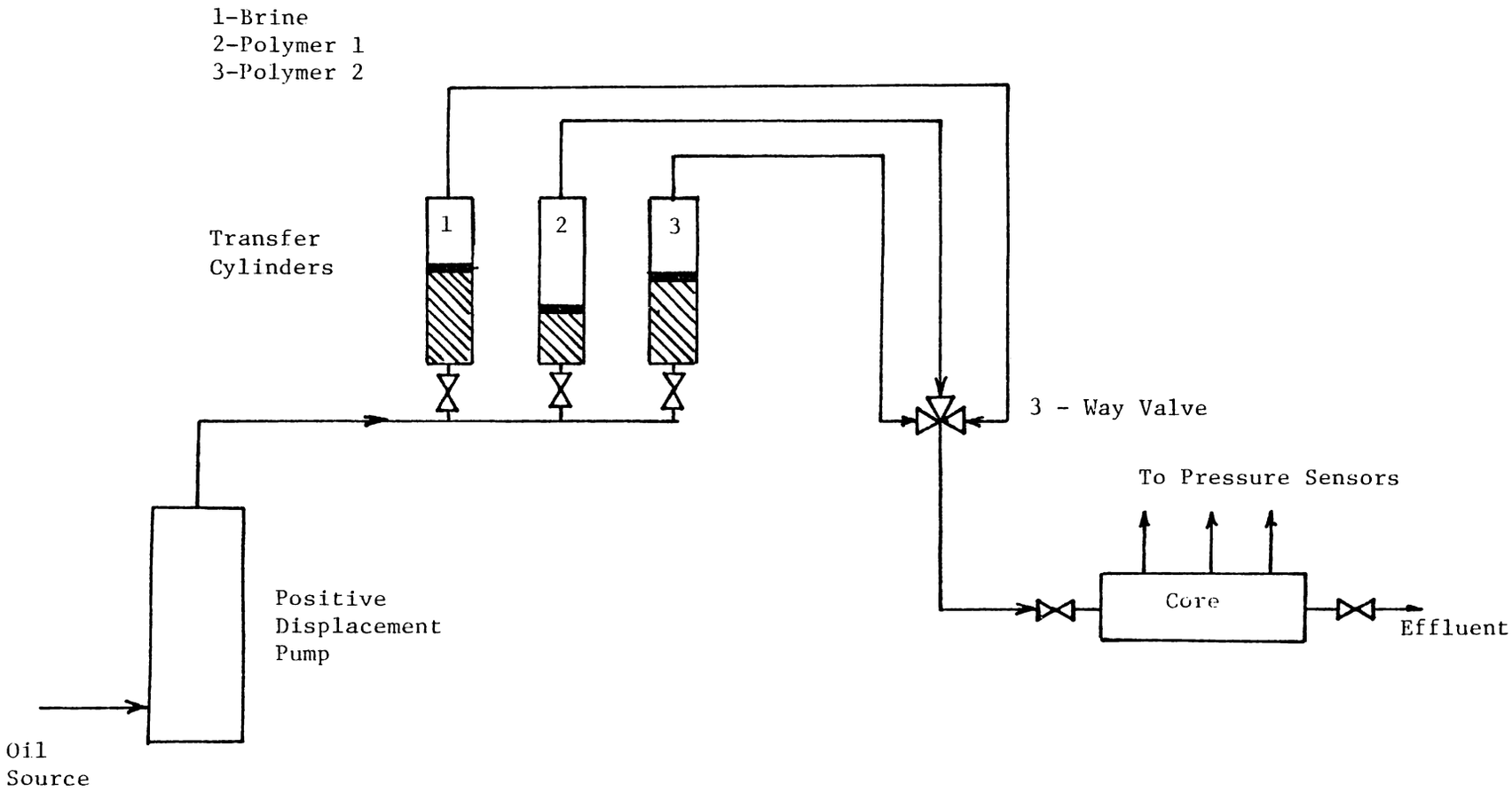

Figure 3.2 Schematic Diagram of Laboratory Core Flood Apparatus.

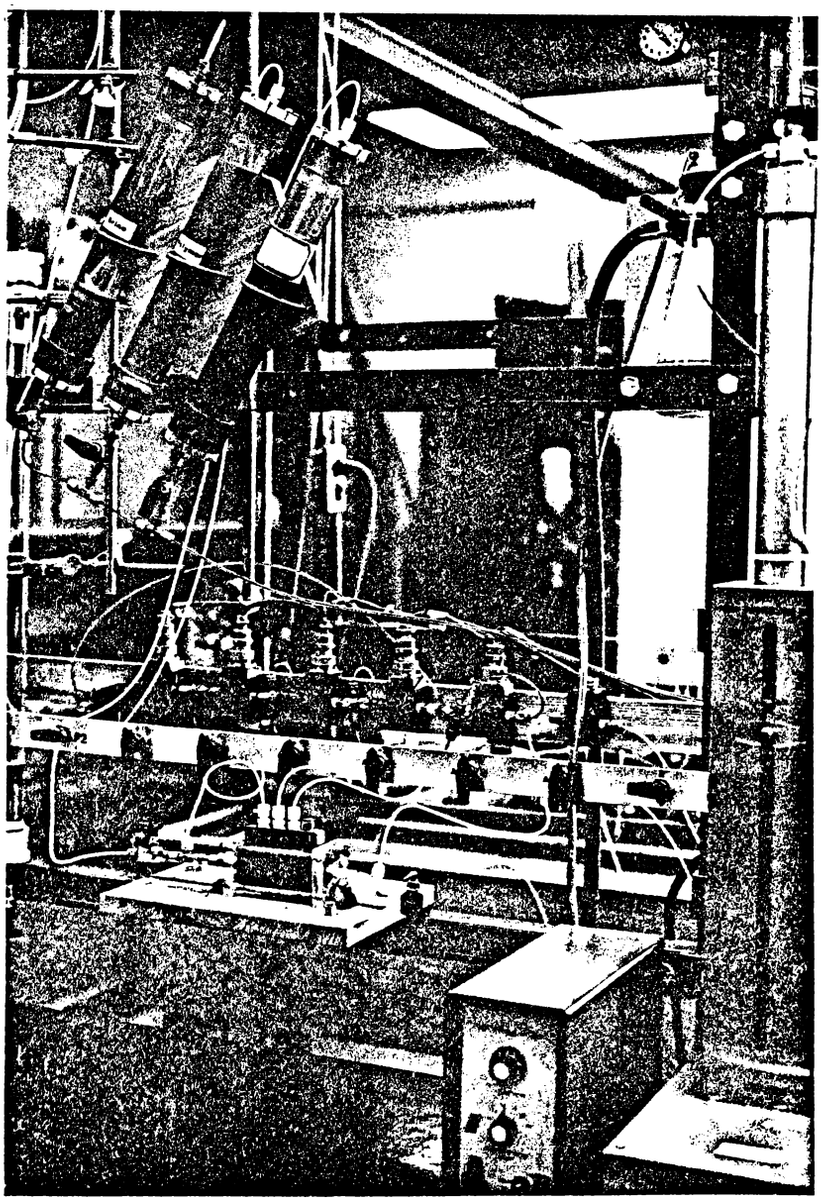

Figure 3.3 Laboratory Core Flood Experimental Apparatus.

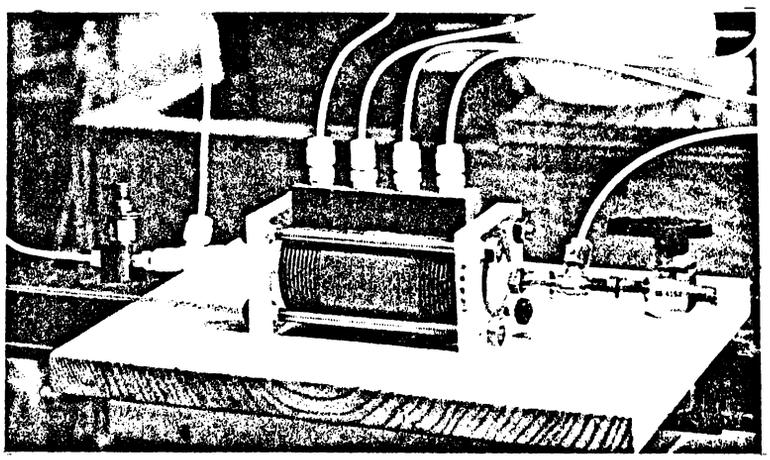

Figure 3.4 Laboratory Core Flood Cell.

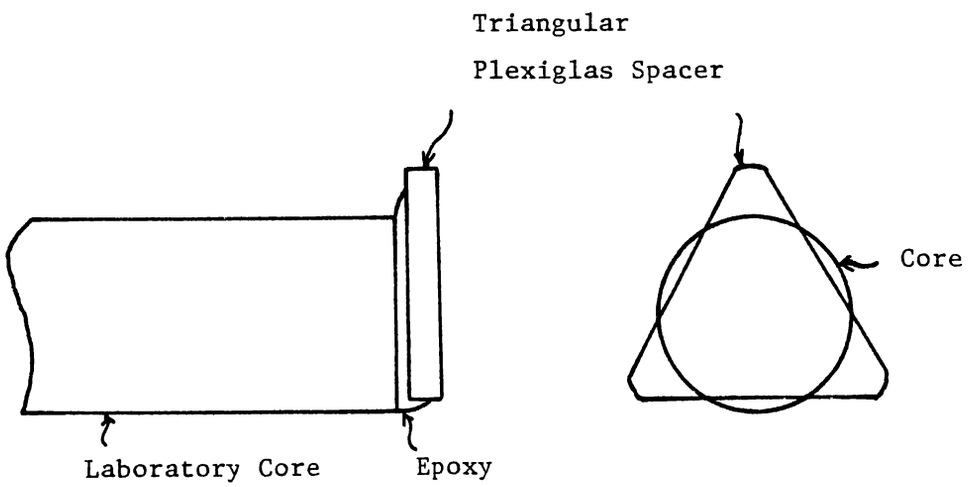

Figure 3.5 Preparation of Core for Encapsulation.

Prior to flood tests, the absolute permeability of the core to gas was determined by flowing air through the core and measuring pressure drop and flow rate. The calculation of the absolute air permeability is given in appendix B. To measure the porosity, the core was first saturated with carbon dioxide and then evacuated from 30 minutes to 1 hour. Distilled water at 480 kPa (70 psi) was introduced to saturate the core, and water was flowed for approximately 5 pore volumes. Dry weight and wet weight measurements were used to determine the pore volume and porosity of the core. The core was dried in a vacuum oven at 85°C (185°F). Holes were then drilled down to the core through the pressure tap boss, pipe, and epoxy. The pressure taps were determined open when gas flowed freely out the taps once the core was pressurized.

3.3.4 Fluid Preparation

A synthetic brine was prepared to simulate the field brine produced from the Brooks Number 6 well. Only the three major ions, sodium, calcium, and magnesium, were used in the synthetic brine preparation The brine was prepared on a weight basis. The final mixture was vacuum filtered through a 0.4 micrometer Nucleopore filter using a vacuum type Millipore filter holder.

Betz 1160, a cationic polyacrylamide, was the polymer used in all the experiments. The polymer was mixed according to the procedure described in Appendix A to the desired concentrations by weight. The uniform solution was filtered by gravity through a 1.2 micrometer Millipore filter. A hydraulic pressure head of 9 kPa (3 ft of liquid) was placed on the filter. The filtering process re-

quired approximately 12 hours for polymer concentrations up to 750 ppm and 3 to 4 days for 2000 ppm polymer. Filters were replaced when plugging was indicated by a cessation of flow. The filtered solutions were stored at 1°C (34°F) until ready for use.

3.3.5 Preparation for Flow

A series of Validyne transducers were used to measure the pressure along the core length. The transducers were adjusted and calibrated according to manufacturer's specifications.

Brine and polymer solutions were placed in the Plexiglas transfer cylinders and air was removed by drawing a vacuum on the solution and tapping on the cylinder to dislodge any air bubbles. Flow lines leading to the core inlet were purged of any air. The core was saturated with carbon dioxide while maintaining 345 kPa (50 psi) of pressure on the core. The pressure taps were plugged and the core was evacuated and brine introduced under pressure. Flow lines were connected to the core and a small amount of brine was passed through the core. The end valves to the core were shut off and the core was allowed to equilibrate for several hours. Pressure drops were measured along the core to provide a basis for pressure calculations.

3.3.6 Water Permeability Determination

The permeability of the core to brine was measured by flowing brine at three rates and measuring the pressure drop across each section of the core. Pressure measurements were taken every 30 seconds for a 5 minute period to enable the determination of an average permeability to brine.

3.3.7 Flooding Procedure

The core flooding procedure for the Baker dolomite core BAK5 involved the following sequence of steps:

1) Brine was injected at a rate of 0.328 (1 ft/da) for five pore volumes.
2) Polymer of 250 ppm concentration was injected at 0.328 m/da for five pore volumes. The rate was increased to 0.656 m/da (2 ft/da), 0.984 m/da (3 ft/da), and 1.64 m/da (5ft/da) maintaining flow for 1.5 pore volumes at each rate.
3) Polymer of 500 ppm concentration was injected at 0.328 m/da for five pore volumes. The rate again was increased to 0.656, 0.984, 1.64 m/da and the flow rate was maintained at each rate for 1.5 pore volumes.
4) Polymer of 750 ppm concentration was injected at 0.656 m/da for five pore volumes. The rate was increased to 0.984 and 1.64 m/da and the flow rate was maintained for 1.5 pore volumes at each rate.
5) Brine was injected at 1.64 m/da for five pore volumes. The flow rate was decreased to 0.984 m/da for 2.5 pore volumes.

Pressures were monitored continuously and were recorded on data files on a Data General minicomputer.

3.4 Phase III - Geology

In order to both understand and interpret the flow behavior of fluids in carbonate rocks, it is necessary to understand the petrography

or the description and systematic classification scheme of these rocks. The complex make-up of carbonate rocks is the result of complicated and varied depositional patterns and extensive post-depositional alterations. Thin sections of rock slabs, scanning electron photomicrographs, and mercury porosimetry data taken from rock samples are three techniques used to aid in the interpretation of the fluid flow behavior.

These geological studies are discussed in this section. The discussion will be limited to technique alone with the results and interpretation to be presented later in Chapters 4 and 5.

3.4.1 Thin Sections

One petrographic technique used to study mineral content, grains, textures, cements, and porosities in the carbonate samples involved the preparation of rock thin sections. Thin sections consist of samples of rock mounted to glass slides with clear epoxy. The rock is then ground down to a thickness of about 30 micrometers. The slides can then be viewed with a light microscope.

Epoxy cemented thin sections of samples of the pure dolomite and reservoir core before and after flooding were prepared by an outside source*. Before flooding, the dolomite and reservoir core were selected to indicate differences in mineralogy, pore structure, grain size, and cementation. Portions of the thin section samples were stained to distinguish calcite ($CaCO_3$) from dolomite ($CaMg(CO_3)_2$) and to indicate iron content. The stain consisted of a mixture of Alizarin Red-S stain in a 0.2% HCl solution (cold) and potassium fer-

---

Central Petrographic Service Inc.,
2514 Nicholson Drive, Dallas, Texas 75224.

ricyanide stain in a weak HCl solution. The Alizarin Red-S stain turns calcite red[49]. Dolomite remains colorless. The potassium ferricyanide stains ferroan minerals a pale to deep turquoise. Non-ferroan minerals remain colorless.

Samples from the flooded cores were selected for thin section preparation from areas in the core in which both low and high resistance factors were measured. These samples were impregnated with blue epoxy before mounting to indicate connected pore space. Dead end pores not connected to the fluid flow stream would not fill with the blue epoxy. In addition, the colored epoxy distinguishes actual pore space from space caused by grain loss during the grinding process.

The thin sections were covered with glycerine and a cover slip and mounted on a Zeiss microscope** equipped with a camera mount. Photographs of the thin sections were taken using various exposures. Shutter speed and ASA were the only exposure controls. The ASA was set to the proper film speed and the correct exposure indicated by a light meter equipped with the microscope was bracketed one stop up and one stop down by varying the shutter speed.

3.4.2 Rock Pore Casts

Pore casts are plastic replicas of the pore system made by impregnating the rock with plastic epoxy and dissolving the rock with acid. Samples of core flooded in the laboratory were used for the

---

** ZEISS WL BINOCULAR RESEARCH MICROSCOPE equipped with 2.5x, 10x, 25x, and 40x objectives; 12.5x oculars.
OLYMPUS camera and light meter; 0.5x magnifier.

preparation of pore casts.

A small piece of the thin-section butt remaining after preparation of the thin section was used to prepare the pore cast. The sample was placed in a series of dilute hydrochloric acid (HCl) solutions of 5, 10, and 15% concentrations. The sample was placed in the solution of next higher concentration when the effervescing action subsided. The integrity of the delicate pore cast structure was preserved by controlling vigorous effervescence caused by the reaction between HCl and carbonate material. The samples were finally washed with distilled water and dried in a vacuum oven.

3.4.3 Scanning Elecron Micrographs

A technique used to examine more closely the fine-grained sediments of the carbonate rocks involves use of the scanning electron microscopy (SEM). Specimens are fixed to aluminum SEM mounts with a conductive silver paint* and are typically coated with approximately 200 angstroms of gold-paladium alloy in vacuo and are placed in the SEM. Electrons reflected from the surface of the specimen form an image which is photographed to give the photomicrograph.

Samples of flooded core and pore casts were dried and mounted on aluminum SEM mounts. The samples were coated and photographed using a Polaroid camera attached to the SEM unit. Several magnifications were used to show detail of pore configuration, grain size, and degree of cementation.

---

*Silver paint No. 1481 supplied by Ernest F. Fullam, Inc.

3.4.4 Mercury Porosimetry

The last portion of the third phase of the experimental program involved the measurement** of a capillary pressure curve for each rock sample and the calculation of pore sizes for each rock sample. This was achieved by a technique called mercury porosimetry.

Samples of both pure dolomite from the quarry and core taken from the reservoir and flooded in the laboratory were selected for testing. The flooded samples were chosen from sections within one core exhibiting low and high resistance to polymer flow. The samples were washed with water and dried before testing. The procedure used in this study was that described by Purcell [45].

** Laboratory measurements performed by Randall B. Ivey, student in Chemical Engineering at the University of Kansas.

CHAPTER 4

Presentation of Results and Discussion

4.1 Core Selection

Reservoir core sampled in the Lansing and Kansas City Group from the Brooks, Denker, and Souchek wells provided material with adequate porosity and permeability for flooding with polymer solutions in the laboratory. Results of the measurements of core physical properties are presented in Table 4.1. Each core plug tested is listed along with the corresponding depth, porosity, and permeability. Material selected for laboratory floods is marked with an asterisk.

Core material from each well having the highest permeability and porosity was selected for the laboratory floods. Porosities of the core ranged from essentially 0 to approximately 38%. Absolute permeabilities to air, determined by the procedure described in Appendix B, ranged from 0 to 940 md. The three wells provided core material with a wide variation in porosity and permeability, conditions frequently found in carbonate reservoirs.

4.2 Polyacrylamide Brine Compatibility

4.2.1 Polymers Tested

Twenty commercially available polyacrylamides were tested for compatibility with various brine mixtures. A list of the polymers investigated is given in Table 4.2.

Table 4.1 Porosity and Air Permeability for Core Plugs Sampled from the Brooks, Denker, and Souchek Wells

WELL	CORE PLUG	DEPTH (m)	DEPTH (ft)	POROSITY (m^3/m^3)	PERMEABILITY (md)
Brooks	H1*	11119	3390	0.085	0.38
	H2	11109	3387	0.249	1.15
	H3	11139	3396	---**	7.68
	H5	13120	4000	0.091	0.00
	H6A*	11100	3384	---	4.58
	H6B*	11100	3384	0.474	6.44
	H9	11132	3394	---	2.80
Denker	D1*	11447	3490	0.173	939.30
	D2	11447	3490	---	824.60
	D3	11040	3366	0.090	5.65
	D4	11040	3366	0.054	1.30
	D5	11027	3362	0.019	0.00
	D6	10991	3351	0.017	0.00
	D7	10972	3345	0.026	0.00
	D8	11470	3497	0.003	0.00
	D9	11047	3368	0.158	80.10
	D10	11319	3451	0.142	17.20
	D11	11319	3451	0.134	4.95
	D12	11267	3435	0.204	0.38
	D13	11316	3450	0.143	465.30
	D14	11316	3450	0.108	59.95
	D15	11398	3475	0.049	0.33
	D16	11346	3459	0.079	0.83
	D25	11375	3468	0.060	2.24
	D26	11437	3487	0.061	0.22
	D27	11329	3454	0.099	35.36
	D28	11109	3387	0.295	114.67
	D29	11309	3448	0.054	4.30
	D30	11237	3426	0.022	0.00
	D31*	11044	3367	0.214	648.18
	D32	11434	3486	0.073	2.85
	D33	11346	3459	0.152	129.58

* material selected for laboratory floods.
** porosity values not obtained

Table 4.1 (continued)

WELL	CORE PLUG	DEPTH (m)	DEPTH (ft)	POROSITY (m^3/m^3)	PERMEABILITY (md)
Souchek	S1A	13025	3971	0.279	9.12
	S1B	13025	3971	0.272	8.86
	S2A	13015	3968	0.00	0.00
	S2B	13015	3968	0.026	0.00
	S3A	13022	3970	0.231	2.29
	S3B	13022	3970	0.225	2.16
	S4	13140	4006	0.100	4.37
	S5A	13140	4006	0.218	10.24
	S5B	13140	4006	0.127	7.23
	S6A	13146	4008	0.027	0.00
	S6B	13146	4008	0.055	0.00
	S7A	13153	4010	0.129	7.50
	S7B	13153	4010	0.137	5.35
	S8A	13156	4011	0.083	0.00
	S9A	13215	4029	0.017	0.00
	S9B	13215	4029	0.018	0.00
	S10A	13225	4032	0.021	0.00
	S10B	13225	4032	0.040	0.00
	S11A*	13517	4121	---**	63.91
	S11B	13517	4121	0.289	28.65
	S12	13523	4123	0.168	5.32
	S13A	13592	4144	0.150	22.51
	S13B	13592	4144	0.201	46.07
	S14A	13596	4145	0.312	45.41
	S14B	13596	4145	0.351	77.83
	S15A	13605	4148	0.185	0.00
	S15B	13605	4148	0.176	0.00
	S16A	13605	4148	0.171	3.51
	S16B	13605	4148	0.157	0.87
	S17A	13605	4148	0.258	67.8
	S17B*	13605	4148	---	67.57
	S18A*	13605	4148	0.380	67.94
	S18B	13605	4148	0.302	58.81
	S19	13622	4153	0.181	13.76

material selected for laboratory floods.
** porosity values not obtained

Table 4.2 Polyacrylamide Tested for Compatibility with Brine Mixtures

POLYMER	MANUFACTURER	AVERAGE MOLECULAR WEIGHT	DESCRIPTION
Solid Polymers			
ALCOFLOOD 1100	Allied Colloids Inc.	--*	--
BETZ Polymer 1160	Betz Co.	5 x106	cationic copolymer
MAGNIFLOC 905N	American Cyanamid	15 x106	non-ionic polymer
Polymer 340	Calgon Corp.	3 x106	anionic unhydrolyzed copolymer
Polymer 454	Calgon Corp.	--	18% hydrolyzed
Polymer 800	Calgon Corp.	3 x106	nonionic unhydrolyzed
Polymer 815	Calgon Corp.	3 x106	15% hydrolyzed
Polymer 825	Calgon Corp.	3 x106	25% hydrolyzed
Polymer 835	Calgon Corp.	3 x106	35% hydrolyzed
PUSHER 500	Dow Chemical Co.	2 -3 x106	anionic
PUSHER 700	Dow Chemical Co.	3-10 x106	anionic
Water-Cut 110	Tiorco Inc.	10 x106	anionic copolymer
Water-Cut 160	Tiorco Inc.	5 x106	anionic copolymer
Liquid Polymer			
CYANATROL 930S	American Cyanamid	6 x106	anionic
CYANATROL 950S	American Cyanamid	15 x106	anionic
CYANATROL 960S	American Cyanamid	20 x106	anionic
Nal-flo 30	Nalco Chemical Co.	10 x106	anionic copolymer
Nal-flo 50	Nalco Chemical Co.	15 x106	anionic copolymer
Bx-2606	Nalco Chemical Co.	--	anionic copolymer
Ws-001	Nalco Chemical Co.	--	anionic copolymer

* Information not available.

The 900 series of American Cyanamid CYANATROL polymers are anionic polyacrylamides composed of four grades; 930S, 940S, 950S, and 960S, and designed for a wide range of viscosity development and mobility control properties.** Each grade is an opaque, white liquid with a bulk viscosity of 1200 cp at 25°C (77°F). CYANATROL 940S polymer was not

** Information from manufacturer's data sheet.

tested.

The Nalco products, NAL-FLO 30 and NAL-FLO 50, are high molecular weight, anionic acrylate-acrylamide copolymers.** The molecular weight* of NAL-FLO 30 is about 10 to 11 million. That of NAL-FLO 50 is 15 million or greater. The Nalco WS-001 copolymer is tolerant to high-salinity brines and has been employed in Germany as a pre-sweep agent in reservoirs.* Nalco BX-2606 copolymer is designed for low permeability reservoirs. The WS-001 polyacrylamide has a high molecular weight yet a low anionic charge. The molecular weight of BX-2606 is lower than NAL-FLO 30 yet the anionic charge is high. All four Nalco products are viscous, white liquids.

MAGNIFLOC 905N flocculant is a granular, ultra-high molecular weight, non-ionic polymer manufactured by American Cyanamid Co.** The polymer is a white solid used commercially in water clarification processes.

TIORCO Water-Cut 160 is a cationic acrylamide copolymer with a molecular weight of 5 million and charge density of 20%.** The polymer is a white granular solid.

Calgon 340 is a copolymer of acrylamide and 2-acrylamido-2- methyl propyl sulfonate.** Calgon 454 is an 18% hydrolyzed and slightly cross-linked polyacrylamide. The 800 series of Calgon polymers are linear polyacrylamides. Calgon 800 is a non-ionic unhydrolyzed polyacrylamide. Calgon 815, 825, and 835 are hydrolyzed to 15%, 25%, and 35% respectively.

Information from manufacture's data sheets.
* Correspondence with W. J. Fratt, Sales Manager, Nalco Chemical Co.

The Dow Chemical Company PUSHER 500 and PUSHER 700 are 25% partially hydrolyzed anionic polyacrylamides. The molecular weight of PUSHER 500 is 2 to 3 million and PUSHER 700 is 3 to 10 million. Both are white powdered solids.

BETZ Polymer 1160 is a cationic, high-molecular weight, copolymer of acrylamide and a quaternized cationic monomer.** The molecular weight is 5 million. BETZ 1160 is a white, granular solid.

4.2.2 Brine Formulations

The predominant ions found present in brines produced from the Lansing and Kansas City Group in Kansas were sodium, calcium, and magnesium. Sodium chloride (NaCl), calcium chloride dihydrate ($CaCl_2 \cdot 2H_2O$), and magnesium chloride hexahydrate ($MgCl_2 \cdot 6H_2O$), all reagent grade, were used to formulate the brine mixtures. The highest levels of each cation determined from the compiled brine water analyses were ,

80,000 ppm Na

30,000 ppm Ca

15,000 ppm Mg.

Brines containing 200,000 ppm NaCl and 100,000 ppm $CaCl_2 \cdot 2H_2O$ were chosen for use in the polymer-brine compatibility study. The effect of magnesium ion was not investigated. The sodium and calcium ion concentrations corresponding to the salt levels are as follows,

---

** Information from manufacturer's data sheets.

78,675 ppm Na

27,262 ppm Ca.

The concentrations of salt used to make the Brooks synthetic brine are given in Table 4.3. The water analysis report* for water produced from the Husky Oil Company's Brooks No. 6 well showed cation concentrations of 34,137 ppm Na, 2,636 ppm Ca, and 2,088 ppm Mg.

Table 4.3 Synthetic Brooks No. 6 Well Brine Composition

SALT	CONCENTRATION (μg/g) (ppm)	CATION	CONCENTRATION (μg/g) (ppm)
NaCl	86,870	Na	34,137
$CaCl_2 \cdot 2H_2O$	9,670	Ca	2,636
$MgCl_2 \cdot 6H_2O$	8,890	Mg	2,088

4.2.3 Low Temperature Studies (25°C).

The polyacrylamides which did not form a visible solid precipitate after mixing with 200,000 ppm NaCl in distilled water at 25°C are listed in Table 4.4. The polymer concentration used was 2,000 ppm. The period of time during which the polymers were observed for precipitate formation is also listed. All solid polyacrylamides were optically clear. The liquid polyacrylamides were white and translucent after mixing. Samples centrifuged exhibited a phase separation with the white translucent phase on top

---

Report compiled by the Operations Research Section of the KGS.

and a clear phase on the bottom. No precipitate was observed at the bottom of the centrifuge tube. CYANATROL 950S, Nalco BX-2606, and NAL-FLO 50 separated slightly after about one week leaving a white layer on top.

Polyacrylamides which did not form a precipitate after mixing 2,000 ppm of the polymer with brine consisting of 100,000 ppm $CaCl_2 \cdot 2H_2O$ in distilled water at 25°C were as follows,

BETZ Polymer 1160
MAGNIFLOC 905N
Polymer 800
Water-Cut 160

Solid precipitates were not visible in the translucent mixture for the liquid polymers until the solutions were centrifuged. The solutions of liquid polyacrylamides separated into a white, cloudy phase on top, clear phase on the bottom, and slight amount of precipitate at the bottom of the clear phase. All the solid polyacrylamides mixed in the calcium chloride brine grew molds after about five months. The liquid polymers stored for the same period of time as the solids either grew molds, separated, or formed a visible precipitate at the bottom of the sample.

Calgon 815, 825, 835 and PUSHER 700 were found not to be compatible with 100,000 ppm $CaCl_2 \cdot 2H_2O$ when the solid polymer was added to the brine mixture. Each polymer was also tested by dissolving the solid first in distilled water and then by adding the solid salt. The Calgon series was cloudy on mixing and eventually separated leaving a solid at the bottom. The PUSHER 700 solution remained optically clear in the second test.

Table 4.4 Polyacrylamides Stable at 2,000 ppm Concentration in 200,000 ppm NaCl Brine and at 25°C (77°F).

	POLYMER	TEST PERIOD (days)	(months)
Solids	ALCOFLOOD 1100	209	6.97
	BETZ Polymer 1160	208	6.93
	MAGNIFLOC 905N	208	6.93
	Polymer 800	209	6.97
	Polymer 815	208	6.93
	Polymer 825	208	6.93
	PUSHER 700	208	6.93
	Water-Cut 160	163	5.43
Liquid	Cyanatrol 930S	207	6.90
	Cyanatrol 950S*	162	5.40
	Cyanatrol 960S	200	6.67
	Nal-flo 30	172	5.73
	Nal-flo 50*	179	5.97
	Nalco Bx-2606*	162	5.4
	Nalco WS-001	162	5.4

separated slightly leaving white layer on top.

Polyacrylamides stable after mixing 2,000 ppm of the polymer with Brooks Well Number 6 synthetic brine at 25°C are listed in Table 4.5. Time periods are given for those polymers still stable after the listed period of time. No liquid polymers were tested in this brine.

Table 4.5 Polyacrylamides Stable at 2,000 ppm Concentration in Brooks Synthetic Brine at 25°C (77°F).

	POLYMER	TEST PERIOD (days)	(months)
Solids	BETZ Polymer 1160	224	7.5
	MAGNIFLOC 905N*	150	5.0
	Polymer 340	224	7.5
	Polymer 454*	150	5.0
	Polymer 800*	150	5.0
	Polymer 815*	150	5.0
	Polymer 825*	150	5.0
	Polymer 835*	150	5.0
	Water-Cut 160*	150	5.0

* solutions grew molds.

4.2.4 High Temperature Studies (43.3°C).

Solutions found stable at 25°C were tested at an elevated temperature, 43.3°C (110°F), a maximum temperature reported* for the Lansing and Kansas City Group. Polyacrylamides stable in 200,000 ppm NaCl at a polymer concentration of 2,000 ppm are listed in Table 4.6. TIORCO Water-Cut 160 formed a trace amount of precipitate. CYANATROL 950S, 960S, and all four Nalco polymers separated slightly, yet did not form precipitates. The times during which the samples were observed are also listed.

* Report compiled by the Operations Research Section of the Kansas Geological Survey.

Table 4.6 Polyacrylamides Stable at 2,000 ppm Concentration in 200,000 ppm NaCl Brine and at 43.3°C (110°F).

	POLYMER	TEST PERIOD (days)	(months)
Solids	ALCOFLOOD 1100	163	5.43
	BETZ Polymer 1160	208	6.93
	MAGNIFLOC 905N	208	6.93
	Polymer 800	209	6.97
	Polymer 815	208	6.93
	Polymer 825	208	6.93
	Polymer 835	209	6.97
	PUSHER 700	208	6.93
	Water-Cut 160**	215	7.17
Liquids	Cyanatrol 930S	207	6.90
	Cyanatrol 950S*	162	5.40
	Cyanatrol 960S*	202	6.73
	Nal-flo 30*	162	5.4
	Nal-flo 50*	179	5.97
	Nalco Bx-2606*	162	5.4
	Nalco WS-001*	162	5.4

* separated slightly leaving white layer on top.
** trace amount of precipitate.

Polyacrylamides stable in 100,000 ppm $CaCl_2 \cdot 2H_2O$ at a polymer concentration of 2,000 ppm are listed in Table 4.7. TIORCO Water-Cut 160 formed a trace amount of precipitate. All liquid polymers separated slightly.

Polyacrylamides stable after mixing 2,000 ppm polymer with Brooks Well Number 6 synthetic brine are listed in Table 4.8 with observation times.

Table 4.7 Polyacrylamides Stable at 2,000 ppm Concentration in 100,000 ppm $CaCl_2 \cdot 2H_2O$ Brine and at 43.3°C (110°F).

	POLYMER	TEST PERIOD (days)	(months)
Solids	BETZ Polymer 1160	215	7.17
	MAGNIFLOC 905N	211	7.03
	Polymer 454	209	6.97
	Polymer 800	215	7.03
	Water-Cut 160**	163	5.43
Liquids	Cyanatrol 930S*	207	6.90
	Cyanatrol 950S*	162	5.40
	Cyanatrol 960S*	202	6.73
	Nalco WS-001*	162	5.4

* separated slightly leaving white layer on top.
** trace amount of precipitate.

Table 4.8 Polyacrylamides Stable at 2,000 ppm Concentration in Brooks Synthetic Brine at 43.3°C (110°F).

POLYMER	TEST PERIOD (days)	(months)
MAGNIFLOC 905N	217	7.23
Polymer 800	217	7.23
Water-Cut 160	308	10.27

4.2.5 Polymer Viscosity

The viscosities of several of the polyacrylamide solutions measured after mixing and aging are presented in Table 4.9 to 4.11. Polymer concentration, brine content, viscosity and aging time are listed.

Table 4.9 Viscosities of 2,000 ppm Polyacrylamides in 200,000 ppm NaCl Brine for Various Shear Rates.

	POLYMER	SHEAR RATE (1/sec)	VISCOSITY (cp)	TEST PERIOD (d)	(mo)
Solids	BETZ Polymer 1160	23	9.72	71	2.37
		45	8.12		
		90	7.58		
		225	6.68		
	Polymer 800	90	8.14	74	2.47
		225	6.18		
	Polymer 815	45	16.03	73	2.43
		90	13.29		
	Polymer 825	45	14.22	80	2.67
		90	12.15		
	Polymer 835	90	8.27	81	2.70
		225	7.24		
	PUSHER 700	90	6.83	71	2.37
		225	6.08		
	Water-Cut 160	90	5.53	27	0.90
		225	4.88		
Liquids	CYANATROL 950S	45	13.19	33	1.10
		90	10.99		
	Nalco Bx-2606	90	5.82	26	0.87
		225	5.23		

Table 4.10 Viscosities of 2,000 ppm Polyacrylamides in 100,000 ppm $CaCl_2 \cdot 2H_2O$ Brine for Various Shear Rates.

	POLYMER	SHEAR RATE (1/sec)	VISCOSITY (cp)	TEST (d)	PERIOD (mo)
Solids	BETZ Polymer 1160	45	4.96	78	2.60
		90	4.63		
		225	4.21		
		2.42	2.42		
	Polymer 800	90	5.69	80	2.67
		225	4.96		
	PUSHER 500*	225	2.82	64	2.13
		450	2.43		
	Water-Cut 160	225	3.93	34	1.13
		450	3.62		
Liquids	CYANATROL 950S	90	6.46	33	1.10
		225	5.43		
	Nalco WS-001	90	10.34	33	1.10
		225	8.17		

salt added to dissolved polymer.

Table 4.11 Viscosities of 2,000 ppm Polyacrylamides in Brooks Synthetic Brine for Various Shear Rates.

	POLYMER	SHEAR RATE (1/sec)	VISCOSITY (cp)	TEST (d)	PERIOD (mo)
Solids	MAGNIFLOC 905N	90	10.03	81	2.70
		225	8.01		
	Polymer 800	90	6.36	82	2.73
		225	5.22		
	PUSHER 700**	225	2.17	80	2.67
		450	2.07		
	Water-Cut 160	225	4.69	172	5.73
		450	4.04		

polymer concentration of 1,000 ppm.

A graph of the log of the solution viscosity versus log shear rate for 2,000 ppm BETZ 1160 in Brooks synthetic brine is shown in Figure 4.1. High salinities tend to reduce the shear sensitivity of polyacrylamides. For 2,000 ppm BETZ 1160 in Brooks synthetic brine, the viscosity was observed to change by a factor of two over two orders of magnitude of shear rate.

4.3 Core Flood Experiments

The first laboratory core flood was performed using Baker dolomite as the core material. This flood, labelled BAK5, was performed to determine suitable concentrations of polymer and appropriate fluid flow rates to be used for the remaining floods. Three concentrations of BETZ Polymer 1160 of 250, 500, and 750 ppm were used and four fluid frontal velocities of 0.328, 0.656, 0.984, and 1.64 m/d (1,2,3,5 ft/d) were employed.

Each core was divided into sections and pressure drops were measured across the individual sections as discussed in Chapter 3. The section were labelled with the entrance section being termed the "Front", the next section termed section 1, "Sect1", the next section 2, "Sect2", etc., and finally the exit section being termed the "Back".

The pressure data from BAK5 are graphed in Figures 4.2A through 4.2F, as pressure drop per unit length (kPa/cm) versus pore volume fluid injected (Vp), for each section and for the total core length. Problems were encountered with pressure measurements during flow of the 250 ppm polymer solution and these data were not plotted.

The pressure data in Figures 4.2A through 4.2F show that a polymer concentration of 500 ppm gave sufficiently high resistance and residual

resistance to obtain suitable pressure measurements with the equipment. Pressure drops per unit length over the flow rate range studied with the 500 ppm polymer concentration ranged in value from 14 to 84 kPa/m (0.6 to 3.7 psi/ft). These pressure gradients are typical of those encountered in a reservoir. The lower concentration of 250 ppm was also chosen for later floods to investigate the effect of concentration on polymer resistance. Figures 4.2A through 4.2F show that for rates higher than 0.984 m/d (3 f/d), the polymer resistance factors as indicated by pressure drop were a function of flow rate. At 1.64 m/d (5 f/d), the resistance factors computed from the pressure data in these graphs were about two times the values at the lower rates. A frontal velocity of 0.984 m/d (3 f/d) was therefore chosen for the remaining floods.

Once the polymer concentrations and flow rate were selected, ten core floods were conducted in reservoir core material, three in Baker dolomite, and one in Berea sandstone. The resistance factors and residual resistance factors computed using the procedure outlined in Appendix C are listed for these floods in Table 4.12.

Frequency distributions of the resistance factors and residual resistance factors are shown in Figures 4.3 and 4.4. Values for the resistance factors were skewed to the low end with a significant number being between 1 and 14. Similarly, the residual resistance factors were skewed to the low side with a significant number lying between 1 and 20.

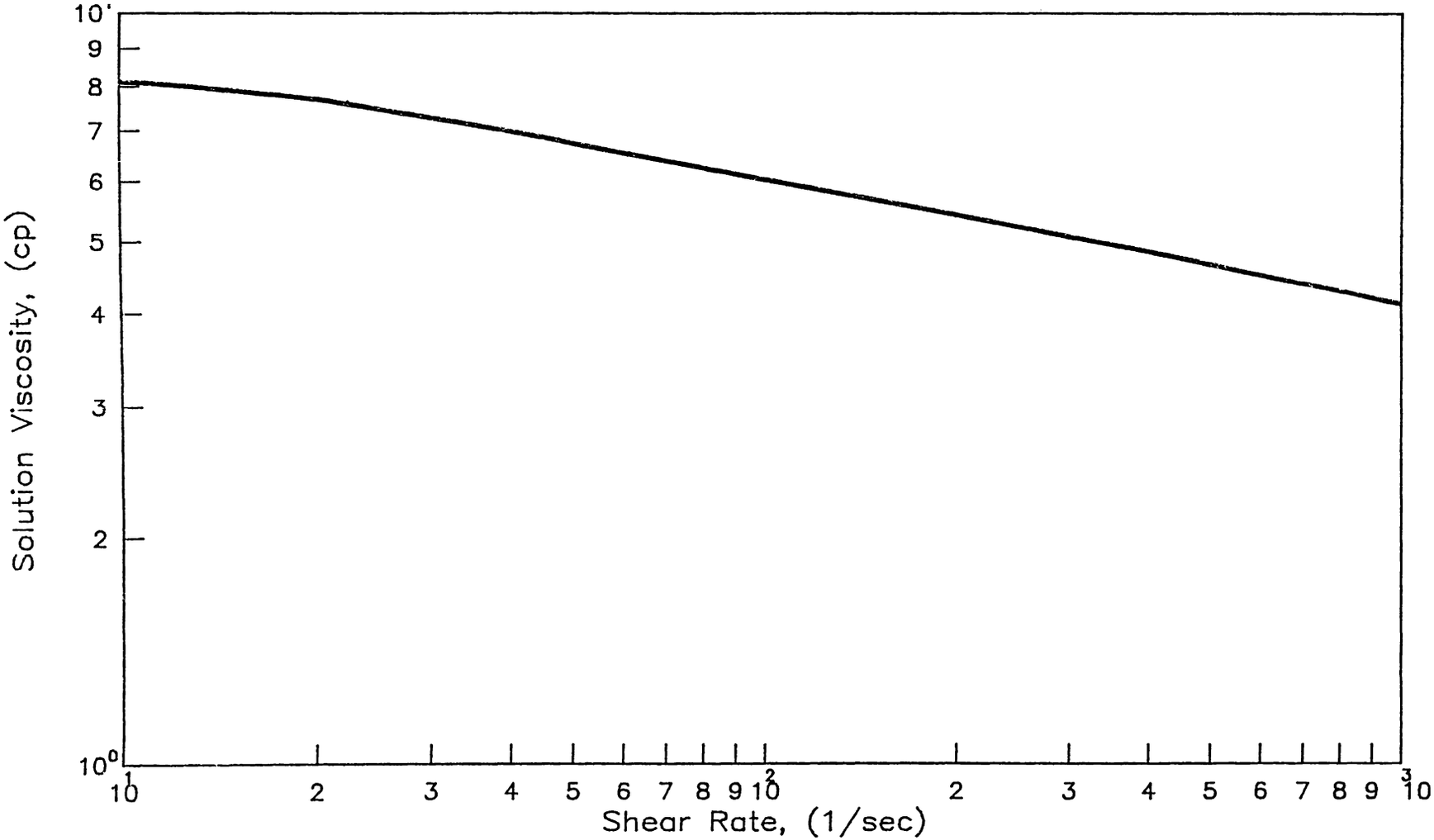

FIGURE 4.1 SHEAR RATE DEPENDENCY OF 2000 BETZ POLYMER 1160 IN BROOKS SYNTHETIC BRINE

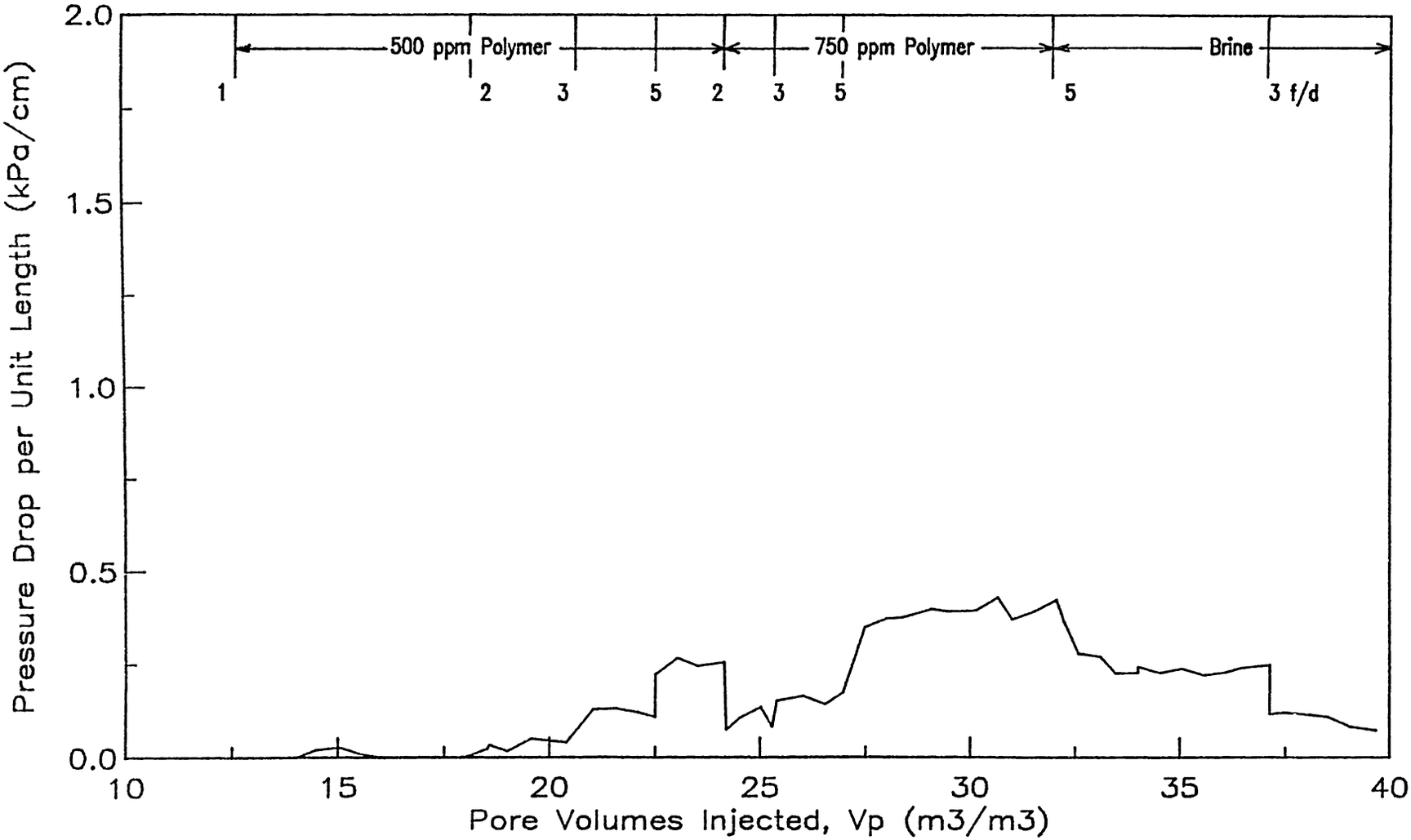

FIGURE 4.2A PRESSURE GRADIENT ACROSS FRONT FACE OF BAKER DOLOMITE CORE FOR FLOOD BAK5 DURING POLYMER AND BRINE FLOW (BETZ 1160 IN BROOKS SYNTHETIC BRINE)

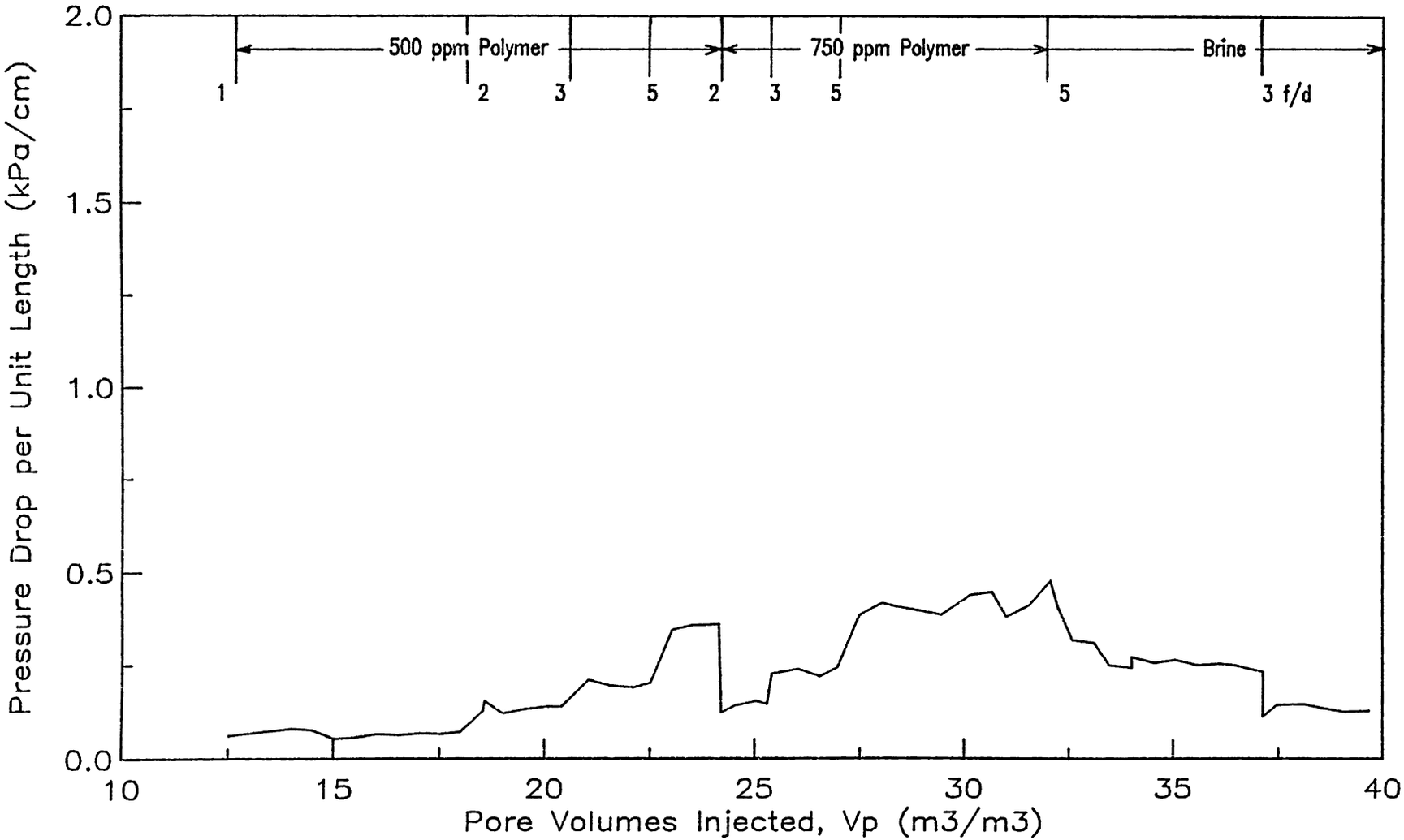

FIGURE 4.2B PRESSURE GRADIENT ACROSS SECTION 1 OF BAKER DOLOMITE CORE FOR FLOOD BAK5 DURING POLYMER AND BRINE FLOW (BETZ 1160 IN BROOKS SYNTHETIC BRINE)

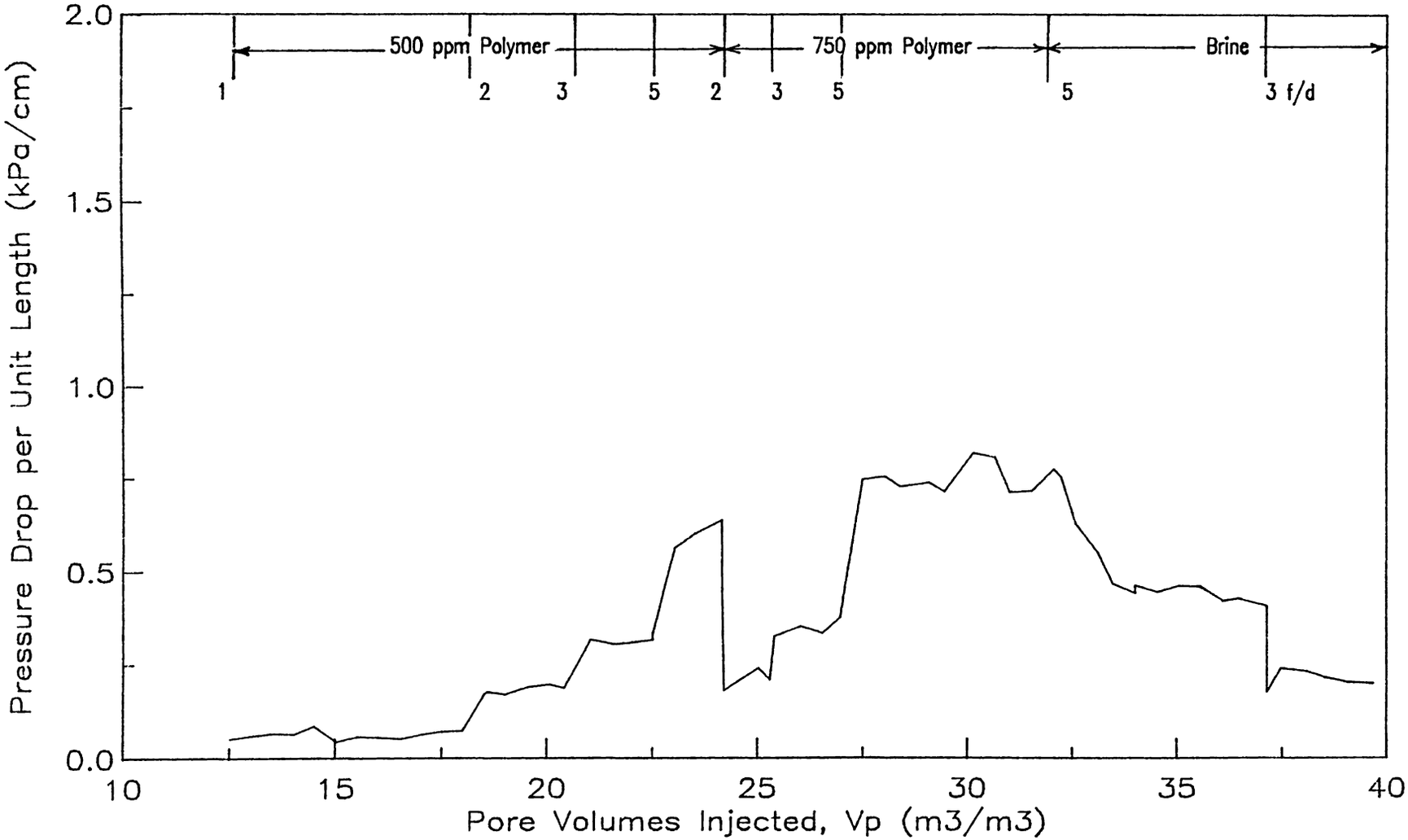

FIGURE 4.2c PRESSURE GRADIENT ACROSS SECTION 2 OF BAKER DOLOMITE CORE FOR FLOOD BAK5 DURING POLYMER AND BRINE FLOW (BETZ 1160 IN BROOKS SYNTHETIC BRINE)

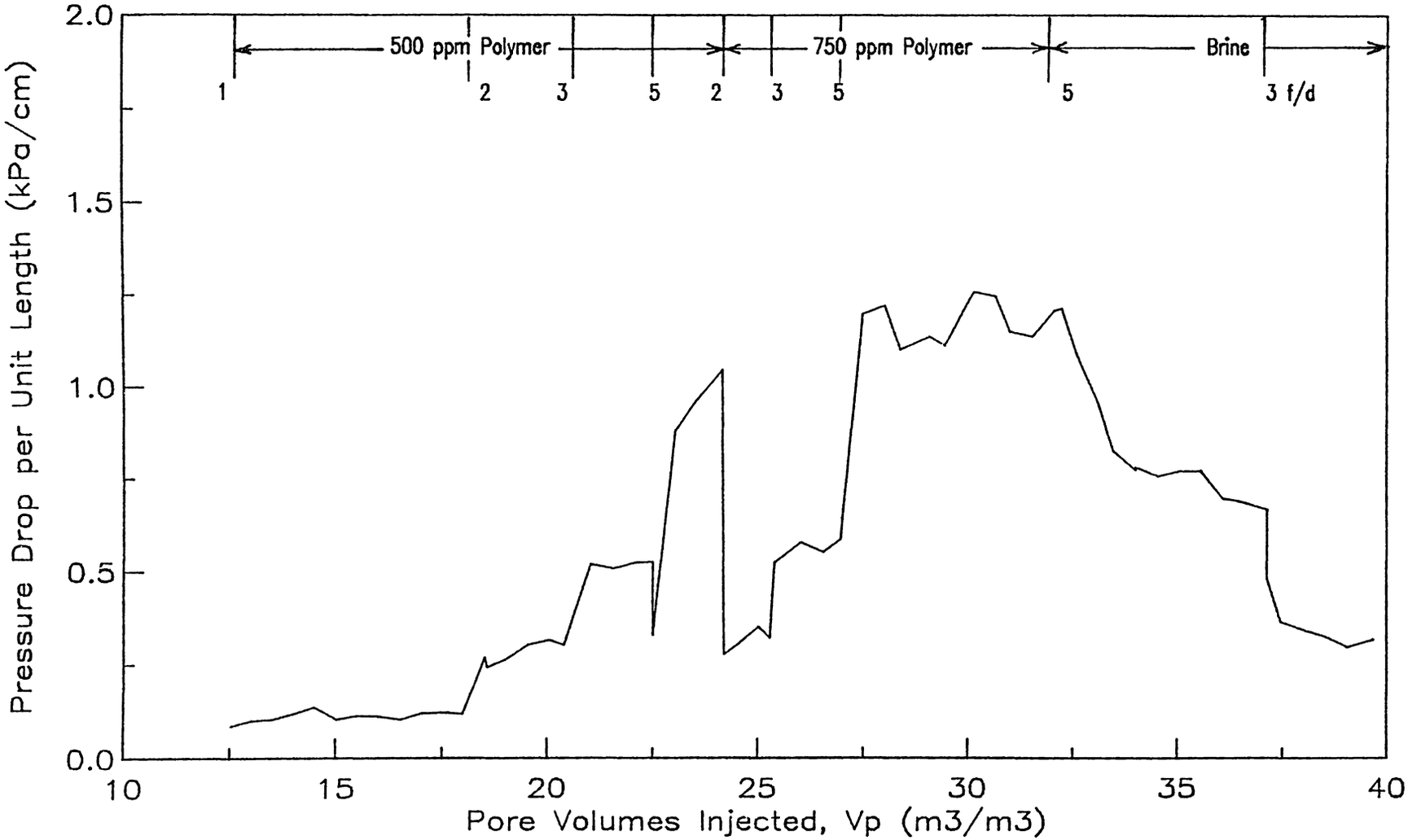

FIGURE 4.2D PRESSURE GRADIENT ACROSS SECTION 3 OF BAKER DOLOMITE CORE FOR FLOOD BAK5 DURING POLYMER AND BRINE FLOW (BETZ 1160 IN BROOKS SYNTHETIC BRINE)

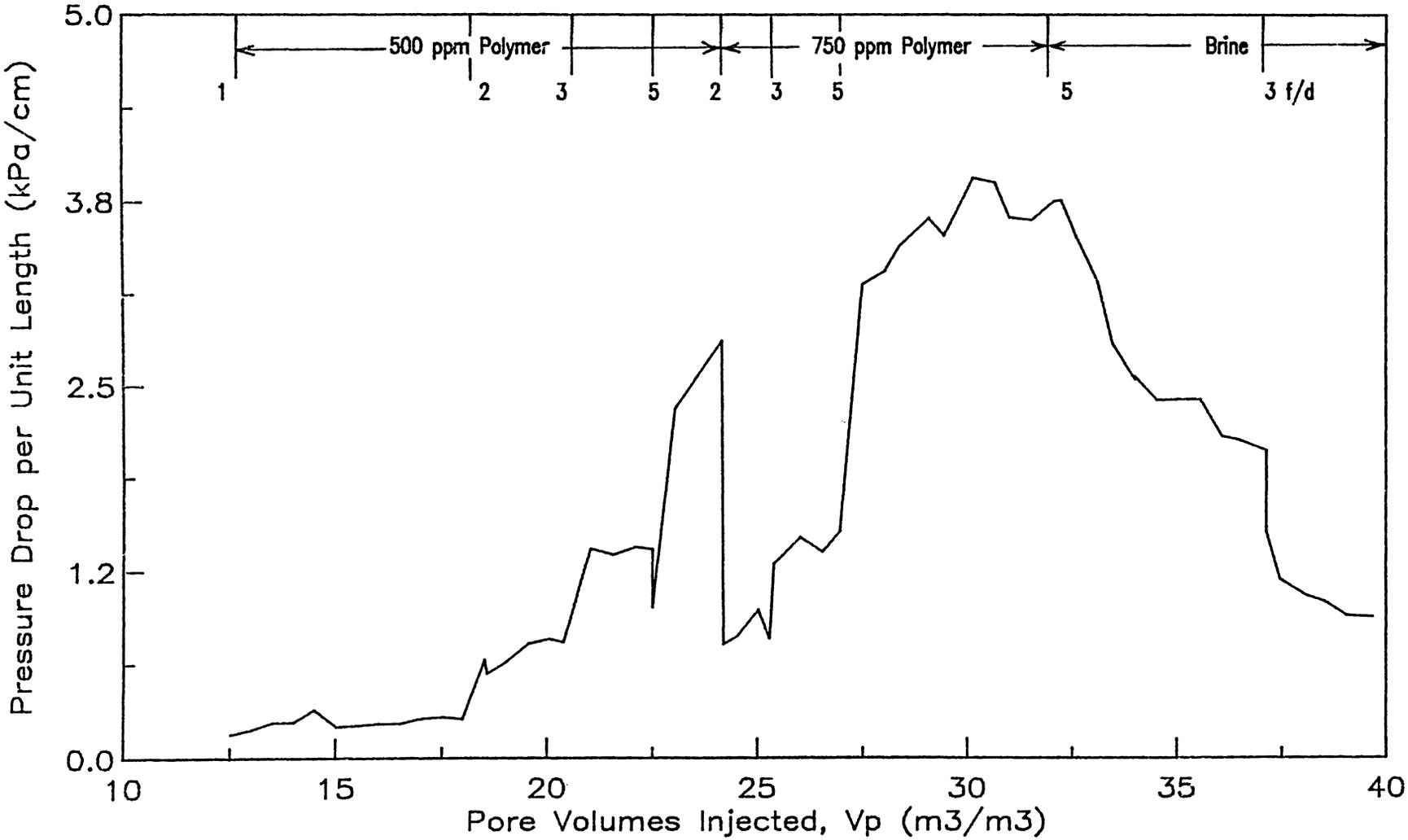

FIGURE 4.2 E PRESSURE GRADIENT ACROSS BACK FACE OF BAKER DOLOMITE CORE FOR FLOOD BAK5 DURING POLYMER AND BRINE FLOW (BETZ 1160 IN BROOKS SYNTHETIC BRINE)

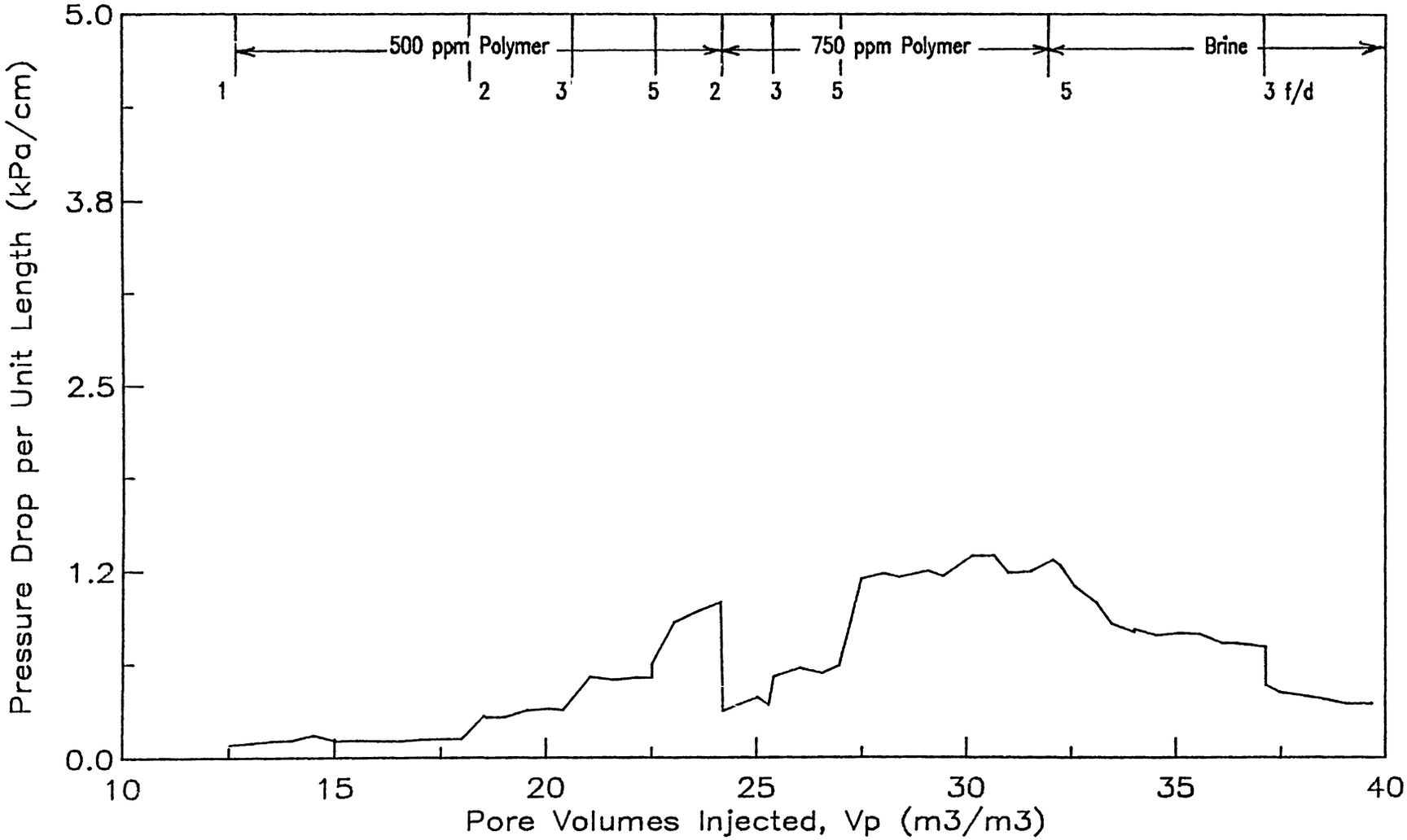

FIGURE 4.2 F PRESSURE GRADIENT ACROSS TOTAL BAKER DOLOMITE CORE FOR FLOOD BAK5 DURING POLYMER AND BRINE FLOW (BETZ 1160 IN BROOKS SYNTHETIC BRINE)

Table 4.12 Resistance Factors and Residual Resistance Factors for Laboratory Core Floods.

CORE	LENGTH (cm)	POROSITY (m^3/m^3)	kw (md)	RF (250)	RRF (250)	RF (500)	RRF (500)
DENK1	4.92	0.17	349.77	4.32	3.89	11.24	-
Front	1.11		627.45	2.33	0.78	5.04	3.10
Sect1	2.70		990.2	1.53	1.22	2.54	-
Back	1.11		122.95	5.47	4.86	14.59	-
DENK2	4.37	0.20	743.13	2.88	2.60	4.89	4.89
Front	1.11		927.74	4.30	2.80	4.00	4.00
Sect1	2.22		888.64	1.68	1.49	3.45	3.45
Back	1.03		579.88	2.25	2.03	4.75	4.75
DENK3	4.37	0.14	434.99	1.83	1.15	2.91	1.35
Front	1.35		198.52	1.98	0.74	2.97	0.99
Sect1	1.67		1487.96	1.85	1.16	3.24	1.85
Back	1.35		653.28	1.12	2.44	3.66	2.44
HUSK1	7.46	0.21	82.82	14.18	11.26	19.36	17.02
Front	1.27		82.97	3.13	2.09	7.79	3.66
Sect1	2.38		117.95	2.97	2.38	3.17	2.92
Sect2	2.38		160.39	21.81	17.77	44.43	25.04
Back	1.43		35.18	-	-	17.90	17.68
HUSK2	7.70	0.24	32.58	10.58	4.60	19.31	5.52
Front	1.59		7.81	11.69	5.73	20.5	6.17
Sect1	2.38		146.97	3.32	2.07	4.56	-
Sect2	2.38		140.23	12.27	9.90	27.31	13.86
Back	1.35		974.29	9.63	8.25	27.5	15.13
HUSK3	7.46	0.17	35.6	13.94	18.49	-	-
Front	1.91		12.2	17.45	23.88	-	-
Sect1	1.91		157.6	2.37	8.07	-	-
Sect2	1.91		640.3	-	-	-	-
Back	1.75		40.5	7.97	4.47	-	-

Values not obtained or computed less than 1.

Table 4.12 (continued).

CORE	LENGTH (cm)	POROSITY (m^3/m^3)	kw (md)	RF (250)	RRF (250)	RF (500)	RRF (500)
SOU1	5.24	0.28	122.5	0.74	0.56	2.23	1.11
Front	1.11		249.4	6.42	4.53	18.50	10.57
Sect1	3.02		63.1	0.12	0.15	0.23	0.07
Back	1.11		10.4	-*	-	-	-
SOU2	4.29	0.27	952.3	3.51	3.14	5.68	3.58
Front	1.11		814.7	3.90	3.07	5.37	2.68
Sect1	2.22		1593.1	2.25	2.00	3.50	2.00
Back	0.95		646.8	3.09	2.79	5.98	3.09
SOU3	4.45	0.27	316.5	1.80	1.00	3.10	1.73
FRONT	1.59		339.6	-	-	-	-
Sect1	1.43		1264.7	1.01	1.62	2.64	1.73
Back	1.59		210.1	2.40	1.90	1.01	2.70
SOU4	5.56	0.19	42.5	8.62	6.89	29.54	11.32
Front	1.91		265.00	-	-	-	-
Sect1	1.83		37.00	10.31	5.15	35.43	9.88
Back	1.83		27.2	9.46	-	29.0	14.82
BAK7	9.21	0.20	98.7	11.64	9.02	22.62	14.10
Front	1.27		55.0	25.9	24.58	87.41	47.48
Sect1	2.22		121.1	11.44	8.84	28.59	17.88
Sect2	2.22		132.6	6.28	5.09	15.87	7.27
Sect3	2.22		94.5	13.12	10.79	37.99	18.99
Back	1.27		99.5	9.23	7.69	26.24	14.08
BAK6	9.21	0.22	193.0	-	-	7.93	5.16
Front	1.27		203.2	-	-	6.54	2.58
Sect1	2.22		244.8	-	-	6.89	4.82
Sect2	2.22		155.7	-	-	11.47	6.57
Sect3	2.22		203.2	-	-	6.54	5.81
Back	1.27		181.2	-	-	6.93	4.60
BEREA	8.57	0.18	457.97	1.86	1.45	2.54	1.72
Front	1.75		367.60	2.02	1.05	2.46	1.40
Sect1	1.75		463.47	1.88	1.49	2.65	1.77
Sect2	1.67		504.87	1.72	1.27	2.47	1.51
Sect3	1.59		591.83	2.26	1.87	2.61	1.41
Back	1.98		429.74	1.87	1.36	2.46	1.74

Values not obtained or computed less than 1.

Figure 4.3 Frequency Distribution of Resistance Factors for Carbonate Cores

Figure 4.4 Frequency Distribution of Residual Resistance Factors for Carbonate Cores

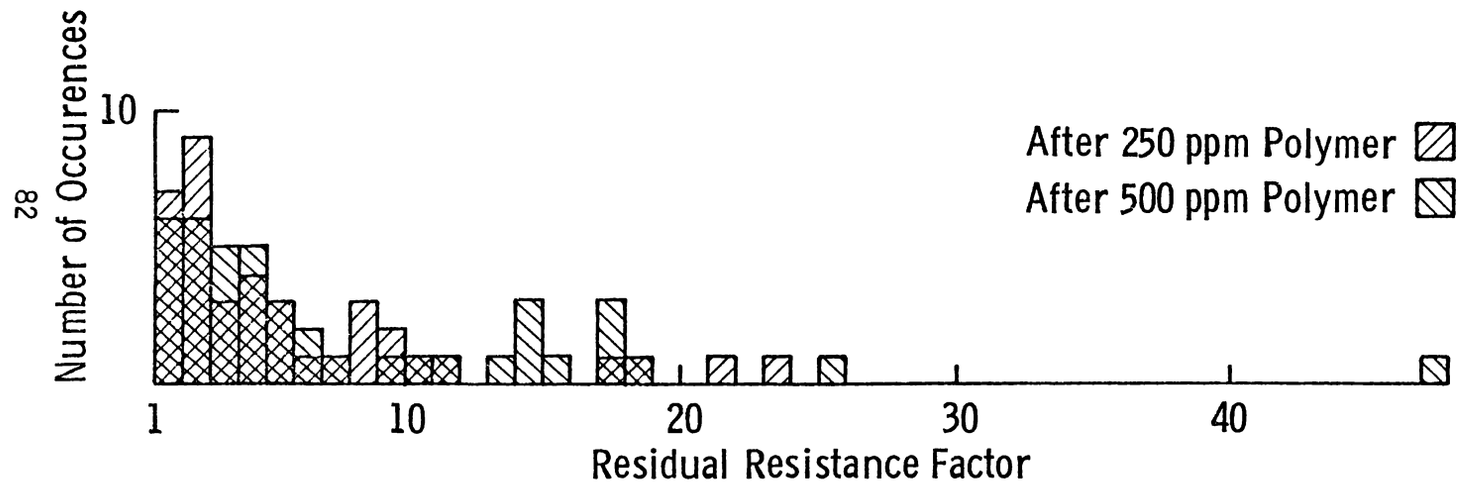

Length, porosity, and permeability information for the individual sections are also listed.

It was observed during several of the core floods that resistance factors and residual resistance factors increased as the water permeability decreased. For example, in the BAK5 flood, the Back section of the core had the lowest permeability and the highest resistance factor and residual resistance factor. An attempt was made to correlate both resistance factors and residual resistance factors with water permeability for all the floods, but the data did not correlate.

One unexpected result was that the resistance factors were quite variable in the Baker dolomite, a quarry rock. It was thought that this material might be rather uniform and could serve as a laboratory standard. However, the large variability in the resistance factors in the Baker cores diminish the laboratory utility of this material.

The resistance factors for all the carbonate cores were quite variable. The error associated with the pressure measurements was on the order of 1% maximum for transducers operated over a 30 day period. The variability in the resistance factors was much larger; up to 5 times in value in some of the floods. This variability is assumed to be a result of the heterogeneities which exist in the cores. These heterogeneities are further indicated by the variation in water permeability measured along the core length. The large variability in the resistance factors does diminish the utility of the polymer applications in the sense that uniform mobility control would be difficult to achieve. Predictions of polymer behavior would also be extremely difficult.

The resistance and residual resistance factors for the Berea sandstone were generally an order of magnitude smaller than those for the carbonate material and the variability was much less in the Berea. The Berea sandstone was correspondingly much more uniform in water permeability than were the other carbonate materials.

4.4 Thin Section Descriptions

Thin sections prepared from epoxy impregnated core samples previously flooded in the laboratory were examined and described.* These descriptions are summarized in this section with emphasis placed on geologic aspects related to observed core flood behavior.

4.4.1 Baker Dolomite

A thin section prepared from the BAK7 core was found to be a fine to medium crystalline dolomite. The original sediment was unrecognizable due to complete recrystallization to pure dolomite. The crystals are approximately 0.10 mm and are classed as being fine sand size. Porosity of the Baker dolomite as viewed from thin section showed complete intergranular porosity most probably created by shrinkage of grains as the dolomite crystals were formed. Much of the porosity viewed in the thin section and thin section butt did not fill with epoxy and therefore was not connected pore space. No relationship was observed between porosity in the thin section and the resistance and residual resistance factors.

Thin section descriptions by Marvin D. Woody and Patricia N. StClair, students in the Department of Geology at the University of Kansas.

4.4.2 Denker Core

A thin section prepared from the DENK2 core showed the rock to be a mixed skeletal grainstone or packstone. The sediment was originally deposited in a high energy, nearshore, shoal environment experiencing wave activity and occasional subarial exposure. Calcite and dolomite were both present along with peloids and organic constituents such as echinoderms and foraminifera. The rock is grain-supported with the grains being moderately well-rounded and well-sorted.

A large proportion of Section 1 of the core as viewed in the thin section was vuggy while the front face of the core was not. The resistance and residual resistance factors listed in Table 4.12 are lower for section 1 of the core. A higher permeability was also observed for this portion of the core than for the rest of the core. The vuggy porosity in section 1 may account for the lower resistance and residual resistance factors measured.

4.4.3 Brooks Core

Thin sections were prepared for the front and back sections of the Brooks HUSK1 core. Rock material in both sections was a skeletal pellet packstone originally deposited in a low-energy, lagoonal, restricted environment. The mineral content was about 90% calcite. Pellets, echinoderms, and shell fragments were also present. The rock is grain-supported with most grains being very fine grain microspar or re-crystallized, micrite mud. Many pellets had been dissolved forming abundant moldic porosity.

Section 1 was highly fractured and exhibited a high permeability. The resistance and residual resistance factors listed in Table 4.12 were lower for section 1 than were the values for section 2 and the back section. Fracture porosity was evident in the back section of the core but was particularly close to the contact between section 2 (Sect2) and the back section. Polymer solution could preferentially flow through the fracture and not exhibit significant resistance to flow.

4.4.4 Souchek Core

A thin section prepared from the SOU1 core showed the rock to be composed of coated grains and peloids thereby classifying it as a mixed skeletal packstone. The sediment was deposited in a fairly high energy, open marine environment. The rock is composed of calcite, ferroan calcite, and dolomite. Pellets or peloids were present mostly as micritized skeletal grains. Echinoids, foraminifera, brachiopods, ostracods, and coral were also found present. A bimodal distribution of well-rounded and well-sorted grains was found.

Section 1 of the core was extremely vuggy in comparison with the front section. The resistance and residual resistance factors for section 1 computed less than one and are not feasible. If no resistance to polymer flow and brine flow after polymer is assumed for section 1, (resistance and residual resistance factors equal to one), then low values in section 1 compared with values in the front section may be explained by the vuggy nature of section 1.

4.5 Scanning Electron Photomicroscopy (SEM)

4.5.1 Description

The SEM photographs called photomicrographs taken of core material and resin pore casts are presented at the end of this section. The photomicrographs are labelled at the bottom with the core name and section together in the left field, the magnification and correction factor in the center field, and the date in the right field. For example in Figure 4, DENK2B indicates the material was sampled from the back section of the laboratory core used for Denker core flood number 2 (DENK2). This core was cut from the Denker well reservoir material. The magnification used was 160/1.2 times or 133.3X. The dashed line at the bottom indicates the scale in the photomicrograph. Each white line is a measure of picture scale in micrometers and varies with magnification according to the following convention.

20 to 160X -100 micrometers per white line

320 to 2500X - 10 micrometers per white line

4.5.2 Denker Photomicrographs

Scanning electron photomicrographs for core material sampled from the Denker Well and flooded in the laboratory are shown in Figures 4.5A to 4.5E. The Denker core was composed of large (250 micrometers) rounded grains seen in Figure 4.5C and coarse calcite crystals visible in Figure 4.5D. Most of the grains were lined with fine calcite cement and were coated with a clay-sized (less than 1 micrometer) material. The cement lining is visible in Figure 4.5C

surrounding the large grain positioned to the right-of-center. Figures 4.5A and 4.5B show material from the front and back sections of the core used in flood DENK2. The average pore sizes of the material in the front section are larger and less uniform than pore sizes in the back section. The lower resistance and residual resistance factors measured in the front section of the core as listed in Table 4.12 correspond with the larger pore sizes viewed for the front section in the SEM photomicrographs.

Figure 4.5E is a photomicrograph of a resin pore cast made out of material from the back section of the core in DENK2 core flood. Void space in the photograph was previously carbonate grains and cement. Solid material is plastic remaining after dissolution of the rock. Four shapes of pore structure are visible in the micrograph. (1) A long tubular pore is visible in the upper-right quadrant. (2) Sheet-like pore connections between carbonate crystals can be seen in the center of the picture. (3) Smaller pores and pore connections between small crystals can be seen in the lower-right quadrant. (4) In the upper-left quadrant a large pore resembling the grain visible to the right-of-center in Figure 4.5C, has a very fine porous texture. This indicates the large, rounded grains may be composed of a fine calcite or microspar leaving the grains with a very microporous structure.

4.5.3 Brooks (Husky) Photomicrographs

Photomicrographs for core material sampled from the Brooks No. 6 Well and flooded in core HUSK1 in the laboratory are shown in Figures 4.6A to 4.6F. The predominant feature of the Brooks core was

the presence of very uniform pores depicted in Figure 4.6A in a matrix of small yet somewhat uniform calcite crystals and microspar visible in Figures4.6B and 4.6D. The uniform pores appear to be peloids which have been leached or dissolved from the rock. In Figure 4.6C, magnification of a pore reveals the circular void lined by secondary, calcite crystal growth.

Much of the pore system is not visible by viewing the rock directly. Figure 4.6E, a photomicrograph of a resin pore cast, shows a lobe-shaped pore network. On magnification in Figure 4.6F, the lobes consist of a mass of sheet-like pore connections. The resin cast of pores to the left-of-center in Figure 4.6F correspond to small pores and pore throats between the crystals occupying the center of the photograph in Figure 4.6C.

As indicated from the resin pore casts, much of the peloid shaped pores are not visible and are assumed to be lost during dissolution and SEM sample preparation. This indicated these larger pores are not the main source of porosity. Most of the porosity consists of small sheet-like micropores between microspar calcite. This would substantiate the very low permeabilities measured in the Brooks core. However, the resistance factors and residual resistance factors were not relatively large as might be expected.

4.5.4 Souchek Photomicrographs

Photomicrographs for the core sampled from the Souchek well and flooded in core flood SOU1 in the laboratory are shown in Figures 4.7A through 4.7F. Figures 4.7A and 4.7B show material sampled from the front and back sections of the SOU1 core.

Figure 4.7A shows the front section of the core to be very vuggy with irregularly shaped pores. The back section of the core is seen in Figure 4.7B to be very granular with regular pore sizes. The granular nature of the rock correlates with its description as a packstone (grainstone). Most of the grains are surrounded with lime mud (micrite) or microspar visible in Figure 4.7C. On magnification in Figure 4.7D, the small crystalline nature of the material indicates it to be microspar, or crystallized micrite. Resistance and residual resistance factors were not obtained for the back section of the core and no relationship between these values and porosity could be drawn.

A microporous system in addition to the larger pores and vugs is visible in Figures 4.7E and 4.7F. The pore connections between crystals appear sheet-like in shape.

4.5.5 Baker Dolomite Photomicrographs

Photomicrographs for the Baker dolomite core from BAK7 core flood are shown in Figure 4.8A through 4.8D. Figure 4.8A shows the rock is composed of both large crystals coated with a very fine micrite or microspar. On magnification of material from Section 2 of the BAK7 core in Figure 4.8B, these particles are actually small crystal overgrowths.

A pore cast of the Baker dolomite in Figure 4.8C gives evidence of a dual pore system. Both large, sheet-like pores between crystals and a small microporous system are visible. The microporous system was not visible in the thin section. As with the thin sections, the SEM photomicrographs did not show a relationship between resistance

and residual resistance factor and porosity for the baker dolomite.

4.5.6 Polyacrylamide Photomicrographs

Photomicrographs taken of evaporated polyacrylamide solutions prepared in distilled water and brine are shown in Figure 4.9A through 4.9C. Large aggregates of polymer ranging in size from 25 to 500 micrometers are visible in Figure 4.9A for polyacrylamide prepared in distilled water. Magnification of this polymer in Figure 4.8B showed a web-like structure. It is unknown whether the polymer aggregates were formed by the drying process or were present originally in solution. The web-like structure was not present for polyacrylamides dissolved in Brooks synthetic brine as shown in Figure 4.8C.

4.6 Mercury Porosimetry

The capillary pressure curves for core samples flooded with polymer in the laboratory are shown in Figures 4.10 through 4.14. Figure 4.14 is a capillary pressure curve for fired Berea sandstone presented for comparison with the carbonate materials. Graphed is the capillary pressure represented as the mercury injection pressure versus wetting phase or air saturation.

A tangent line drawn to the curve at the inflection point and extended to 100% air saturation gives the capillary pressure at which the nonwetting phase is present in the pore system as a continuous phase [11]. Based on this, it is assumed that the pore throat diameter computed from this pressure indicates the size of a significant number of pore throats. These pressures and pore throat diameters are listed

in Table 4.13 for each sample tested.

Pore throat diameters were computed assuming the throats are circular in nature. The SEM photomicrographs of the pore casts indicated many of the pore connections to be sheet-like. If the capillary pressure equation is modified to consider the pore throat and the space between parallel plates [61], pore diameters one-half the tabulated values are obtained. The mercury porosimetry measurements were able to account for the microporosity not visible in the thin sections and SEM photomicrographs of the rock.

The capillary pressure curve for Baker dolomite did not correspond with one obtained by Meister [34] for the same material. The second inflection point was not present in Meister's curve. Baker dolomite, a quarry material, may not be uniform in properties similar to Berea sandstone.

Pore size distributions for the Souchek and Denker cores flooded in the laboratory corresponded with resistance factor and residual resistance factor measurements made on these cores. For the DENK2 core, pore sizes of 5 and 10 micrometers measured for the Front and Back sections correspond with resistance factors of 4 and 3 measured at 250 ppm polymer concentration. Resistance factors of 4 and 4.75 for the Front and Back of DENK2 did not correspond with pore size as did the factors measured at the lower polymer concentration. Resistance and residual resistance factors for the Back section of the SOU1 core were determined to be less than one and these values could not be compared with pore sizes. The larger the pore throat diameters, the lower the resistance factor and residual resistance factor. The pore throat diameters deter-

mined for the Brooks core were not significantly different to distinguish polymer resistance behavior. The resistance and pore size behavior for the Baker dolomite core was opposite; low resistance in section with smaller pore throats. However, the bimodal pore size distribution in the Baker dolomite may complicate resistance effects.

Table 4.13 Pore Throat Diameters for Laboratory Core Samples.

CORE	CAPILLARY PRESSURE (kPa)	(psia)	DIAMETER (Hg) (μm)
DENK2F1	21.7	3.2	4.8
DENK2B	11.0	1.6	9.5
HUSK1F1	117.2	17.0	0.9
HUSK1B	100.0	14.5	1.1
SOU1F	34.5	5.0	3.0
SOU11B	16.6	2.4	6.3
BAK7F*	15.7	2.2	6.9
	4.8	0.7	21.7
BAK72*	30.7	4.5	304
	4.1	0.6	25.4
BEREA	35.9	5.2	2.9

bimodal pore size distribution

4.5A

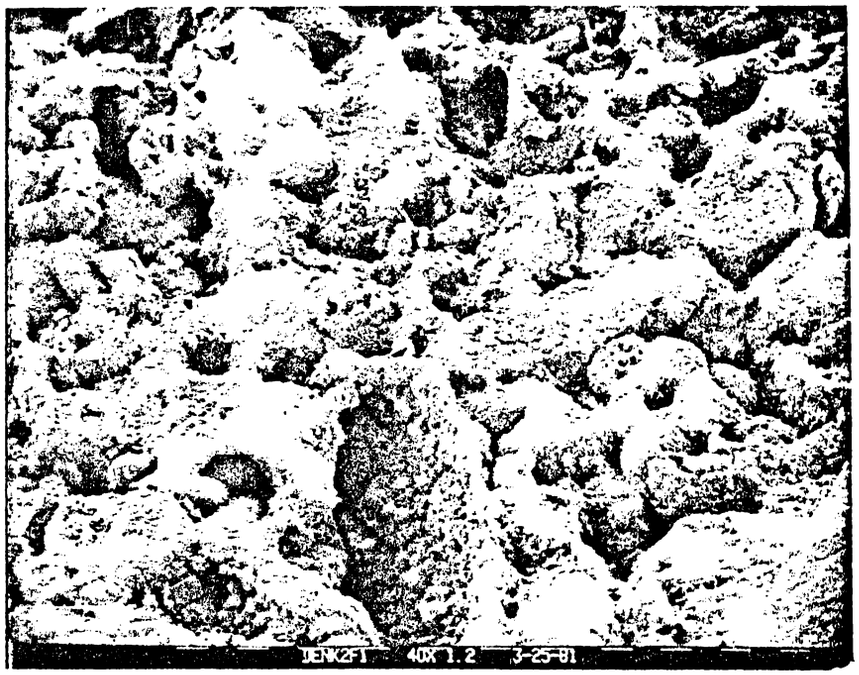

4.5B

Figure 4.5A-E SEM Photomicrographs of Denker Core.

4.5C

4.5D

4.5E

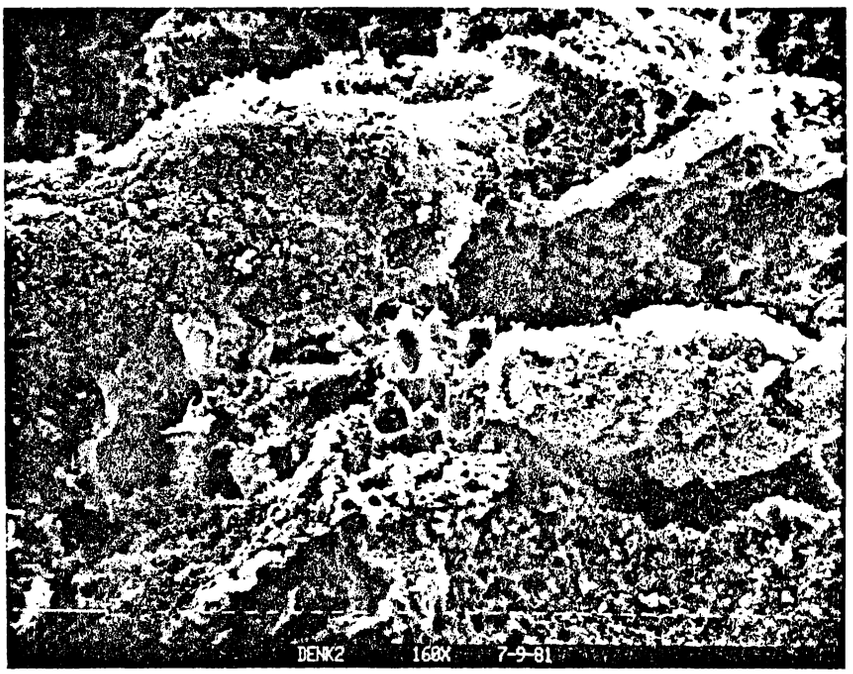

4.6A

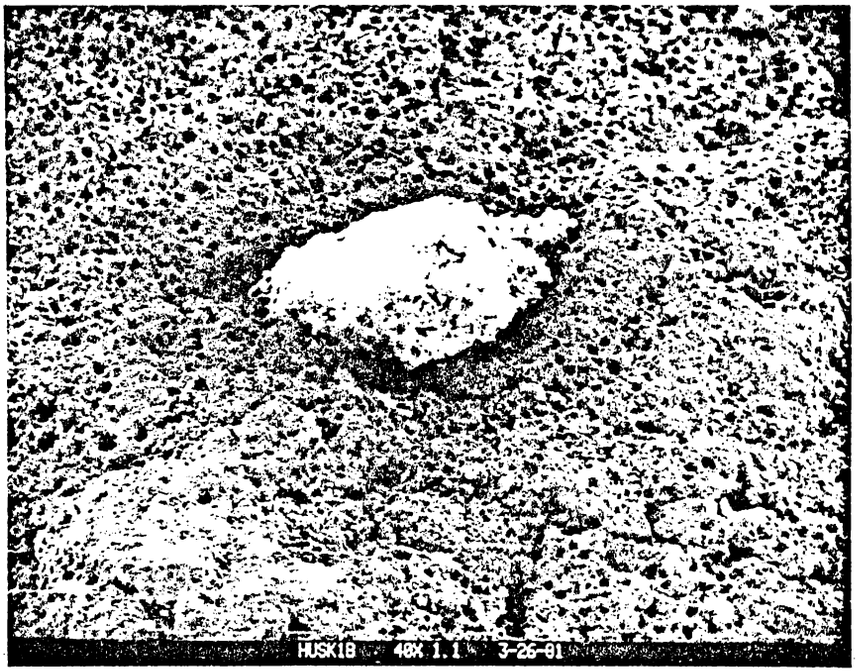

4.6B

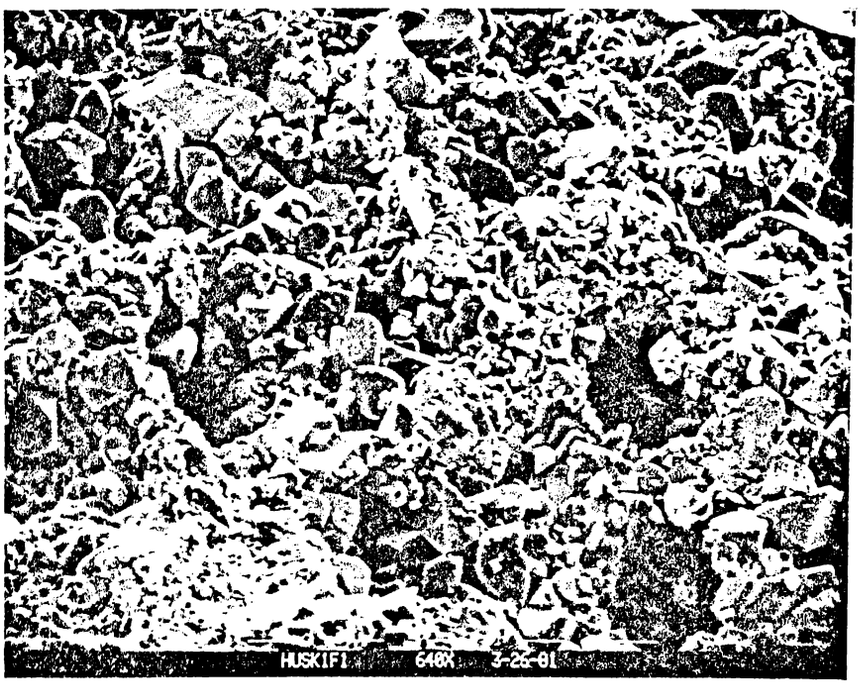

Figure 4.6A-F SEM Photomicrographs of Brooks Core.

4.6C

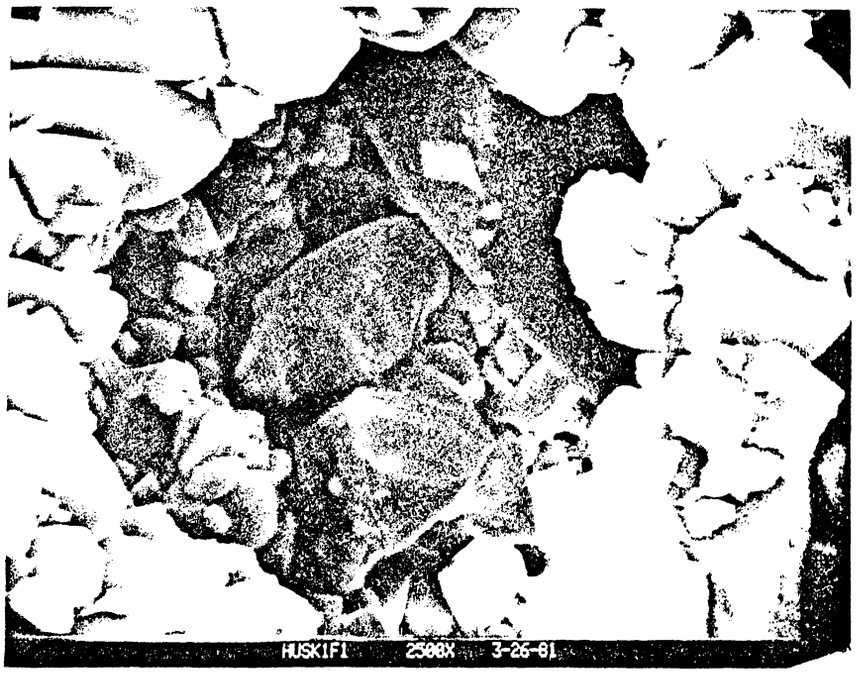

4.6D

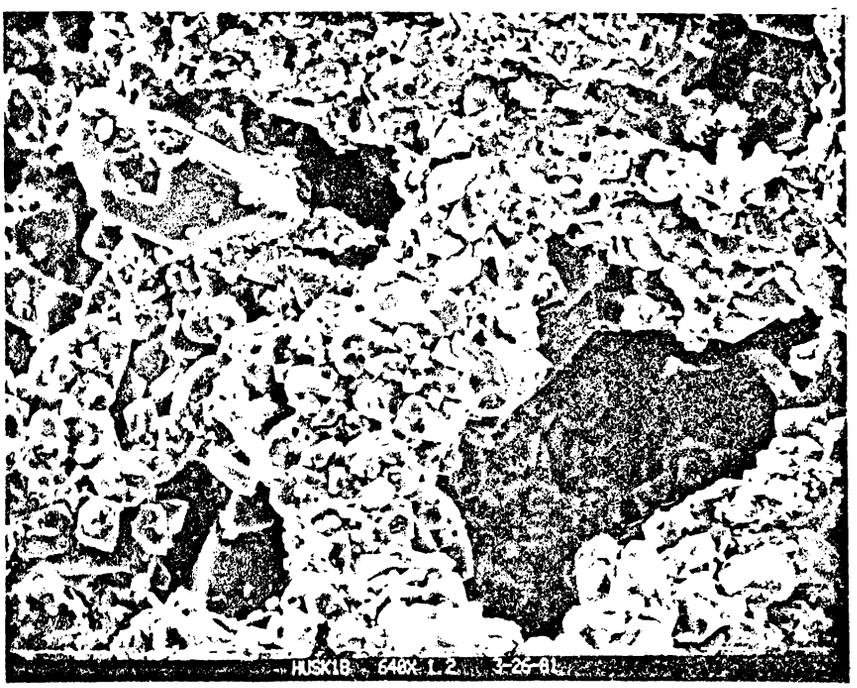

4.6E

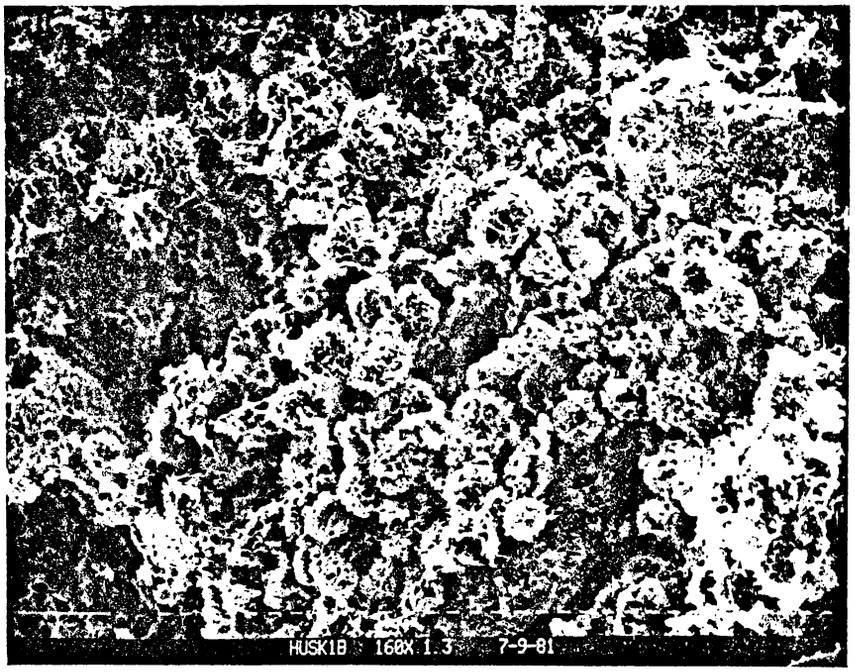

4.6F

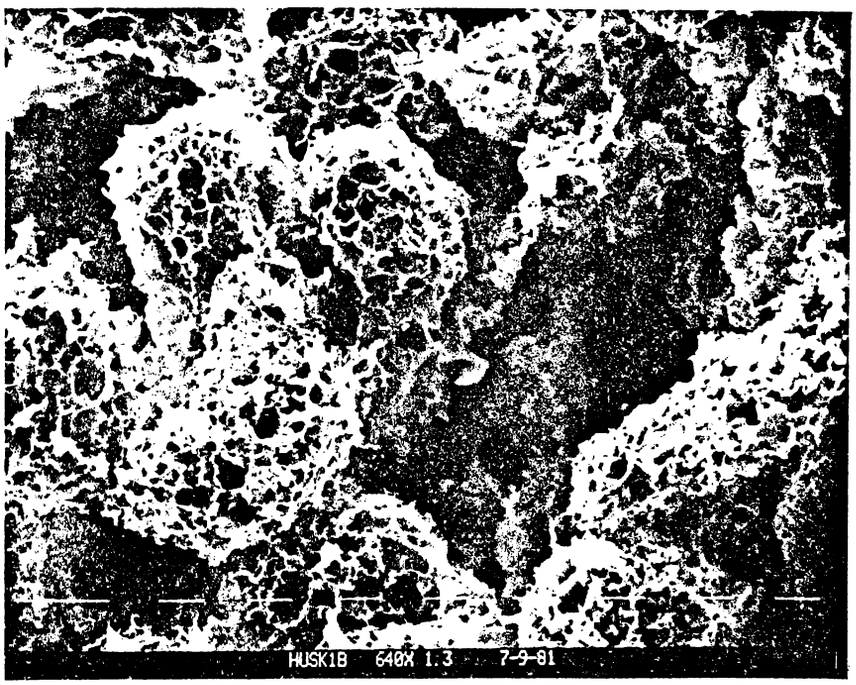

4.7A

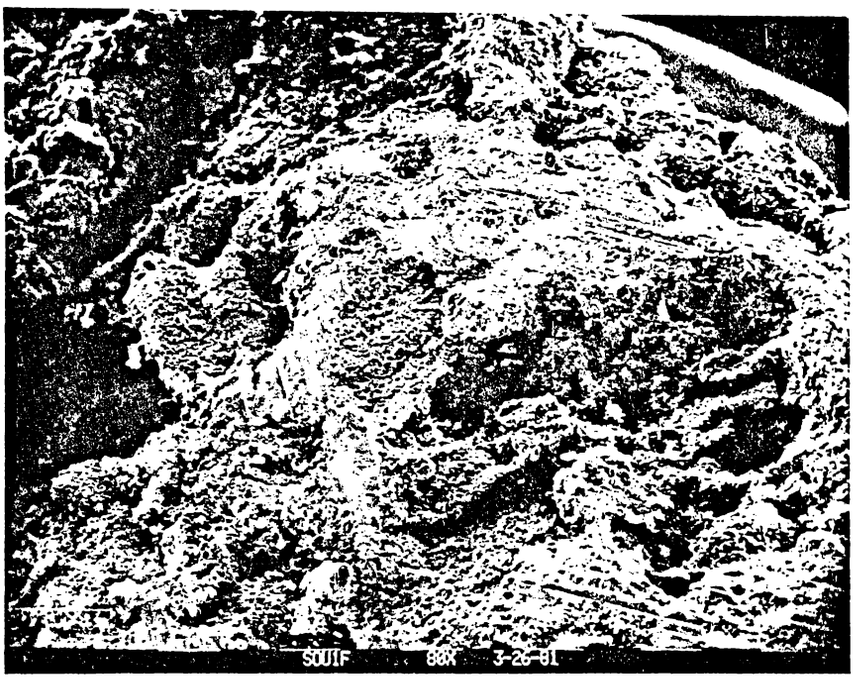

4.7B

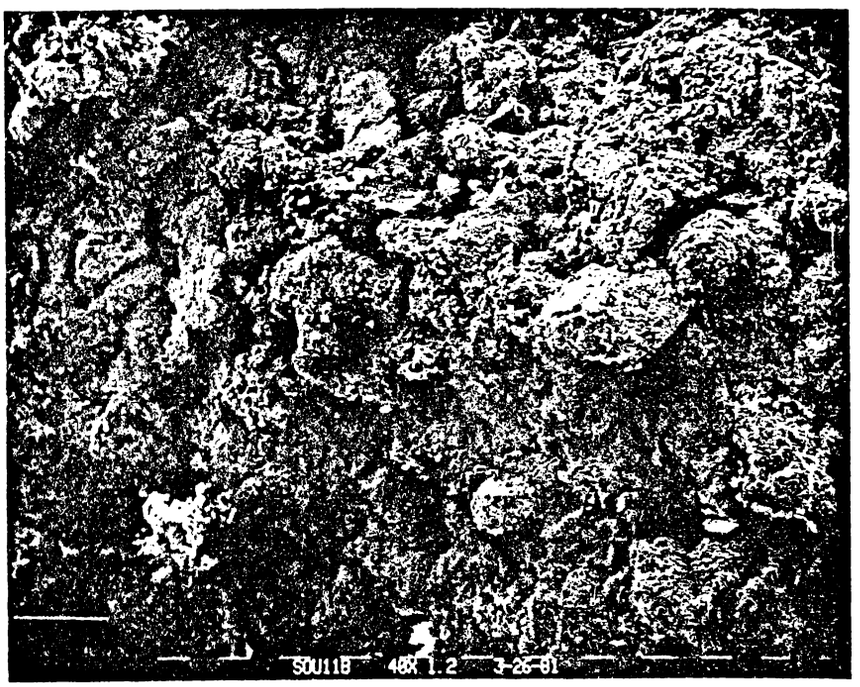

Figure 4.7A-F SEM Photomicrographs of Souchek Core.

4.7C

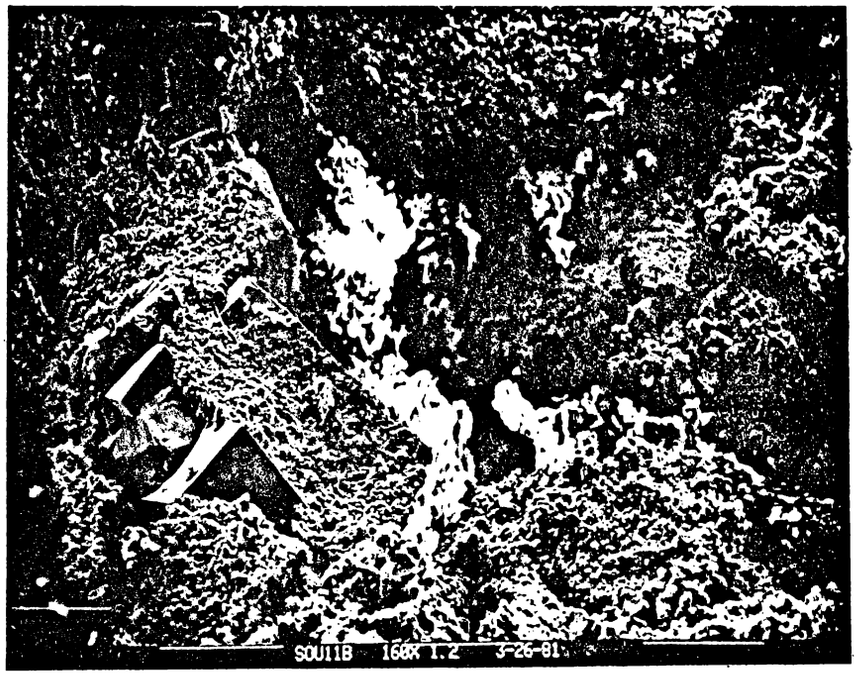

4.7D

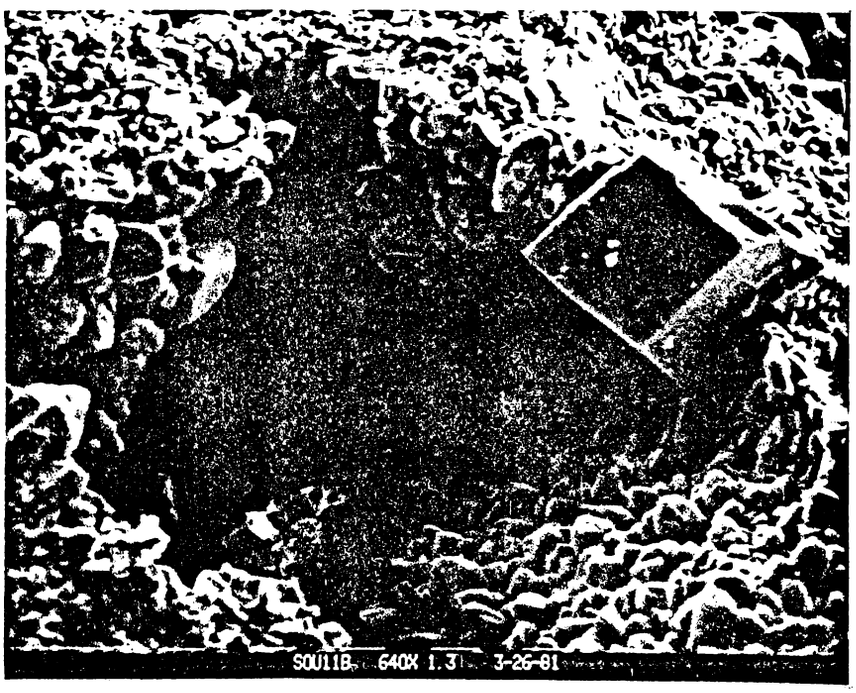

4.7E

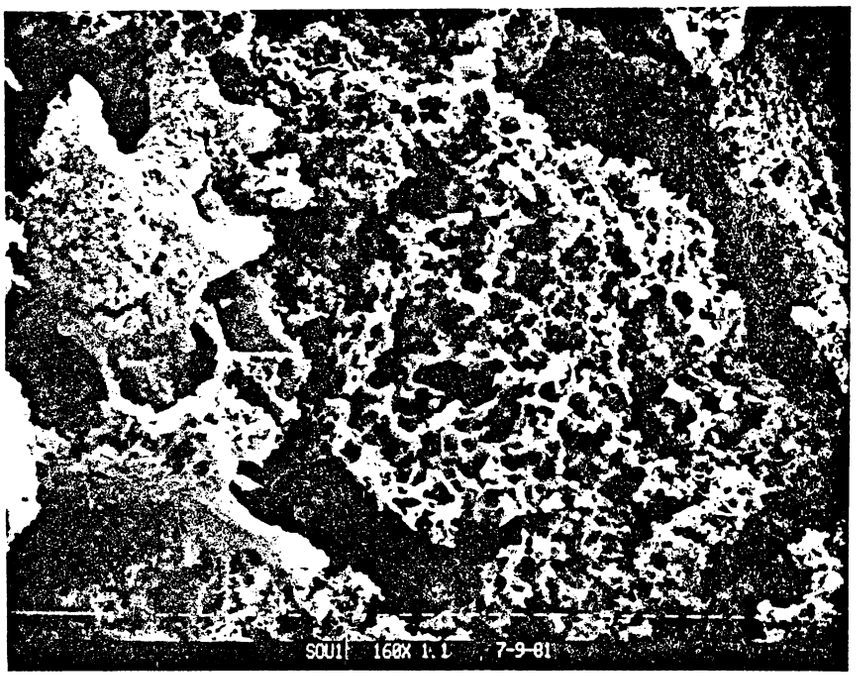

4.7F

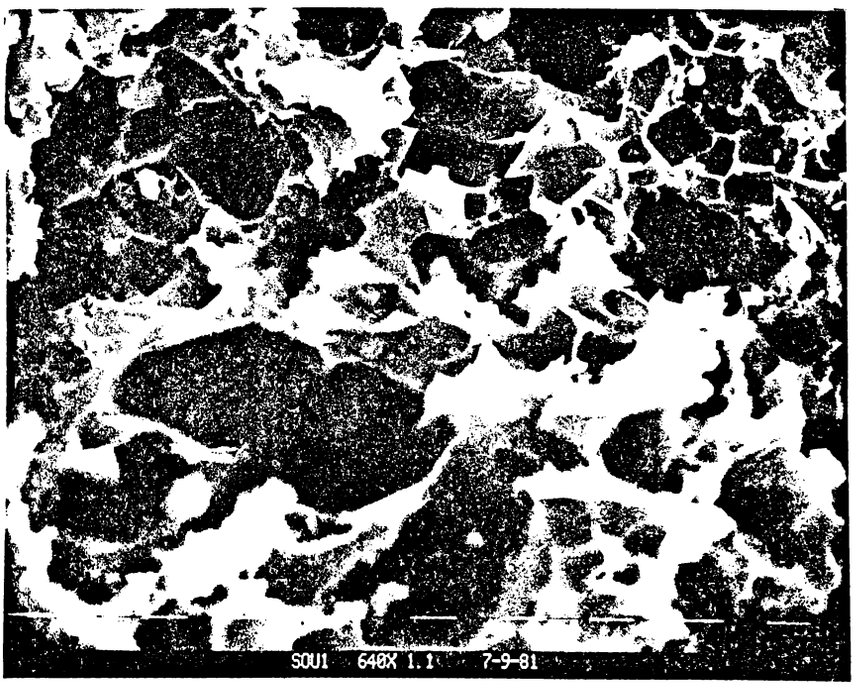

4.8A

4.8B

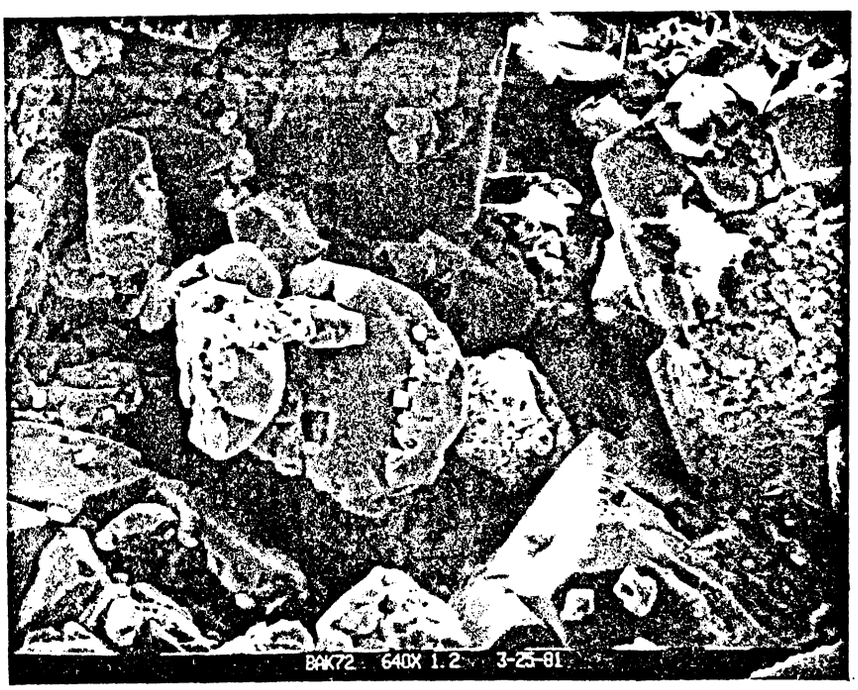

Figure 4.8A-C SEM Photomicrographs of Baker Dolomite.

4.8C

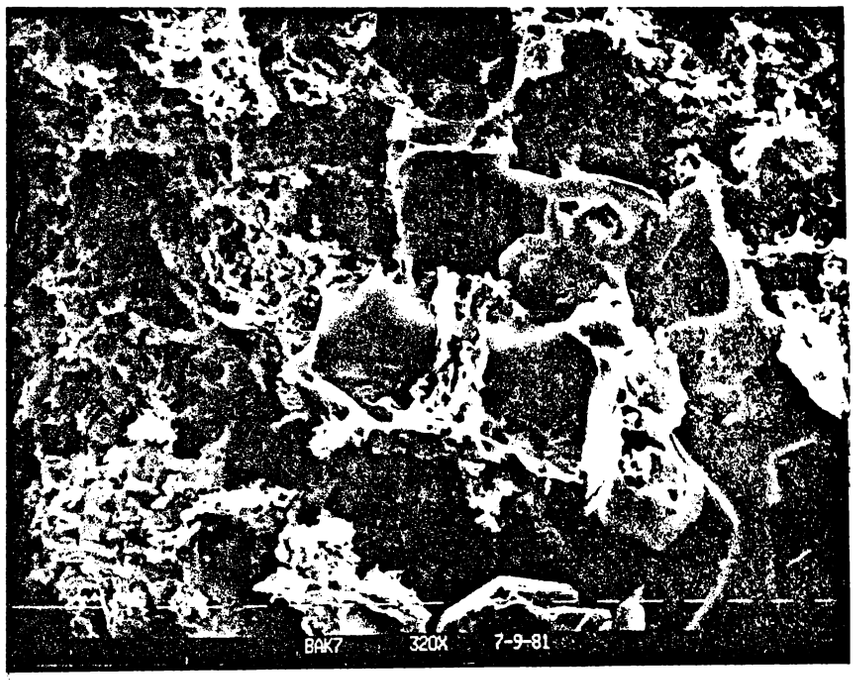

4.9A

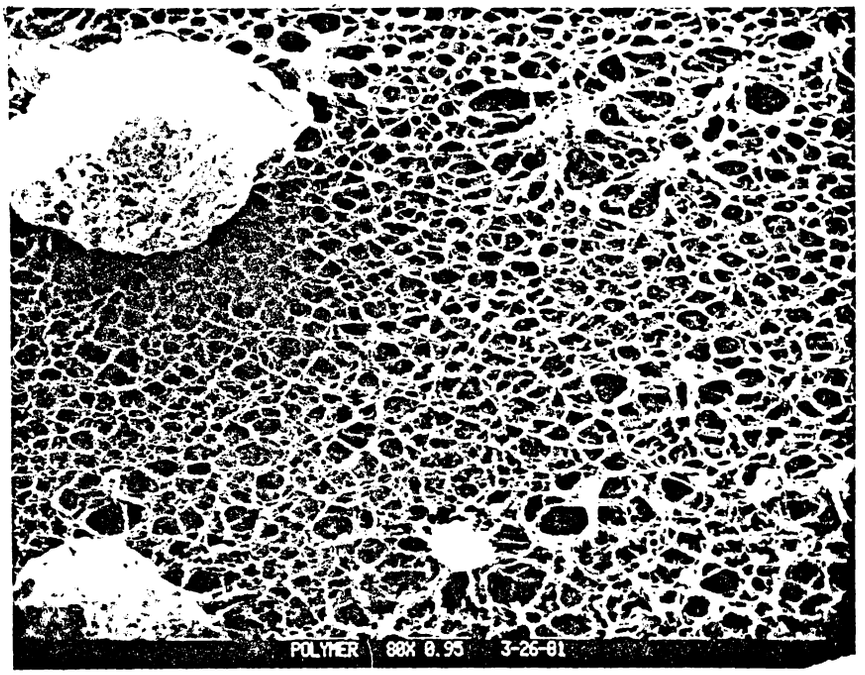

4.9B

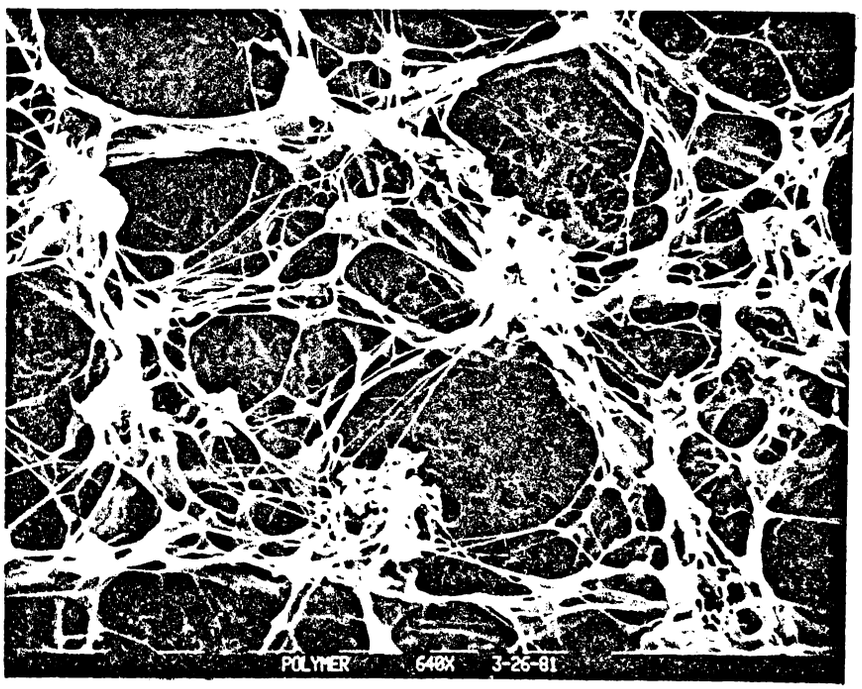

Figure 4.9A-C SEM Photomicrographs of Polyacrylamide Polymer.

4.9C

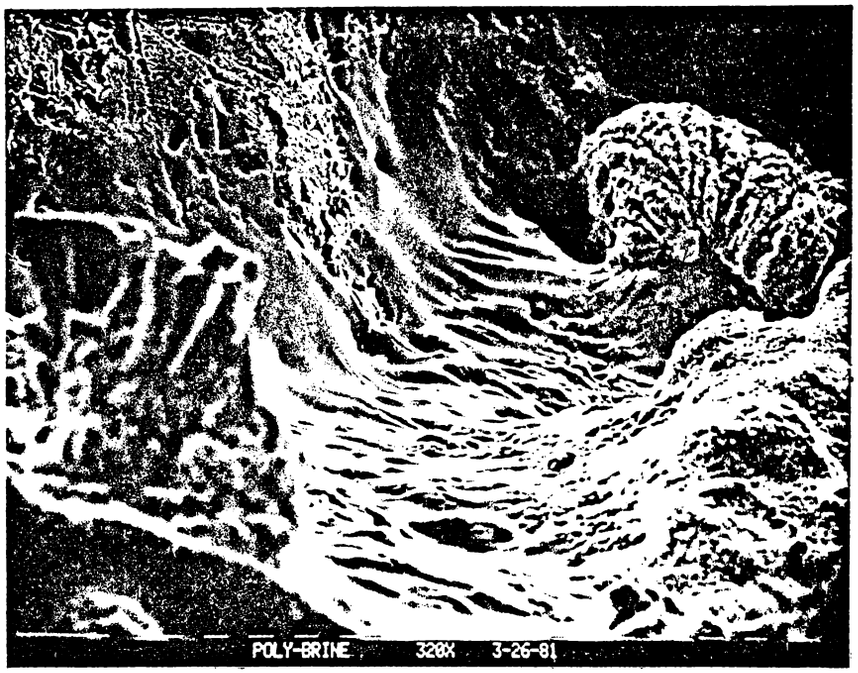

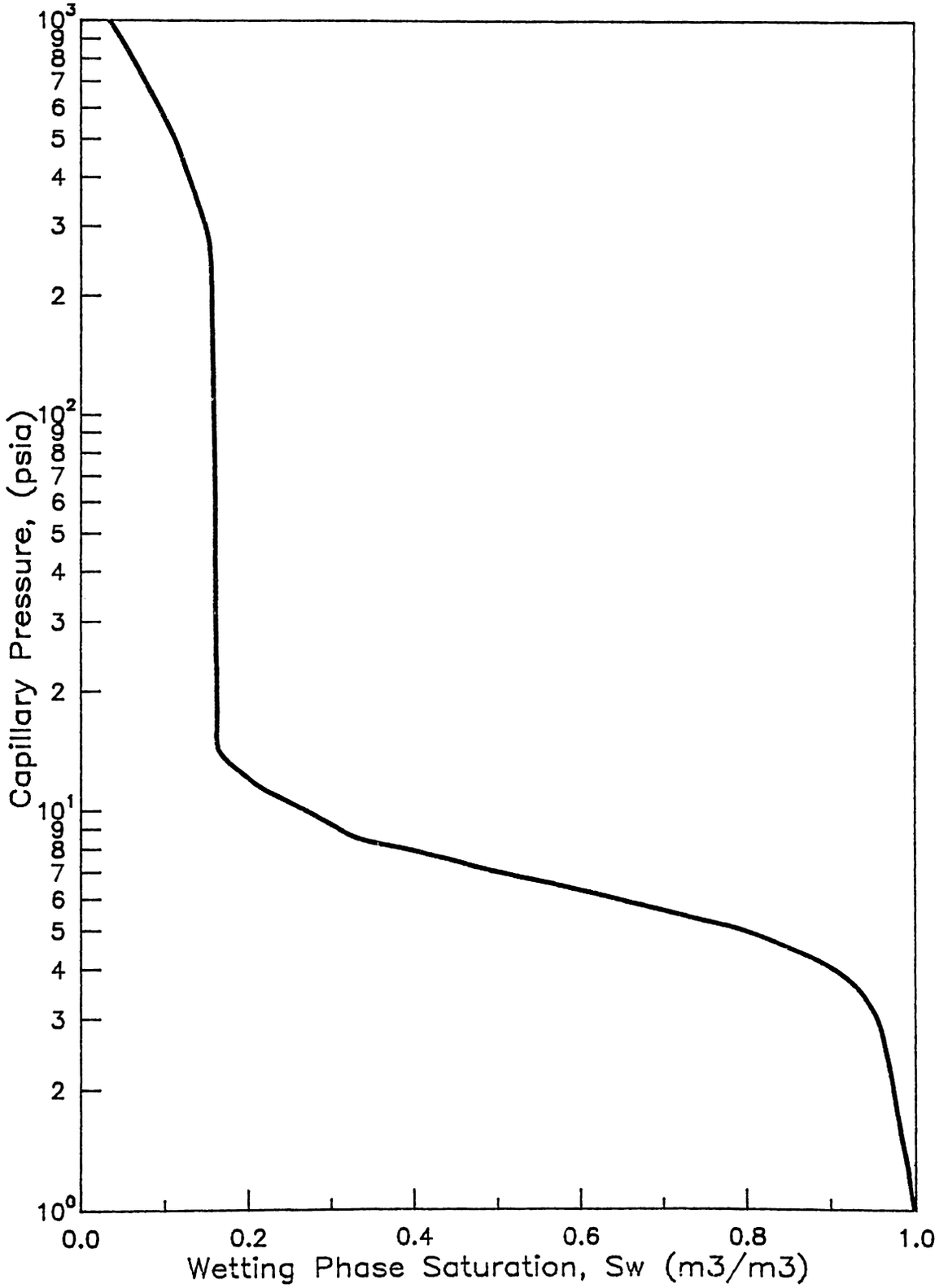

FIGURE 4.10 CAPILLARY PRESSURE CURVE FOR DENK2 CORE

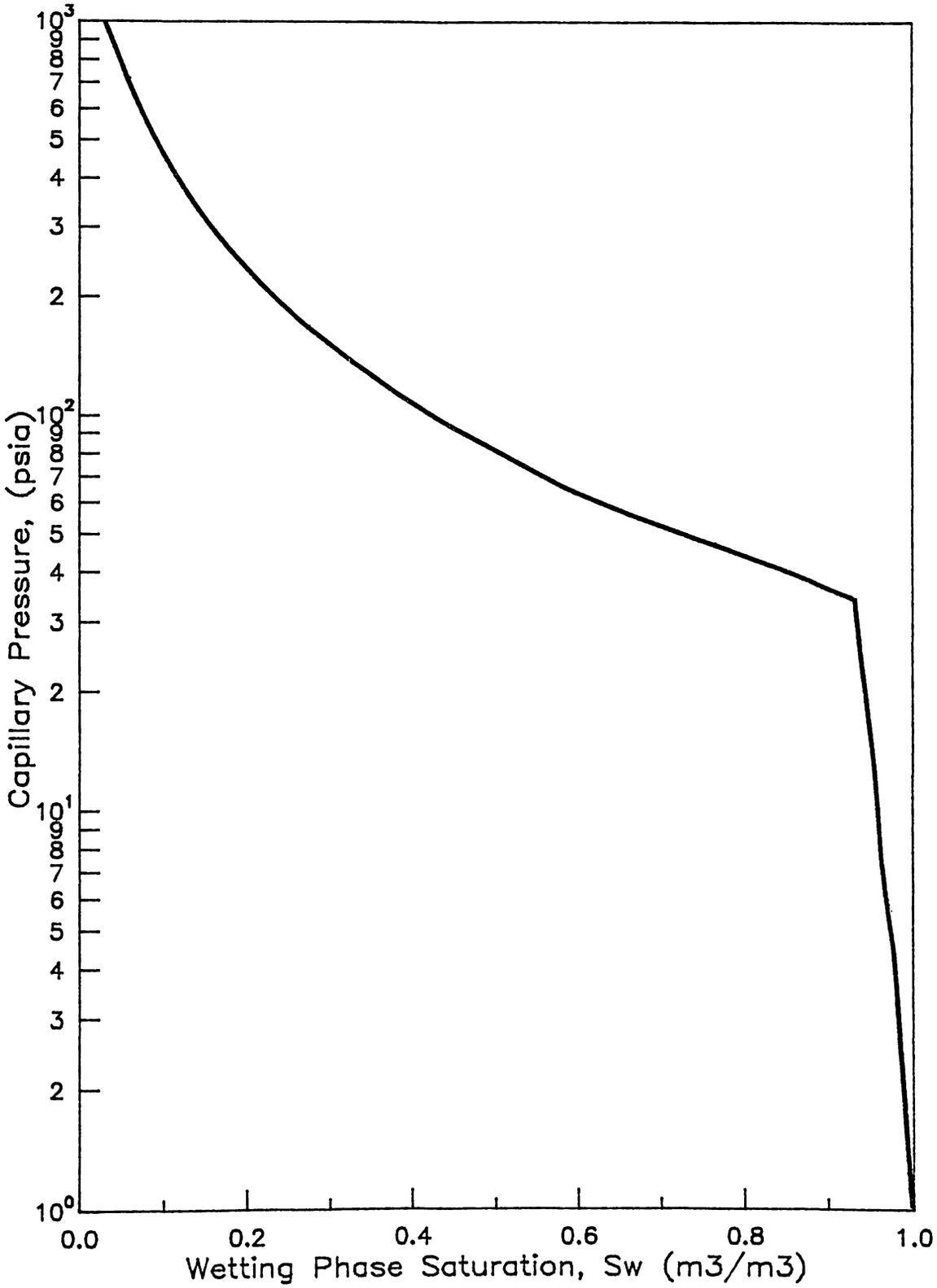

FIGURE 4.11 CAPILLARY PRESSURE CURVE FOR HUSK1 CORE

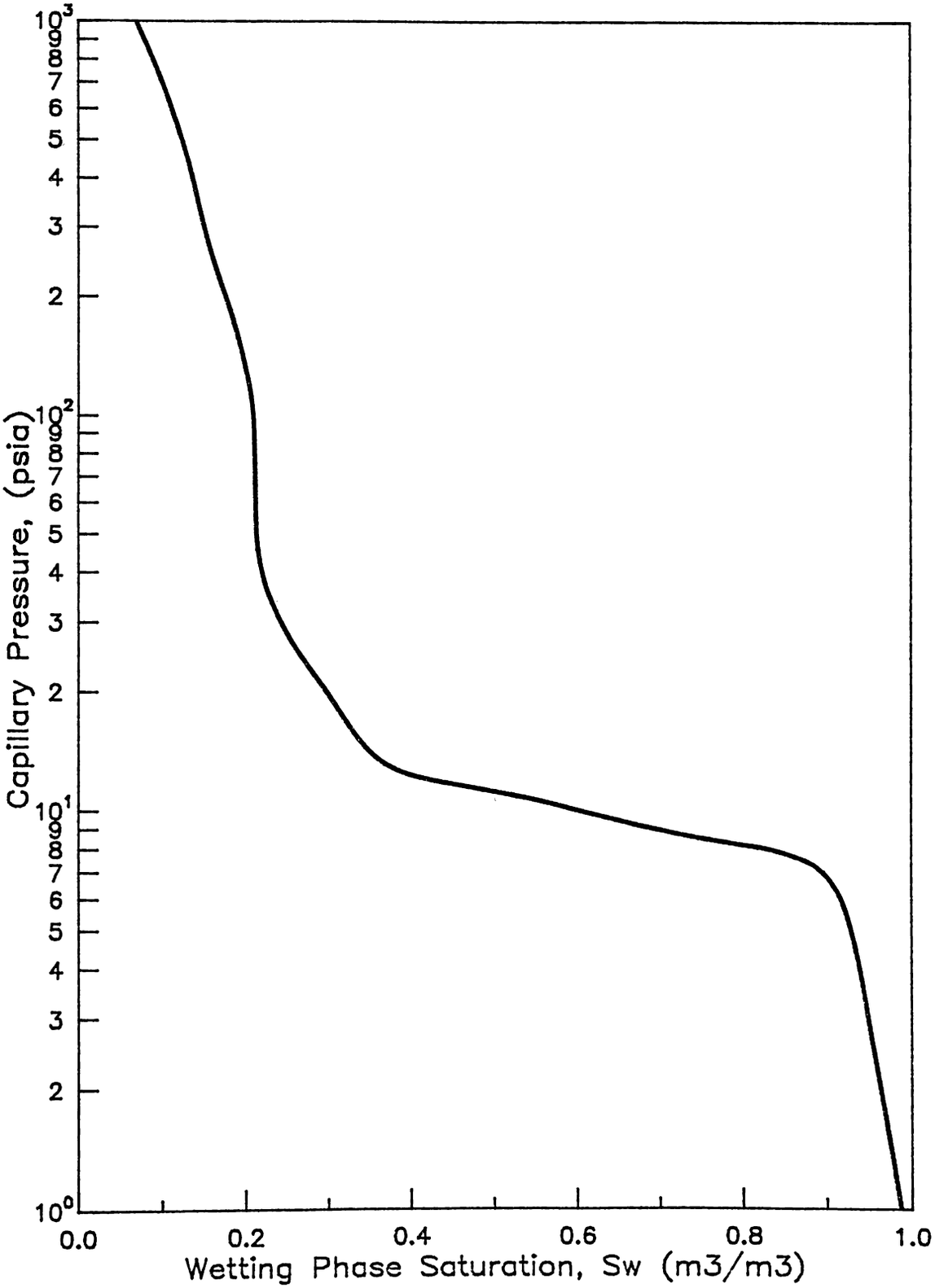

FIGURE 4.12 CAPILLARY PRESSURE CURVE FOR SOU1 CORE

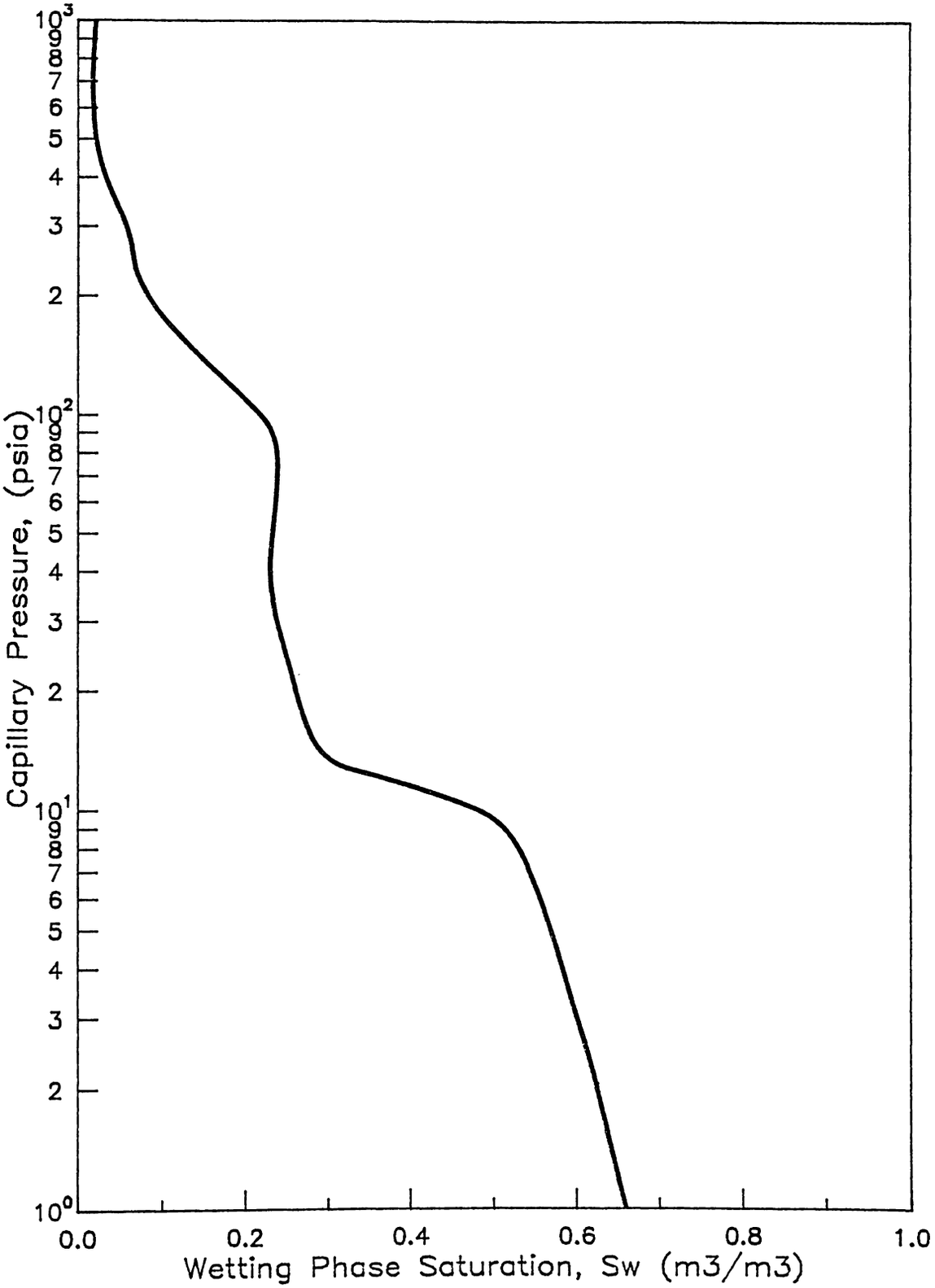

FIGURE 4.13 CAPILLARY PRESSURE CURVE FOR BAK7 CORE

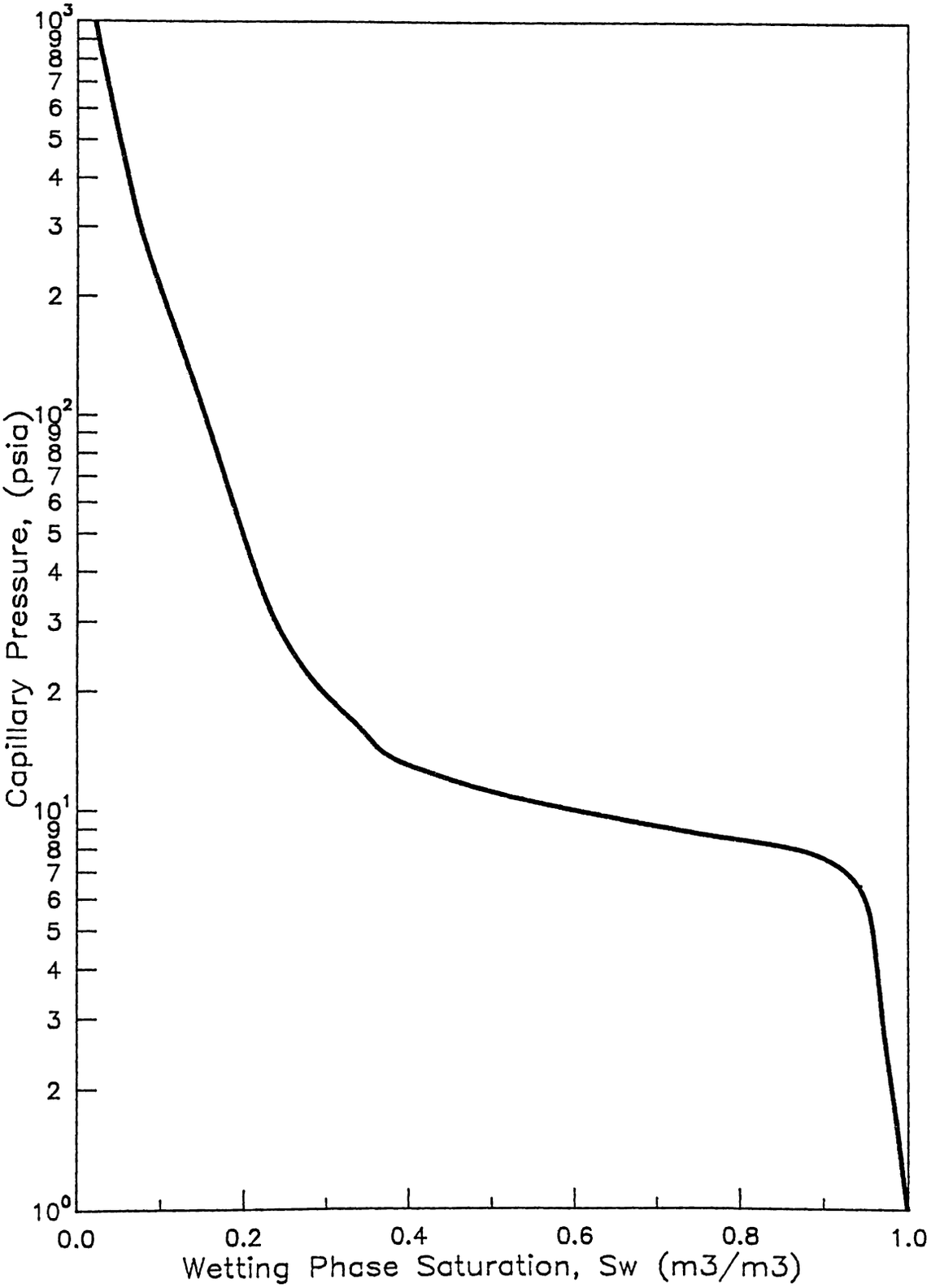

FIGURE 4.14 CAPILLARY PRESSURE CURVE FOR BEREA SANDSTONE

CHAPTER 5

Conclusions and Recommendations

Outlined in this report was an experimental program designed to (1) investigate polymer stability in brines typical of Kansas reservoirs, (2) measure resistance factors and residual resistance factors of polyacrylamide solutions in carbonate rocks, and (3) relate polymer flow behavior with carbonate geology through thin-section, SEM, and mercury porosimetry techniques. Based on this work, conclusions and recommendations are presented.

5.1 Conclusions

(1) Polyacrylamides which tolerate brines of high sodium and calcium content are commercially available.

(2) Significant resistance was generated in carbonates by an unhydrolyzed, cationic polyacrylamide. The resistance factor for this polyacrylamide in carbonate rocks will be on the average between 1 and 14.

(3) Baker dolomite was not as uniform as expected.

(4) Resistance factors and residual resistance factors measured in carbonate materials were extremely variable.

(5) Resistance and residual resistance factors measured in carbonate rocks were much larger than values measured in Berea sandstone. Values in Berea sandstone were also much less variable.

5.2 Recommendations

(1) Polymers found not stable in brine mixtures of salinities tested in this research program can be investigated at lower salinities.

(2) Polymers found stable can be tested in brine mixtures containing combinations of sodium, calcium, and magnesium ion salts.

(3) The effects of other constituents present in reservoir field brines such as iron can be tested on polyacrylamides.

(4) Polymer-brine stability can be tested further by measuring solution viscosities over periods of time.

(5) The flow behavior of other polymers not tested can be studied in carbonate core flood experiments.

(6) Polymer effluent concentrations and pH can be monitored during core flood experiments to study rock matrix-fluid interactions.

(7) Pressure taps can be located around the core circumference to investigate effects of core heterogeneities.

References

1. Akstinat, M.H., "Polymers For Enhanced Oil Recovery in Reservoirs of Extremely High Salinites and High Temperatures," paper SPE 8977 presented at the 5th International Symposium on Oilfield and Geothermal Chemistry, Stanford, Ca., (28-30 May 1980).

2. Bird, B.R., Stewart, W.E., and Lightfoot, E.N., Transport Phenomena, (1960), John Wiley and Sons, Inc., p. 4.

3. Black, J.T., "The Scanning Electron Microscope: Operating Principles," Principles and Techniques of Scanning Electron Microscopy, (1975), I, M.A. Hayat, Van Nostrand Reinhold Co..

4. Burcik, E.J., "Microgel in Polyacrylamide Solutions and Its Role in Mobility Control," Producers Monthly, (September 1968), 32, No. 9, p. 12-14.

5. Burcik, E.J., "Pseudo Dilatant Flow of Polyacrylamide Solutions on Porous Media," Producers Monthly, (March 1967), 31, No. 3, p. 27.

6. Burcik, E.J., "A Note on the Flow Behavior of Polyacrylamide Solutions in Porous Media," Producers Monthly, (June 1965), 29, No. 6, p. 14-16.

7. Burcik, E.J., "The Mechanism of Microgel Formation in Partially Hydrolyzed Polyacrylamide," Journal of Petroleum Technology, (April 1969), 21, No. 4, p. 373-374.

8. Burcik, E.J., and Thakur, G.C., "Some Reactions of Microgel in Polyacrylamide Solutions," Journal of Petroleum Technology, (May 1974), 26, No. 5, p. 545-549.

9. Chang, H.L., "Polymer Flooding Technology -- Yesterday, Today, and Tomorrow," Journal of Petroleum Technology, (August 1978), 30, No. 8, p. 1113-1128.

10. Chatterji, J., and Borchardt, J.K., "Applications of Water-Soluble Polymers in the Oilfield," paper SPE 9288 presented at the Annual Fall Technical Conference and Exhibition of the Society of Petroleum Engineers of AIME, Dallas, Tx. (21-24 September 1980).

11. Chilingar, G.V., Mannon, R.W., and Rieke, H.H. III, Oil and Gas Production from Carbonate Rocks, (1972), American Elsevier Publishing Company, Inc., New York, p. 1-82, 340-354.

12. Choquette, P.W., and Pray, L.C., "Geologic Nomenclature and Classification of Porosity in Sedimentary Carbonates," American Association of Petroleum Geologists Bulletin, (February 1970), 54, No. 2, p. 207-250.

13. Craig, F.F. Jr., The Reservoir Engineering Aspects of - Waterflooding, Monograph, Henry L. Doherty Series, SPE of AIME, (1971), 3, No. New York, Dallas, p. 69.

14. Dauben, D.L., and Menzie, D.E., "Flow of Polymer Solutions through Porous Media," Journal of Petroleum Technology, Petroleum Transactions, (August 1967), 19, No. 8, p. 1065-1073.

15. Davison, P., and Mentzer, E., "Polymer Flooding in North Sea Oil Reservoirs," paper SPE 9300 presented at the 55th Annual Fall Technical Conference and Exhibition of the Society of Petroleum Engineers of AIME, Dallas, Texas, (21-24 September 1980).

16. Dawson, R., and Lantz, R.B., "Inaccessible Pore Volume in Polymer Flooding," Society of Petroleum Engineers Journal, (October 1972), 12, No. 5, p. 448-452.

17. Dominguez, J.G., and Willhite, G.P., "Rentention and Flow Characteristics of Polymer Solutions in Porous Media," Society of Petroleum Engineers Journal, (April 1977), 17, No. 2, p. 111-121.

18. Drake, L.C., and Ritter, H.L., "Macropore - Size Distributions in Some Typical Porous Substances," Industrial and Engineering - Chemistry, Analytical Edition, (December 1945), 17, No. 12, p. 787-791.

19. Dunham, R.J., "Classification of Carbonate Rocks According to Depositional Texture," Classification of Carbonate Rocks,a symposium, Memoir 1, (1962), American Association of Petroleum Geologists, Tulsa, Ok., p. 108-121.

20. Feray, D.E., Heuer, E., and Hewatt, W.G., "Biological, Genetic, and Utilitarian Aspects of Limestone Classification," Classification of Carbonate Rocks,a symposium, Memoir 1, (1962), American Association of Petroleum Geologists, Tulsa, Ok., p. 20-32.

21. Folk, R.L., "Practical Petrographic Classification of Limestones," American Association of Petroleum Geologists Bulletin, (January 1959), 43, No. 1, p. 1-38.

22. Folk, R.L., "Spectral Subdivision of Limestone Types," Classification of Carbonate Rocks, a symposium, Memoir 1, (1962), American Association of Petroleum Geologists, Tulsa, Ok., p. 62-84.

23. Gogarty, W.B., "Mobility Control wtih Polymer Solutions," Society of Petroleum Engineers Journal, (June 1967), 7, No. 2, p. 161-173.

24. Ham, W.E., and Pray, L.C., "Modern Concepts and Classifications of Carbonate Rocks," Classification of Carbonate Rocks, a symposium,

Memoir 1, (1962), American Association of Petroleum Geologists, Tulsa, Ok., p. 2-19.

25. Horowitz, A.S., and Potter, P.E., Introductory Petrography of - Fossils, (1971), Springer - Verlag, New York, p. 1-19.

26. Jardine, D., Andrews, D.P., Wishart, J.W., and Young, J.W., "Distribution and Continuity of Carbonate Reservoirs," Journal of Petroleum Technology, (July 1977), 29, No. 7, p. 873-885.

27. Jennings, R.R., Rogers, J.H., and West, T.J., "Factors Influencing Mobility Control By Polymer Solutions," Journal of Petroleum Technology, (March 1971), 23, No. 3, p. 391-401.

28. Knight, B.L., "Reservoir Stability of Polymer Solutions," Journal of Petroleum Technology, (May 1973), 25, No. 5, p. 618-626.

29. Krynine, P.D., "The Megascopic Study and Field Classification of Sedimentary Rocks," Journal of Geology, (1948), 56, No. 2, p. 130-156.

30. Leighton, M.W., and Pendexter, C., "Carbonate Rock Types," Classification of Carbonate Rocks,a symposium, Memoir 1, (1962), Memoir 1, No. American Association of Petroleum Geologists, Tulsa, Ok., p. 33-61.

31. Lynch, E.J., and MacWilliams, D.C., "Mobility Control with Partially Hydrolyzed Polyacrylamide--A Reply to Emil Burcik," Journal of Petroleum Technology, (October 1969), 21, No. 10, p. 1247-1248.

32. Maerker, J.M., "Mechanical Degradation of Partially Hydrolyzed Polyacrylamide Solutions in Unconsolidated Porous Media," Society of Petroleum Engineers Journal, (August 1976), 16, No. 4, p. 172-174.

33. Maerker, J.M., "Shear Degradation of Partially Hydrolyzed Polyacrylamide Solutions," Society of Petroleum Engineers Journal, (August 1975), 15, No. 4, p. 311-322.

34. Meister, J.J., "A Porous, Permeable Carbonate for Use in Oil Recovery Experiments," Journal of Petroleum Technology, (November 1978), 30, No. 11, p. 1632-1634.

35. Meister, J.J., and Butler, G.B., "Retention of Polyacrylamide by Berea Sandstone, Baker Dolomite, and Sodium Kaolinite During Polymer Flooding," paper SPE 8981 presented at the 5th International Symposium on Oilfield and Geothermal Chemistry, Stanford, Ca., (28-30 May 1980).

36. Mentzer, E., and Meldrum, I.G., to be published in Journal of Polymer Science, cited from reference 15, (1980).

37. Morris, C.W., and Jackson, K.M., "Mechanical Degradation of Polyacrylamide Solutions in Porous Media," paper SPE 7064 presented at the 5th Symposium on Improved Methods for Oil Recovery of the Society of Petroleum Engineers of AIME, Tulsa Ok., (16-19 April 1978).

38. Mungan, N., "Shear Viscosities of Ionic Polyacrylamide Solutions," Society of Petroleum Engineers Journal, (December 1972), 12, No. 6, p. 469-473.

39. Mungan, N., "Rheology and Adsorption of Aqueous Polymer Solutions," Journal of Canadian Petroleum Technology, (April - June 1969), 8, No. 2, p. 45-50.

40. Mungan, N., Smith, F.W., and Thompson, J.L., "Some Aspects of Polymer Floods," Journal of Petroleum Technology Petroleum Transactions, (September 1966), 18, No. 9, p. 1143-1150.

41. Needham, R.B., Threlkeld, C.B., and Gall, J.W., "Control of Water Mobility Using Polymers and Multivalent Cations," paper SPE 4747 presented at the Improved Oil Recovery Symposium of the Society of Petroleum Engineers of AIME, Tulsa, Ok., (1974).

42. Pittman, E.D., "Microporosity in Carbonate Rocks," American - Association of Petroleum Geologists Bulletin, (October 1971), 55, No. 10, p. 1873-1881.

43. Pittman, E.D., and Duschatko, "Use of Pore Casts and Scanning Electron Microscope to Study Pore Geometry," Journal of - Sedimentary Petrology, (December 1970), 40, No. 4, p. 1153-1157.

44. Pittman, E.D., and Thomas, J.B., "Some Applications of Scanning Electron Microscopy to the Study of Reservoir Rock," Journal of Petroleum Technology, (November 1979), 31, No. 11, p. 1375-1380.

45. Purcell, W.R., "Capillary Pressures -- Their Measurement Using Mercury and the Calculation of Permeability Therefrom," Petroleum Transactions,AIME, (February 1949), p. 39-48.

46. Pye, D.J., "Improved Secondary Recovery by Control of Water Mobility," Journal of Petroleum Technology, Petroleum - Transactions, (August 1964), 16, No. 8, p. 911-916.

47. Ritter, H.L., and Drake, L.C., "Pore-Size Distribution in Porous Materials Pressure Porosimeter and Determination of Complete Macropore - Size Distributions," Industrial and Engineering - Chemistry, Analytical Edition, (December 1945), 17, No. 12, p. 782-786.

48. Sandiford, B.B., "Laboratory and Field Studies of Water Floods Using Polymer Solutions to Increase Oil Recoveries," Journal of - Petroleum Technology, Petroleum Transactions, (August 1964), 16,

No. 8, p. 917-922.

49. Scholle, P.A., A Color Illustrated Guide to Carbonate Rock - Constituents, Textures, Cements, and Porosities, Memoir 27, (1978), Rodgers Litho, Tulsa, Ok..

50. Seright, R.S., "The Effects of Mechanical Degradation and Viscoelastic Behavior on Injectivity of Polyacrylamide Solutions," paper SPE 9297 presented at the Annual Fall Technical Conference and Exhibition of the Society of Petroleum Engineers of AIME, Dallas, Tx., (21-24 September 1980).

51. Shah, B.N., Willhite, G.P., and Green, D.W., "The Effect of Inaccessible Pore Volume on the Flow of Polymer and Solvent Through Porous Media," paper SPE 7586 presented at the 53rd Annual Fall Technical Conference and Exhibition of the Society of Petroleum Engineers of AIME, Houston, Tx., (1-3 October 1978).

52. Shupe, R.D., "Chemical Stability of Polyacrylamide Polymers," paper SPE 9299 presented at the 55th Annual Fall Technical Conference and Exhibition of the Society of Petroleum Engineers of AIME, Dallas, Tx., (21-24 September 1980).

53. Smith, F.W., "The Behavior of Partially Hydrolyzed Polyacrylamide Solutions in Porous Media," Journal of Petroleum Technology, (February 1970), 22, No. 2, p. 148-156.

54. Sparlin, D.D., "An Evaluation of Polyacrylamides for Reducing Water Production," Journal of Petroleum Technology, (August 1976), 28, No. 8, p. 906-914.

55. Swanson, B.F., "Visualizing Pores and Nonwetting Phase in Porous Rock," Journal of Petroleum Technology, (January 1979), 31, No. 1, p. 10-18.

56. Szabo, M.T., "An Evaluation of Water-Soluble Polymers for Secondary Oil Recovery--Part 1," Journal of Petroleum Technology, (May 1979), 31, No. 5, p. 553-560.

57. Szabo, M.T., "An Evaluation of Water-Soluble Polymers for Secondary Oil Recovery--Part 2," Journal of Petroleum Technology, (May 1979), 31, No. 5, p. 561-570.

58. Szabo, M.T., "Some Aspects of Polymer Retention in Porous Media Using a C14-Tagged Hydrolyzed Polyacrylamide," Society of Petroleum Engineers Journal, (August 1975), 15, No. 4, p. 323-337.

59. Tolsted, L., and Swineford, A., "Kansas Rocks and Minerals," Kansas Geological Survey, the University of Kansas, (1977).

60. Vollmert, Polymer Chemistry, (1973), Springer-Verlag, New York, p. 493,551.

61. Wardlaw, N.C., "Pore Geometry of Carbonate Rocks as Revealed by Pore Casts and Capillary Pressure," American Association of Petroleum Geologists Bulletin, (February 1976), 60, No. 2, p. 245-257.

62. White, J.L., Goddard, J.E., and Phillips, H.M., "Use of Polymers to Control Water Production in Oil Wells," Journal of Petroleum Technology, (February 1973), 25, No. 2, p. 143-150.

63. Whitten, D.G.A., and Brooks, J.R.V., The Penguin Dictionary of Geology, (1972), Penguin Books, 625 Madison Ave., New York, New York, U.S.A..

64. Willhite, G.P., and Dominguez, J.G., "Mechanism of Polymer Retention in Porous Media," Improved Oil Recovery by Surfactant and Polymer Flooding, (1977), Academic Press, Inc., New York.

Appendix A

Polyacrylamide Mixing Procedures.

A.1 Polymer Inversion Procedure for Brine Make Up Water*

(for preparing 400 grams of solution)

1. Add 300.0 grams of synthetic water to a clean 16 oz wide-mouth jar or 600 ml beaker. Insert a stainless steel caged paddle stirrer** into a cone drive stirrer motor and lower the assembly so that the bottom of the stirrer is no more than 1/4 in above the bottom of the jar. Set stirrer speed so that a good vortex is developed in the make up water.

2. Measure Brine Activator equivalent to 10% of the polymer product to be used.

3. Add Brine Activator to the make up water.

4. Add correctly weighed amount of polymer latex to the stirred synthetic water as follows:

   Fill a 1 ml plastic syringe (no needle) with the latex, then discharge contents. Wipe the outside of the syringe with a paper towel and tare on an analytical balance to 0.00 grams with the cleaned syringe. Fill the syringe, wiping the outside of the syringe with a paper towel, and discharge excess latex until desired amount remains. Discharge the syringe contents into the vortex of the make up water in one continuous stroke.

5. When the polymer solution becomes viscous, after about a minute of stirring, increase the stirring speed to about 1000 rpm and stir for 10 minutes.

6. Add the remaining water necessary to bring the total sample weight to 400.0 grams.

7. Stir at about 1000 rpm for 30 additional minutes.

---

* Obtained from Nalco Chemical Company, Sugar Land, Texas

** Jiffy Mixer Company, Irvine, California

A.2 Preparation of Cyanatrol(R) WF Polymer Solutions

Suggested Laboratory Mixing Procedures*

A. Equipment

1. Variable Transformer (e.g., Powerstat, Staco)
2. Blender-type Stirrer (e.g., Waring Blender, Oster)
3. 5 ml Plastic Syringe

B. Procedure

1. Connect the blender through the variable transformer to an electrical outlet.

2. Add 500 ml of fresh water or brine to the blender vessel and attach to its base. Turn on blender and adjust variable transformer so that the fluid vortex just reaches down to the blender blades. (A Waring Blender at the low setting and a 25-30 volt setting on a Staco transformer gave the desired degree of agitation.)

3. Agitate sample of Cyanatrol WF Polymer thoroughly by shaking bottle.

4. Withdraw sample using syringe and add the Cyanatrol polymer to the shoulder of the vortex as rapidly as possible.

5. Turn off blender 15-20 seconds after sample addition. Longer mix times are not necessary (see data below). Excessive high speed stirring of the polymer solution should be avoided.

6. Typical viscosities of solutions prepared as above and measured within minutes after preparation and after two hours standing were as follows:

Cyanatrol	Concentration, g/500 ml**	Visc.,Cp.(UL/25°C/6 rpm) Initial	After 2 Hours
950S	2.02	48.0	48.0
940S	2.06	37.8	37.5
930S	2.04	28.6	27.9

Obtained from American Cyanamid Company.

** Synthetic Injection Water, 2376 ppm TDS.

A.3 Solid Polyacrylamide Mixing Procedure.

Solid polyacrylamides were prepared by weight. Brine of the amount necessary to make a known quantity of polymer solution was weighed into a beaker. A vortex was created with a magnetic stirrer which extended to the bottom of the beaker. Solid polymer was added slowly to the shoulder of the vortex. After addition of the polymer was complete, the stirrer was slowed to about 60 rpm and the solution was covered and allowed to stir overnight.

Appendix B

Air Permeability Measurement Procedure.

B.1 Air Permeability Determination*

The absolute permeability of plugs sampled from field cores was measured using a Ruska gas permeameter. The device was adapted by replacing the pressure regulator with a connection for a constant pressure source and by replacing the triple range flowmeter with a soap bubble buret used to measure the flow rate.

The Ruska Gas Permeameter is an instrument for measuring the permeability of consolidated core sections by forcing a gas of known viscosity through a core sample of known cross section and length. Pressure, temperature, and flow rate of the gas through the sample are measured.

The apparatus consists of a core holder with (1) built-in thermometer, (2) soap bubble buret flowmeter, (3) gas inlet connection, and (4) constant pressure source**

The core sample is sealed in the coreholder in such a manner that any gas entering can escape to the atmosphere only after having passed lengthwise through the sample. The thermometer indicates the temperature of the gas before it enters the core. The desired gas pressure (upstream pressure) is applied by adjusting the controller.*** The gas flow is determined by measuring the time required for a soap bubble to traverse a known length of the buret corresponding in cubic centimeters. Soap bubbles are generated by squeezing the rubber bulb filled with a soap solution and located at the bottom of the buret.

The dimensions of a clean and dry plug cut from the field core were recorded. The plug was inserted into the tapered rubber sleeve and this sleeve was then placed into the steel coreholder sleeve and locked into place by tightening the clamp. Air pressure was applied and slowly increased until a reasonable flow rate was observed (0.5 cc per second). Flow readings were recorded until a stable flow rate occurred. The absolute permeability to air was calculated for each plug using the following equation.

---

* Adapted procedure from Ruska Instrument Corporation instructions for Ruska Gas Permeameter Number 1011; publication 1011 113-58

** Mensor Quartz Manometer/Controller

*** Mensor Quartz Manometer/Controller Operating Instructions publication B10300-001 Rev. A, 1970

$$k_g = \frac{2.0(\mu)QL}{A\left[(\Delta P + 1.0)^2 - 1.0\right]}$$

where,

k_g = absolute air permeability in md

μ_g = air viscosity in cp

L = core length in cm

A = core area in cm^2

ΔP = pressure drop in atm

Q = flow rate in cm^3

Appendix C

Resistance Factor and Residual Resistance Factor

Resistance Factor

The resistance factor, RF, is defined as the ratio of the water mobility, λ_w, to polymer mobility, λ_p.

$$RF = \frac{\text{water mobility}}{\text{polymer mobility}} = \frac{\lambda w}{\lambda p}$$

The mobility is defined as the permeability, k, divided by the fluid viscosity, μ. Therefore,

$$RF = \frac{\frac{k}{\mu w}}{\frac{k}{\mu p}} = \frac{\Delta Pp}{\Delta Pw}$$

where,

ΔP = pressure drop to polymer

ΔP_w^p = pressure drop to water

Residual Resistance Factor

The residual resistance factor, RRF, is defined as the ratio of the mobility to water before polymer to the mobility to water after polymer. Therefore,

$$RRF = \frac{\lambda w \text{ (initial)}}{\lambda w \text{ (after polymer)}}$$

Appendix D

Unexplained Polymer Behavior

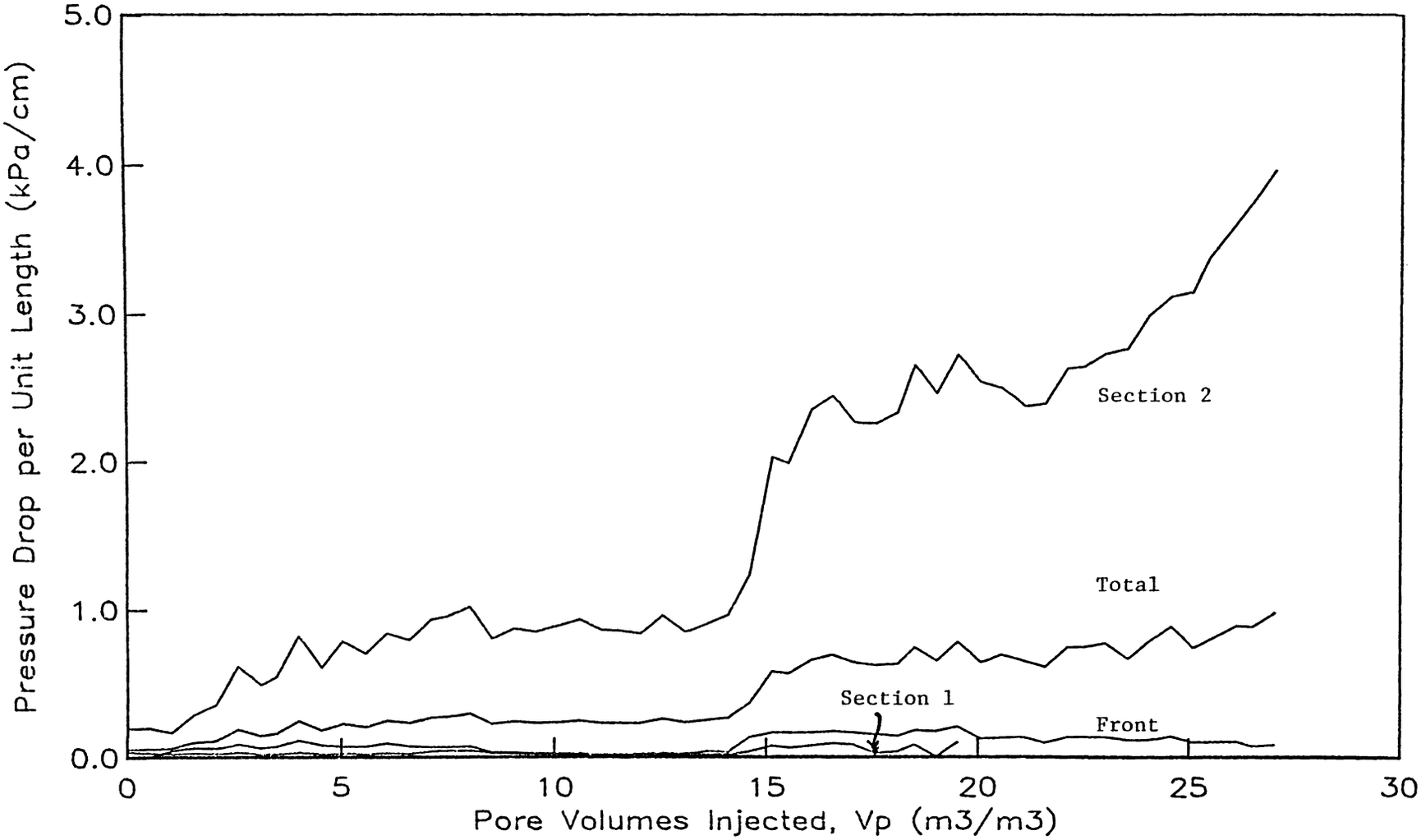

FIGURE D–1 PRESSURE GRADIENT ACROSS SECTIONS AND TOTAL CORE LENGTH FOR DENK1 FLOOD (BETZ 1160 IN BROOKS SYNTHETIC BRINE)

Appendix E

References Not Discussed.

1. Abdel-Alim, A.H., and Hamielec, A.E., "Shear Degradation of Water-Soluble Polymers. I. Degradation of Polyacrylamide in a High-Shear Couette Viscometer," Journal of Applied Polymer Science, (1973), 17, p. 3769-3778.

2. Bernard, G.G., "Effect of Clays, Limestone, and Gypsum on Soluble Oil Flooding," Journal of Petroleum Technology, (February 1975), 27, No. 2, p. 179-180.

3. Bernard, G.G., "Composition and Method for Enhanced Oil Recovery Utilizing Aqueous Polyacrylamide Solutions," U.S. Patent 4,060,490, (29 November 1977).

4. Bondor, P.L., Hirasaki, G.J., and Tham, M.J., "Mathematical Simulation of Polymer Flooding in Complex Reservoirs," Society of Petroleum Engineers Journal, (October 1972), 12, No. 5, p. 369-382.

5. Burcik, E.J., and Thakur, G.C., "Reaction of Polyacrylamide with Commonly Used Additives," Journal of Petroleum Technology, (September 1972), 24, No. 9, p. 1137-1139.

6. Capelle, H.T., "Water - Analysis Diagrams -- Kansas Oil-field Brines," paper presented at the Spring meeting of the Mid-Continent District, Div. of Prod., Wichita, Kansas, (April 1956), p. 238-248.

7. Chauveteau, G., and Kohler, N., "Polymer Flooding: The Essential Elements for Laboratory Evaluation," paper SPE 4745 presented at the Improved Oil Recovery Symposium of the Society of Petroleum Engineers of AIME, Tulsa, Ok., (22-24 April 1974).

8. Clampitt, R.L., and Curzon, J.E., "Secondary Recovery Methods," U.S. Patent 3,757,863, (11 September 1973).

9. Dabbous, M.K., "Displacement of Polymers in Waterflooded Porous Media and Its Effects on a Subsequent Micellar Flood," Society of Petroleum Engineers Journal, (October 1977), 17, No. 5, p. 358-368.

10. Dingman, R.J., and Angino, E.E., "Chemical Composition of Selected Kansas Brines as an Aid to Interpreting Change in Water Chemistry with Depth," Chemical Geology, (1969), 4, p. 325-339.

11. Duda, J.L., Klaus, E.E., and Fan, S.K., "The Influence of Polymer Molecule - Wall Interactions on Mobility Control," paper SPE 9298 presented at the Annual Fall Technical Conference and Exhibition of the Society of Petroleum Engineers of AIME, Dallas, Tx., (21-24 September 1980).

12. Ferrer, J., "Some Mechanistic Features of Flow of Polymer Through Porous Media," paper SPE 4029 presented at the 47th Annual Fall Meeting of the Society of Petroleum Engineers of AIME, San An-

tonio, Tx., (8-11 October 1972).

13. Gogarty, W.B., "Rheological Properties of Pseudoplastic Fluids in Porous Media," Society of Petroleum Engineers Journal, (June 1967), 7, No. 2, p. 149-160.

14. Gogarty, W.B., "Micellar/Polymer Flooding--An Overview," Journal of Petroleum Technology, (August 1978), 30, No. 8, p. 1089-1101.

15. Gogarty, W.B., and McAtee, R.W., "Method for Stabilizing the Mobility of Polyacrylamide Solutions Flowing Through Porous Media," U.S. Patent 3,580,337, (25 May 1971).

16. Gogarty, W.B., Meabon, H.P., and Milton, H.W.,Jr., "Mobility Control Design for Miscible-Type Waterfloods Using Micellar Solutions," Journal of Petroleum Technology, (February 1970), 22, No. 2, p. 141-147.

17. Gupta, S.P. and Trushenski, S.P., "Micellar Flooding--The Propagation of the Polymer Mobility Buffer Bank," Society of Petroleum Engineers Journal, (February 1978), 18, No. 1, p. 5-12.

18. Harbaugh, J.W., and Davie, W. Jr., "Upper Pennsylvanian Calcareous Rocks Cored in Two Wells In Rawlins and Stafford Counties, Kansas," State Geological Survey of Kansas, Bulletin 170, Part 6, The University of Kansas, (1964).

19. Harvey, H.A., and Menzie, D.E., "Polymer Solution Flow in Porous Media," Society of Petroleum Engineers Journal, (June 1970), 10, No. 2, p. 111-118.

20. Hill, H.J., Brew, J.R., Claridge, E.L., Hite, J.R., and Pope, G.A., "The Behavior of Polymers in Porous Media," paper SPE 4748 presented at the Improved Oil Recovery Symposium of the Society of Petroleum Engineers of AIME, Tulsa, Ok., (22-24 April 1974).

21. Jewett, R.L., and Schurz, G.F., "Polymer Flooding--A Current Appraisal," Journal of Petroleum Technology, (June 1970), 22, No. 6, p. 675-684.

22. Klinkerberg, L.J., "Pore Size Distribution of Porous Media and Displacement Experiments with Miscible Liquids," Petroleum Transactions,AIME, (1957), 210, p. 366-369.

23. Knight, R.K., "Mobility Control of Aqueous Fluids in Porous Media," U.S. Patent 4,039,028, (2 August 1977).

24. Krauskopf, K.B., Introduction to Geochemistry, 2nd edition, (1979), McGraw Hill Book Co., from the International Series in the Earth and Planetary Sciences, p. 40-76.

25. Lange, W., and Rehage, G., "Recent Results on the Use of Polymers in Tertiary Oil Recovery in Brines of High Salinity," paper SPE

8983 presented at the 5th International Symposium on Oilfield and Geothermal Chemistry, Stanford, Ca., (28-30 May 1980).

26. Lapre, J.F., "Reservoir Potential as a Function of the Geological Setting of Carbonate Rocks," SPE 9246 55th, (21-24 September 1980).

27. Legere, R.F., "Reduction of Water-Oil Ratio Using Polyacrylamides in Vugular Carbonate Reservoirs," Journal of Canadian Petroleum - Technology, (October - December 1978), 17, No. 4, p. 51-60.

28. Maerker, J.M., "Dependence on Polymer Retention on Flow Rate," Journal of Petroleum Technology, (November 1973), 25, No. 11, p. 1307-1308.

29. Martin, F.D., and Sherwood, N.S., "The Effect of Hydrolysis of Polyacrylamide on Solution Viscosity, Polymer Retention and Flow Resistance Properties," paper SPE 5339 presented at the SPE-AIME Rocky Mountain Regional Meeting, Denver, Co., (7-9 April 1975).

30. McKennon, K.R., "Method of Degrading Water-Soluble Polymers with Ferrous Salts and a Ferric Chelating Agent," U.S. Patent 3,240,737, (15 March 1966).

31. Meyer, H.I., "Pore Distribution in Porous Media," Journal of - Applied Physics, (May 1953), 24, No. 5, p. 510-512.

32. Murphy, C.L., "Method of Recovering Oil Using Sacrificial Agent and Viscosifier," U.S. Patent 3,478,823, (18 November 1969).

33. Needham, R.B., Threlkeld, C.B., and Gall, J.W., "Control of Water Mobility Using Polymers and Multivalent Cations," paper SPE 4747 presented at the Improved Oil Recovery Symposium of the Society of Petroleum Engineers of AIME, Tulsa, Ok., (22-24 April 1974).

34. Norton, C.J., and Falk, D.O., "Salinity Effects on Water Thickeners for Enhanced Oil Recovery," paper SPE 7141 presented at the Regional Meeting of the Society of Petroleum Engineers of AIME, San Francisco, Ca., (12-14 April 1978).

35. Norton, C.J., anf Falk, D.O., "Carboxy Vinyl Polymer and Partially Hydrolyzed Polyacrylamide Mobility Control Agent and Process," U.S. Patent 3,891,567, (24 June 1975).

36. Petitt, D.J., "Guar Gum - Polyacrylamide Compositions," U.S. Patent 3,658,734, (25 April 1972).

37. Pye, D.J., "Water Flooding Process for the Recovery of Petroleum and Improved Water Flooding Process," U.S. Patent 3,399,725, (3 September 1968).

38. Pye, D.J., "Waterflooding Process for the Recovery of Petroleum," U.S. Patent 3,282,337, (1 November 1966).

39. Quayle, D.V., "An Electron Microscopical Study of Polyacrylamide," Journal of the Royal Microscopical Society, (December 1967), 87, p. 353-359.

40. Rhudy, J.S., and Haws, G.W., "Method of Polymer Flooding," U.S. Patent 3,842,909, (22 October 1974).

41. Rhudy, J.S., and Haws, G.W., "Method of Polymer Flooding," U.S. Patent 3,726,342, (10 April 1973).

42. Rhudy, J.S., and Knight, B.L., "Mobility Control in Low Permeability Reservoirs," U.S. Patent 3,858,652, (7 January 1975).

43. Rhudy, J.S., Gogarty, W.B., Knight, B.L., and Fullinwider, J.H., "Polymer Flooding in High Permeability Reservoirs," U.S. Patent 4,011,910, (15 March 1977).

44. Sloat, B.F., Fitch, F.P., and Taylor, J.T., "How to Produce More Oil and More Profit with Polymer Treatments," paper SPE 4185 presented at the 43rd Annual California Regional Meeting of the Society of Petroleum Engineers of AIME, Bakersfield Ca., (8-10 November 1972).

45. Smith, F.W., "A Rapid Method for Determining Characteristics of Liquid Flow in Porous Media," Journal of Petroleum Technology, (November 1968), 20, No. 11, p. 1219-1220.

46. Szabo, M.T., "Laboratory Investigations of Factors Influencing Polymer Flood Performance," Society of Petroleum Engineers - Journal, (August 1975), 15, No. 4, p. 338-346.

47. Szabo, M.T., "Molecular and Microscopic Interpretation of the Flow of Hydrolyzed Polyacrylamide Solution Through Porous Media," paper SPE 4028 presented at the 47th Annual Fall Meeting of the Society of Petroleum Engineers of AIME, San Antonio, Tx., (8-11 October 1972).

48. Szabo, M.T., "A Comparative Evaluation of Polymers for Oil Recovery -- Rheological Properties," paper SPE 6601-A presented at the 1977 SPE-AIME International Symposium on Oilfield and Geothermal Chemistry, La Jolla, Ca., (27-28 June 1977).

49. Szabo, M.T., "A Comparative Evaluation of Polymers for Oil Recovery -- Flow and Retention in Porous Media," paper SPE 6601-B presented at the 1977 SPE-BIME International Symposium on Oilfield and Geothermal Chemistry, La Jolla, Ca., (27-28 June 1977).

50. Thomas, C.P., "The Mechanism of Reduction of Water Mobility by Polymers in Glass Capillary Arrays," Society of Petroleum - Engineers Journal, (June 1976), 16, No. 3, p. 130-136.

51. Tinker, G.E., Bowman, R.W., and Pope, G.A., "Determination of In-Situ Mobility and Wellbore Impairment From Polymer Injectivity Data," Journal of Petroleum Technology, (May 1976), 28, No. 5,

p. 586-596.

52. Townsend, W.R., Becker, S.A., and Smith, C.W., "Polymer Use in Calcareous Formations," paper SPE 6382 presented at the Permian Basin Oil and Gas Recovery Conference of the Society of Petroleum Engineers of AIME, Midland, Tx., (10-11 March 1977).

53. Tysee, D.A., and Vetter, O.J., "Chemical Characterization Problems of Water Soluble Polymers," paper SPE 8977 presented at the 5th International Symposium on Oilfield and Geothermal Chemistry, Stanford, Ca. (28-30 May 1980).

54. Uzoigwe, A.C., Scanlon, F.C., and Jewett, R.L., "Improvements in Polymer Flooding: The Programmed Slug," paper SPE 4024 presented at the 47th Annual Fall Meeting of the Society of Petroleum Engineers of AIME, San Antonio, Tx., (8-11 October 1972).

55. Ward, J.S., and Martin, F.D., "Prediction of Viscosity for Partially Hydrolyzed Polyacrylamide Solutions in the Presence of Calcium and Magnesium Ions," paper SPE 8978 presented at the 5th International Symposium on Oilfield and Geothermal Chemistry, Stanford, Ca., (28-30 May 1980).

56. Wardlaw, N.C., and Taylor, R.P., "Mercury Capillary Pressure Curves and the Interpretation of Pore Structure and Capillary Behaviour in Reservoir Rocks," Bulletin of Canadian Petroleum - Geology, (June 1976), 24, No. 2, p. 225-262.